SCUOLA DI DOTTORATO
UNIVERSITÀ DEGLI STUDI DI MILANO-BICOCCA

Department of Medicine and Surgery
PhD program in Translational and Molecular Medicine
Cycle XXXIII

Improving Outcome of Cardiac Arrest: from Cardiopulmonary Resuscitation Interventions to Post Resuscitation Care

Magliocca Aurora, MD

Registration number 776979

Tutor: Prof. Giacomo Bellani, MD, PhD

Co-tutor: Prof. Giuseppe Ristagno, MD, PhD

Coordinator: Prof. Andrea Biondi, MD, PhD

ACADEMIC YEAR 2019-2020

Table of Contents

Chapter 1. Introduction

Cardiac arrest (CA) is a leading cause of death worldwide with poor outcome (1). Significant improvements have been achieved in the last decades in both resuscitation from cardiac arrest and post-resuscitation care, but mortality remains high. Cardiopulmonary resuscitation (CPR), including chest compression (CC), often in conjunction with electrical defibrillation (DF), has the potential of re-establishing spontaneous circulation. According to the American Heart Association's "Heart Disease and Stroke Statistics—2019 Update," (1) there are ≈356 000 cases of out-of-hospital cardiac arrest (OHCA) and 209000 cases of in-hospital cardiac arrest (IHCA) in the United States. The survival to hospital discharge was 12% for OHCA and 25% for IHCA. For OHCA, survival with good neurological outcome is 8% (1). The European Registry of Cardiac Arrest Project provided information about resuscitation events during October 2014 across 28 countries in Europe. In a population of almost 179 million inhabitants, 37054 OHCA were reported, with CPR onset confirmed in 25171 cases. The bystander CPR showed high variability ranging from 13% to 82%. ROSC was achieved in 33% of cases and 8% of patients was discharged from hospital alive. Association of CPR with ventilation showed a higher survival to hospital discharge compared to CPR only (14% versus 8% respectively). No bystander CPR was associated to a 4.3% survival (2).

Prompt cardiopulmonary resuscitation (CPR) is the major determinant of successful resuscitation (3-4), but its quality heterogeneity may contribute to the variable survival rates reported in different regions

(5-6). The vast majority of patients successfully resuscitated from cardiac arrest present in coma or with an altered level of consciousness caused by the widespread nature of brain injury after cardiac arrest. Although most of the deaths in patients initially resuscitated from cardiac arrest are attributed to brain injury, only ≈10% of these deaths meet the clinical criteria for brain death (7-8). Instead, most deaths associated with brain injury after cardiac arrest result from active withdrawal of life-sustaining treatment (WLST) because a poor neurological outcome is predicted. For this reason, neurological prognostication in comatose cardiac arrest survivors is of utmost importance to avoid both pursuing futile treatments in patients destined for a poor outcome and making an inappropriate WLST in patients who may have a chance for neurological recovery. The molecular events that cause neurodegeneration after cardiac arrest occur over hours to days after ROSC. This time course suggests a potentially broad therapeutic window for neuroprotective drug therapy. However, the number of clinical trials performed to date is limited and has failed to demonstrate improved neurological outcome with potential neuroprotective drugs given after cardiac arrest. Novel therapeutic target are needed to reduce post-CA brain injury and improve outcomes.

CPR interventions

Prompt delivery of cardiopulmonary resuscitation with an emphasis on high-quality chest compressions improves successful resuscitation from cardiac arrest (9). During cardiac arrest, coronary blood flow ceases. This determines a progressive and critical energy failure. The

presence of myocardial acidosis – due to high carbon dioxide - is associated with depletion of high-energy phosphates and a severe ischemia of the myocardium (10-11). Ischemia injures the left ventricle (LV) that becomes contracted and is therefore named "stone heart" (12-13). In the presence of a stone heart, a successful DF becomes hardly achievable. In order to delay onset of ischemic myocardial injury and facilitates DF, the application of early CPR can partially restore coronary perfusion pressure (CPP) and myocardial blood flow (14). Interestingly, delays in CPR, ineffective and frequently interrupted CC, and limited access to, or delayed DF are major contributing factors to the poor outcome after cardiac arrest (15-17).

Indeed, ineffective and frequently interrupted CC is often provided even by well-trained rescuers, leading to unsuccessful resuscitative efforts (18-19). The challenge is even greater during special circumstances like transport, a condition characterized by the presence of acceleration, deceleration, and rotational forces that may affect manual CC (20-23).

Monitoring effectiveness of CC

The quality of CC is a major predictor of success of ROSC (17-19). There are two specific determinants of good quality CPR that successful predict resuscitation: coronary perfusion pressure (CPP) (24-27), and end-tidal CO_2 ($EtCO_2$) (28-30).

CCs during CPR generate blood flow by the pressure gradient that is developed among the aortic and the venous return pressure (31). CPP is defined as the difference between simultaneously measured

diastolic aortic pressure and the right atrial pressure during decompression diastole (32). CPP is highly correlated with the coronary blood flow during CPR and it is considered as most proficient indicator of the likelihood of success of DF and ROSC (33). According to experimental and clinical observations, levels of CPP above 15 mmHg during CC are good predictors of ROSC (25). Given this pathophysiologic background, it becomes clear how resuscitative strategies aiming at increasing CPP – which include high quality CC (34) and the use of vasopressors (35) - have been supported to restore an effective spontaneous circulation.

Exhaled CO_2 is determined by cardiac output and arterial partial pressure of CO_2, which is in turn determined by the production of metabolic CO_2 and by the alveolar ventilation. If cardiac output (CO) is not impaired, pulmonary perfusion is adequate and $EtCO_2$ is mainly driven by the alveolar minute ventilation. In contrast, during cardiac arrest and CPR, CO usually decreases less than one-third of normal; consequently, pulmonary blood flow and $EtCO_2$ drastically decrease. Therefore, $EtCO_2$ can indirectly infer on the levels of CO - and then pulmonary blood flow - produced by CCs. As the $EtCO_2$ is strongly correlated with CPP during CPR it may serve as a non-invasive surrogate of CPP. Accordingly, $EtCO_2$ has emerged as another valuable tool – together with CPP – to monitor the effectiveness of CCs and therefore the quality of CPR (35-36). Levels of $EtCO_2$ above approximately 10 to 15 mmHg during CPR are correlated with a greater likelihood of successful ROSC (35). Furthermore, $EtCO_2$ may be used to suggest the earliest clinical evidence of ROSC (36).

Blood pressure assessment during CPR is – theoretically - of utmost importance. However, invasive measurements of aortic and right atrial pressures are available or feasible during resuscitation in a limited proportion of patients, which is even lower in pre-hospital settings. Similarly, $EtCO_2$ is not widely available yet. However, portable infrared capnometers could be successfully used in pre-hospital settings during CPR, although monitoring of $EtCO_2$ requires airway adjuncts. Out of hospital endotracheal intubation is associated with a high failure rate and a 30% incidence of traumatic injury to the airway. Furthermore, epinephrine administration during CPR leads to significant decreases of $EtCO_2$ by the increase of pulmonary shunting (37). This might induce a significant bias in the $EtCO_2$ interpretation during the monitoring and guiding of the resuscitative maneuvers.

Post-cardiac arrest syndrome

After the initial success of CPR, the majority of resuscitated patients die within 72 hr, due to what is now termed “post cardiac arrest syndrome” (38). Indeed, ROSC after cardiac arrest is an unnatural pathophysiological state created by successful CPR. In the early 1970s, Dr. Vladimir Negovsky recognized that the pathology caused by complete, whole-body ischemia and reperfusion was unique in that it had a clearly definable cause, time course, and constellation of pathophysiological processes (39). Negovsky named this state “post resuscitation disease”. Although appropriate at the time, the term “resuscitation” is now used more broadly to include treatment of various shock states in which circulation has not ceased. Moreover,

the term “post resuscitation” implies that the act of resuscitation has ended. Negovsky stated that “a second, more complex phase of resuscitation begins when patients regain spontaneous circulation after cardiac arrest” (39). Therefore, the term “post-cardiac arrest syndrome” seems more appropriate. The 3 key components of this syndrome are: 1) post cardiac arrest brain injury; 2) post cardiac arrest myocardial dysfunction; 3) systemic ischemia/reperfusion response (38, 40-41). Pathophysiology, clinical manifestations and potential treatments of the post cardiac arrest syndrome are summarized in Table 1 (42).

Post-cardiac arrest lung damage

The presence of lung injury in the context of post-CA syndrome and its association with outcomes has been recently highlighted (43-45). It has been reported that up to 50% of OHCA survivors develop acute respiratory distress syndrome (ARDS) within 48h after hospital admission, and that early ARDS is associated with hospital mortality and poor neurological outcome (43). Indeed, a post-resuscitation lung protective ventilation strategy is suggested, since low tidal volume ventilation may improve neurocognitive outcome after cardiac arrest. In a study comparing a tidal volume less than or greater than 8 ml/kg in OHCA survivors, it was observed that a lower tidal volume in the first 48 h post-ROSC was associated with a favorable neurological outcome, more ventilator and shock-free days (44). In the TTM trial non-survivors at 28 days had worst oxygenation, higher respiratory rates, driving pressures, plateau pressures and lower compliance of the

respiratory system compared to survivors (45).

Lung injury after CA has ben attributed to several mechanisms, including pulmonary ischemia–reperfusion, pulmonary aspiration, mechanical injury from chest compressions and associated thoracic fractures, and systemic inflammation characteristic of post-CA syndrome (Table 2).

However, a comprehensive understanding of the trigger mechanism, pathophysiology and evolution of lung injury after CPR is still lacking; especially after the introduction of mechanical CC. Mechanical chest compression devices could deliver consistently high-quality CC, nevertheless the optimal ventilation strategy during mechanical CC is still elusive: how to provide adequate blood oxygenation and carbon dioxide (CO_2) removal while minimizing lung injury remains uncertain, with a substantial lack of robust evidence and conclusive recommendations (46). Lung injury related to CPR has been previously reported in OHCA (47-48) and in experimental models of CA. A recent autopsy-based comparison between manual and mechanical CC revealed that lung lesions are present respectively in 4% and 18.6% of patients undergoing manual and mechanical CC, respectively (49). In contrast, imaging studies using Computed Tomography (CT) showed that lung injuries, mainly ground glass opacity and airspace consolidation, are frequent complications in CA patients who undergo CPR, detectable in up to 79% of cases (50-51). Experimental studies showed that the severity of lung injury is correlated with the duration of CA (52-53). Taken altogether these evidences suggest that lung injury related to CPR is a frequent complication and it is more represented in patients

undergoing mechanical CC. Furthermore, lung injury may significantly contribute to morbidity in CA patients and may represent a potentially reversible cause of resuscitation failure.

Post-cardiac arrest brain injury

The unique vulnerability of the brain is attributed to its limited tolerance of ischemia as well as its unique response to reperfusion. The mechanisms of brain injury triggered by cardiac arrest and resuscitation are complex and include excitotoxicity, disrupted Ca^{2+} homeostasis, free radical formation, pathological protease cascades, and activation of cell death signaling pathways (38, 54-55). Both neuronal necrosis and apoptosis have been reported after cardiac arrest. Histologically, selectively vulnerable neuron subpopulations in the hippocampus, cortex, cerebellum, corpus striatum, and thalamus, degenerate over hours to days (56-60). Levels of high-energy metabolites such as ATP and phosphocreatine decrease within seconds when oxygen supply to the brain is interrupted (61). The breakdown of ATP and the switch of intracellular metabolism to anaerobic glycolysis lead to an increase in intracellular levels of inorganic phosphate, lactate, and hydrogen ion, resulting in both intra- and extracellular acidosis. The above processes lead to influx of Ca^{2+} into the cell. Loss of ATP and acidosis also inhibit the mechanisms that normally deal with excessive intracellular Ca^{2+} by sequestering Ca^{2+} from the cell, further aggravating intracellular Ca^{2+} overload. These problems are compounded by failure of ATP–dependent (sodium-potassium) Na^{+}-K^{+} pumps and K^{+}, Na^{+}, and Ca^{2+} channels, leading to an additional influx of Ca^{2+}. The excess Ca^{2+} induces mitochondrial

dysfunction (increasing intracellular Ca^{2+} influx yet further, in a vicious cycle) and activates numerous intracellular enzyme systems (kinases and proteases). In addition, immediate early genes are activated and a depolarization of neuronal cell membranes occurs, with a release of large amounts of the excitatory neurotransmitter glutamate into the extracellular space. This leads to prolonged and excessive activation of membrane glutamate receptors, further stimulating Ca^{2+} influx through activation of Ca^{2+} channels in another vicious cycle. Under normal circumstances, neurons are exposed to only very brief pulses of glutamate; prolonged glutamate exposure induces a permanent state of hyperexcitability in the neurons (the *excitotoxic cascade*), which can lead to additional injury and cell death. A destructive process that is closely linked to but distinct from the mechanisms discussed above is the release of ROS following ischemia/reperfusion. Mediators such as superoxide, peroxynitrite, hydrogen peroxide, and hydroxyl radicals play an important role in determining whether injured cells will recover or die. Free radicals can oxidize and damage numerous cellular components. Although brain cells have various enzymatic and non-enzymatic antioxidant mechanisms that prevent this type of injury under normal circumstances, ROS production following ischemia/reperfusion is so great that these defensive mechanisms are likely to be overwhelmed, leading to peroxidation of lipids, proteins, and nucleic acids. Ischemia/reperfusion can also lead to significant disruptions in the blood–brain barrier (BBB), which can facilitate the subsequent development of brain edema (62). All the above processes contribute to the development of post-cardiac arrest intracranial hypertension,

which further augments brain damage. Mechanisms accounting for BBB loss of integrity include: decreased fluidity and integrity of cell membranes and increased vascular permeability of microvascular endothelial cells in the brain, mediated by inflammatory cytokines and vascular endothelial growth factor, *via* release of nitric oxide (NO). More specifically NO can interact with ROS producing peroxynitrite radicals, which activate matrix metalloproteinases (MMPs) that ultimately disrupt BBB junctions.

Kynurenine pathway (KP)

Metabolism of tryptophan (TRP) to kynurenine, known as the kynurenine pathway (KP), has recently been implicated in a variety of clinical disorders including cerebrovascular disease, sepsis, coronary artery disease and cardiac arrest (Figure 1) (63-69).

Inflammation can modulate the kynurenine pathway via the enzyme indoleamine-2,3-dioxygenase (IDO). That is, IDO expression in cells is induced via IFNγ or TNFα (70-71). Once induced, IDO converts TRP to N-formyl-kynurenine, which in turn becomes kynurenine (KYN). Depending on the cell type involved, KYN may be metabolized further along the kynurenine pathway. Downstream metabolites of KP include kynurenic acid (KYNA), 3-hydroxyanthranilic acid (3-HAA) and Quinolinic acid (QUIN) (72). It has been demonstrated that KYNA has neuroprotective properties, whereas 3-HAA and QUIN have neurotoxic effects (73-76). Furthermore, it has been previously showed that increased KP activation is associated with acute brain dysfunction and mortality in

intensive care unit patients (65) and correlates with infarct volume in stroke patients (64).

Altogether this evidence suggests that KP activation is involved in various neurological disorders. To restore equilibrium among its metabolites, the KP targeting could represent a promising line of investigation.

KP and sepsis

Growing evidence suggests that KP metabolites can play a role in the regulation of blood pressure. Kynurenine has been identified as an endothelium-dependent relaxing factor contributing to the regulation of blood pressure in systemic inflammation (77). It has been demonstrated that IDO activity in resistance vessels is increased and correlates with hypotension in patients with septic shock (63). The KP has been further investigated and the role of xanthurenic acid (XA), a metabolite in the KP, has been highlighted participating in the inflammation-induced hypothension (78). A recent untargeted and targeted metabolomic analysis in septic shock patients showed that high levels of kynurenine were found in non-responders to treatment patients, supporting the role of KP activation in the sepsis outcome (79).

Interestingly, inhibition of the rate-limiting enzyme of the KP (indoleamine-2,3-dioxygenase, IDO) seems to have beneficial effects. In mice injected with LPS, IDO inhibition with 1-methyl-tryptophan (1-MT) prevents the reduction in blood pressure suggesting that IDO activation plays a key role in septic shock (77). The protective effect of the blockade of IDO has been also demonstrated in endotoxin

shock in mice. Specifically, the authors showed that IDO knockout mice ($IDO^{-/-}$) or pharmacological inhibition of the enzyme with 1-MT (pretreatment) increases survival after LPS-induced endotoxin shock and reduces endotoxin shock-induced serum cytokine levels in mice (80). Altogether these evidences suggest that KP is activated and its metabolites are increased in conditions of systemic inflammation like sepsis. KP activation correlates with clinical outcome like hypotension and response to treatment in patients with septic shock. Inhibition of KP via IDO seems to be a promising target, and effectively reduced hypotension and increased survival in experimental models of sepsis.

KP and cardiac arrest (CA)

Our group first proposed KP activation in cardiac arrest and cardiopulmonary resuscitation in animal models and in CA patients. We previously showed that KP is early activated after CA/CPR in a study including both small and large animals (67). We observed a reduction in plasma levels of TRP, together with an increase in plasma levels of KP metabolites: KYN, KYNA and 3-HAA. KP metabolites increase occurred in the first hours following resuscitation and persisted up to 3-5 days after CA/CPR. These findings were consistent in all species studied -rats, pigs and humans- and were correlated with the severity of myocardial dysfunction, cerebral injury, and survival.

Of particular interest, we previously reported that KP is activated early after resuscitation in out-of-hospital CA patients (68). We measured plasma KP metabolites of 245 patients enrolled in a prospective, multi-center, observational study involving 21 intensive care units in Finland (FINNRESUSCI). We found that higher levels of

KP metabolites at ICU admission are associated with hypotension during the first 24 hours after resuscitation and with ICU mortality in out-of-hospital CA patients. KYNA and 3-HAA independently predict poor 12-month neurological outcome. Furthermore, in patients with stable coronary artery disease has been observed the involvement of the KP. In these patients, KP activation strongly predict occurrence of major coronary events, acute myocardial infarction, and cardiovascular mortality (66).

Although KP activation after CA/CPR has been correlated with mortality and neurological outcome, we cannot argue on the causative role of KP activation on neurological damage and outcomes. To date no studies have tested interventions that may inhibit the rate-limiting enzyme of KP after CA/CPR in mice.

Scope of the thesis

The present thesis focuses on different strategies targeting the two main aspects of CA treatment, namely: cardiopulmonary resuscitation interventions and post-resuscitation care. It includes both experimental and translational studies directed to improve hemodynamic support during CPR, to define pulmonary dysfunction related to CPR, and to improve post-resuscitation outcomes.

Chapter 2. In this experimental study, we sought to investigate the hemodynamic support generated by a mechanical piston device or manual chest compression (CC) in a moving ambulance. The hypothesis on whether mechanical CC would improve systemic

perfusion compared with manual CC was tested in a preclinical porcine model of out-of-hospital cardiac arrest.

Chapter 3. The aim of this study was to systematically assess the presence of lung abnormalities associated with cardiopulmonary resuscitation- and to evaluate whether mechanical and manual chest compression could play a different role in their development. The hypothesis was tested in a translational study including 1) a porcine model of CA, and 2) a retrospective multicenter observational cohort study of non-traumatic out-of-hospital CA patients with a lung CT scan at hospital admission.

Chapter 4. This study aimed to investigate the specific pathophysiological role of kynurenine pathway (KP) activation on brain injury and outcomes after CA. We evaluated the effects of genetic deletion of the rate-limiting enzyme of the KP, indoleamine-2,3-dyoxygenase (IDO) on survival and neurological outcome after CA.

References

1. Benjamin EJ, Muntner P, Alonso A, Bittencourt MS, Callaway CW; on behalf of the American Heart Association Council on Epidemiology and Prevention Statistics Committee and Stroke Statistics Subcommittee. Heart disease and stroke statistics—2019 update: a report from the American Heart Association. *Circulation*. 2019;139:e56–e528. doi: 10.1161/CIR.0000000000000659.

2. Jan-Thorsten Gra¨sner, Jan Wnent, Johan Herlitz, Gavin D. Perkins et al. Survival after out-of-hospital cardiac arrest in Europe - Results of the EuReCa TWO study Resuscitation 148 (2020) 218 -226

3. Perkins GD, Handley AJ, Koster RW, Castr_en M, Smyth MA,; Adult basic life support and automated external defibrillation section Collaborators. European Resuscitation Council Guidelines for Resuscitation 2015: Section 2. Adult basic life support and automated external defibrillation. Resuscitation. 2015;95:81–99.

4. Aufderheide TP, Frascone RJ, Wayne MA, Mahoney BD, Swor RA, Domeier RM, Olinger ML, Holcomb RG, Tupper DE, Yannopoulos D, Lurie KG. Standard cardiopulmonary resuscitation versus active compression-decompression cardiopulmonary resuscitation with augmentation of negative intrathoracic pressure for out-of-hospital cardiac arrest: a randomised trial. Lancet. 2011;377:301–311.

5. Okubo M, Schmicker RH, Wallace DJ, Idris AH, Nichol G, Austin MA; Resuscitation Outcomes Consortium Investigators. Variation in survival after out-of-hospital cardiac arrest between emergency medical services agencies. JAMA Cardiol. 2018;3:989–999.

6. Grasner JT, Lefering R, Koster RW, Masterson S, Bottiger BW; EuReCa ONE Collaborators. EuReCa ONE-27 Nations, ONE Europe, ONE Registry: a prospective one month analysis of out-of- hospital cardiac arrest outcomes in 27 countries in Europe. Resuscitation. 2016;105:188–195.

7. Dragancea I, Rundgren M, Englund E, Friberg H, Cronberg T. The influence of induced hypothermia and delayed prognostication on the mode of death after cardiac arrest. *Resuscitation.* 2013;84:337–342. doi: 10.1016/j.resuscitation.2012.09.015

8. Mulder M, Gibbs HG, Smith SW, Dhaliwal R, Scott NL, Sprenkle MD, Geocadin RG. Awakening and withdrawal of life-sustaining treatment in cardiac arrest survivors treated with therapeutic hypothermia. *Crit Care Med.* 2014;42:2493–2499. doi: 10.1097/CCM.0000000000000540

9. SK Wallace, BS. Abella, LB Becker. Quantifying the Effect of Cardiopulmonary Resuscitation Quality on Cardiac Arrest Outcome. Circ Cardiovasc Qual Outcomes. 2013;6:148-156.

10. Johnson BA, Weil MH, Tang W, et al. Mechanisms of myocardial hypercarbic acidosis during cardiac arrest. J Appl Physiol 1995; 78:1579-1584
11. Kern KB, Garewal HS, Sanders AB, et al. Depletion of myocardial adenosine triphosphate during prolonged untreated ventricular fibrillation: effect on defibrillation success. Resuscitation 1990; 20:221-222

12. Klouche K, Weil MH, Sun S et al. Echo-Doppler observations during cardiac arrest and cardiopulmonary resuscitation. Crit Care Med 2000; 28: N212-N213

13. Klouche K, Weil MH, Sun S, et al. Evolution of the Stone Heart After Prolonged Cardiac Arrest. Chest 2002; 122:1006-1011

14. Deshmukh HG, Weil MH, Gudipati CV, et al. Mechanism of blood flow generated by precordial compression during CPR, I: studies on closed chest precordial compression. Chest 1989; 95:1092-1099

15. Iwami T, Kitamura T, Kawamura T, et al. Chest compression-only cardiopulmonary resuscitation for out-of-hospital cardiac arrest with public-access defibrillation: a nationwide cohort study. Circulation 2012; 126:2844-2851

16. Valenzuela TD, Roe DJ, Nichol G, et al. Outcomes of rapid defibrillation by security officers after cardiac arrest in casinos. N Engl J Med 2000; 343:1206–1209

17. Wik L, Kramer-Johansen J, Myklebust H, et al. Quality of cardiopulmonary resuscitation during out-of-hospital cardiac arrest. JAMA 2005; 293:299–304

18. Idris AH, Guffey D, Aufderheide TP, Brown S, Morrison LJ, Nichols P, Powell J, Daya M, Bigham BL, Atkins DL, Berg R, Davis D, Stiell I, Sopko G, Nichol G; Resuscitation Outcomes Consortium (ROC) Investigators. Relationship between chest compression rates and outcomes from cardiac arrest. Circulation. 2012;125:3004–3012.

19. Christenson J, Andrusiek D, Everson-Stewart S, Kudenchuk P, Hostler D, Powell J, Callaway CW, Bishop D, Vaillancourt C, Davis D, Aufderheide TP, Idris A, Stouffer JA, Stiell I, Berg R; Resuscitation Outcomes Consortium Investi- gators. Chest compression fraction determines survival in patients with out-of- hospital ventricular fibrillation. Circulation. 2009;120:1241–1247.

20. Callaway CW, Soar J, Aibiki M, B€ottiger BW, Brooks SC, Deakin CD, Donnino MW, Drajer S, Kloeck W, Morley PT, Morrison LJ, Neumar RW, Nicholson TC, Nolan JP, Okada K, O'Neil BJ, Paiva EF, Parr MJ, Wang TL, Witt J; Advanced

Life Support Chapter Collaborators. Part 4: advanced life support: 2015 international consensus on cardiopulmonary resuscitation and emergency cardio- vascular care science with treatment recommendations. Circulation. 2015;132:S84–S145.

21. Russi CS, Myers LA, Kolb LJ, Lohse CM, Hess EP, White RD. Comparison of chest compression quality delivered during on-scene and ground transport cardiopulmonary resuscitation. West J Emerg Med. 2016;17:634–639.

22. Olasveengen TM, Wik L, Steen PA. Quality of cardiopulmonary resuscitation before and during transport in out-of-hospital cardiac arrest. Resuscitation. 2008;76:185–190.

23. Sunde K, Wik L, Steen PA. Quality of mechanical, manual standard and active compression-decompression CPR on the arrest site and during transport in a manikin model. Resuscitation.1997;34:235–242.

24. Deshmukh HG, Weil MH, Gudipati CV, et al. Mechanism of blood flow generated by precordial compression during CPR, I: studies on closed chest precordial compression. Chest 1989; 95:1092-1099

25. Paradis NA, Martin GB, Rosenberg J, et al. Coronary perfusion pressure and the return of spontaneous circulation in

human cardiopulmonary resuscitation. JAMA 1990; 263:1106–1113

26. Sanders AB, Kern KB, Atlas M, et al. Importance of the duration of inadequate coronary perfusion pressure on resuscitation from cardiac arrest. J Am Coll Cardiol 1985b; 6:113–118

27. Yu T, Weil MH, Tang W, et al. Adverse outcome of interrupted precordial compression during automated defibrillation. Circulation 2002; 106:368-372

28. Falk JL, Rackow EC, Weil MH. End-tidal carbon dioxide concentration during cardiopulmonary resuscitation. N Engl J Med 1988; 318:607-611

29. Lah K, Križmarić M, Grmec S. The dynamic pattern of end-tidal carbon dioxide during cardiopulmonary resuscitation: difference between asphyxial cardiac arrest and ventricular fibrillation/pulseless ventricular tachycardia cardiac arrest. Crit Care 2011; 15:R13

30. Kolar M, Krizmaric M, Klemen P, et al. Partial pressure of end-tidal carbon dioxide successful predicts cardiopulmonary resuscitation in the field: a prospective observational study. Crit Care 2008; 12:R115

31. Andreka P, Frenneaux MP. Haemodynamics of cardiac arrest and resuscitation. Curr Opin Crit Care 2006; 12:198-203

32. Tang W, Weil MH, Sun S, et al: Progressive myocardial dysfunction after cardiac resuscitation. Crit Care Med 1993; 21:1046-1050

33. Povoas HP, Bisera J. Electrocardiographic waveform analysis for predicting the success of defibrillation. Crit Care Med 2000; 28:N210-N211

34. Ristagno G, Tang W, Chang YT, et al. The quality of chest compressions during cardiopulmonary resuscitation overrides importance of timing of defibrillation. Chest 2007; 132:70-75

35. Perkins GD, Ji C, Deakin CD, Quinn T, Nolan JP, Scomparin C, Regan S, Long J, Slowther A, Pocock H, Black JJM, Moore F, Fothergill RT, Rees N, O'Shea L, Docherty M, Gunson I, Han K, Charlton K, Finn J, Petrou S, Stallard N, Gates S, Lall R; PARAMEDIC2 Collaborators. A randomized trial of epinephrine in out-of- hospital cardiac arrest. N Engl J Med. 2018;379:711–721.

36. Neumar RW, Otto CW, Link MS, et al. Part 8: Adult Advanced Cardiovascular Life Support 2010 American Heart Association Guidelines for Cardiopulmonary Resuscitation and Emergency Cardiovascular Care. Circulation 2010; 122;S729-S767

37. Tang W, Weil MH, Gazmuri RJ, et al. Pulmonary ventilation/perfusion defects induced by epinephrine during cardiopulmonary resuscitation. Circulation 1991; 84:2101-2107

38. Nolan JP, Neumar RW, Adrie C, et al. Post-cardiac arrest syndrome: Epidemiology, pathophysiology, treatment, and prognostication A Scientific Statement from the International Liaison Committee on Resuscitation; the American Heart Association Emergency Cardiovascular Care Committee; the Council on Cardiovascular Surgery and Anesthesia; the Council on Cardiopulmonary, Perioperative, and Critical Care; the Council on Clinical Cardiology; the Council on Stroke. Resuscitation 2008; 79:350-379

39. Negovsky VA. The second step in resuscitation: the treatment of the “post-resuscitation disease.” Resuscitation 1972; 1:1–7

40. Adrie C, Adib-Conquy M, Laurent I. Successful cardiopulmonary resuscitation after cardiac arrest as a "sepsis-like" syndrome. Circulation. 2002;106:562-568

41. Adrie C, Laurent I, Monchi M. Postresuscitation disease after cardiac arrest: A sepsis- like syndrome? Curr Opin Crit Care. 2004;10:208-212

42. Hassager Out-of-hospital cardiac arrest: in-hospital intervention strategies. Lancet 2018;391:989-98

43. Johnson NJ, et al. Resuscitation 2019; 135:37-44.

44. Beitler JR, at al. Am J Respir Crit Care Med. 2017;195(9):1198–206.
45. Harmon MBA, et al. Resuscitation. 2018;129:29–36.
46. Olasveengen TM, et al. Circulation 2017;136(23):e424-440.
47. Hillman K, et al. Crit Care Med. 1986;14(7):606-9.

48. Koster RW, et al. European Heart Journal, Volume 38, Issue 40, 21 2017,:3006–3013.

49. Ondruschka et al. Forensic Sci Med Pathol. 2018;14(4):515-525.

50. Cho SH et al. Injury 2013;44(9):1204-1207.

51. Cha et al. Am J Emerg Med 2017;35(1):117-121.

52. Jang Z, et al. J Am Heart Assoc. 2019 Oct;8(19):e012441

53. Liu Z et al, Quant Imaging Med Surg 2018

54. Harukuni I, Bhardwaj A. Mechanisms of brain injury after global cerebral ischemia. *Neurol Clin.* 2006;24:1–21. doi: 10.1016/j.ncl.2005.10.004 21.

55. Greer DM. Mechanisms of injury in hypoxic-ischemic encephalopathy: implications to therapy. *Semin Neurol.* 2006;26:373–379. doi: 10.1055/s-2006-948317

56. Brierley JB, Meldrum BS, Brown AW. The threshold and neuropathology of cerebral ‘‘anoxic-ischemic’’ cell change. Arch Neurol 1973; 29:367-374

57. Taraszewska A, Zelman IB, Ogonowska W, et al. The pattern of irreversible brain changes after cardiac arrest in humans. Folia Neuropathol 2002; 40:133-141

58. BjörklundE,LindbergE,RundgrenM,Cronberg T, Friberg H, Englund E. Ischaemicbrain damage after cardiac arrest and induced hypothermia—a systematic description of selective eosinophilic neuronal death: a neuropathologic study of 23 patients. *Resuscitation.* 2014;85(4):527- 532. doi:10.1016/j.resuscitation.2013.11.022

59. Endisch C, Kenda M, Streitberger KJ, Hypoxic-Ischemic Encephalopathy Evaluated by Brain Autopsy and Neuroprognostication After Cardiac Arrest. JAMA Neurol. Published online July 20, 2020.

60. Björklund E, Lindberg E, Rundgren M, Cronberg T, Friberg H, Englund E. Ischaemic brain damage after cardiac arrest and induced hypothermia—a systematic description of selective

eosinophilic neuronal death: a neuropathologic study of 23 patients. *Resuscitation*. 2014;85(4):527- 532. doi:10.1016/j.resuscitation.2013.11.022

61. Small DL, Morley P, Buchan AM. Biology of ischemic cerebral cell death. Prog Cardiovasc Dis 1999; 42:185–207

62. Fujioka Specific changes in human brain following reperfusion after cardiac arrest. Stroke. 1994;25:2091–2095

63. Changsirivathanathamrong D, Wang Y, Rajbhandari D. Tryptophan metabolism to kynurenine is a potential novel contributor to hypotension in human sepsis. Crit Care Med. 2011;39:2678-2683

64. Darlington LG, Mackay GM, Forrest CM. Altered kynurenine metabolism correlates with infarct volume in stroke. Eur J Neurosci. 2007;26:2211–2221

65. Adams Wilson JR, Morandi A, Girard TD. The association of the kynurenine pathway of tryptophan metabolism with acute brain dysfunction during critical illness. Crit Care Med. 2012;40:835–841

66. Pedersen ER, Svingen GF, Schartum-Hansen H. Urinary excretion of kynurenine and tryptophan, cardiovascular events, and mortality after elective coronary angiography. Heart J. 2013;34:2689–2696

67. Ristagno G, Fries M, Brunelli L. Early kynurenine pathway activation following cardiac arrest in rats, pigs, and humans. Resuscitation. 2013;84:1604–1610

68. Ristagno G, Latini R, Vaahersalo J. FINNRESUSCI Investigators. Early activation of the kynurenine pathway predicts early death and long-term outcome in patients resuscitated from out-of-hospital cardiac arrest. J Am Heart Assoc 2014;4:3

69. Schefold JC, Fritschi N, Fusch G. Influence of core body temperature on Tryptophan metabolism, kynurenines, and estimated IDO activity in critically ill patients receiving target temperature management following cardiac arrest. Resuscitation 2016;107:107– 114

70. Yoshida R, Imanishi J, Oku T. Induction of pulmonary indoleamine 2,3-dioxygenase by interferon. Proc Natl Acad Sci U S A. 1981;78:129-32

71. Werner ER, Hirsch-Kauffmann M, Fuchs D. Interferon-gamma-induced degradation of tryptophan by human cells in vitro. Biol Chem Hoppe Seyler. 1987;368:1407-1412

72. Schwarcz R, Bruno JP, Muchowski PJ. Kynurenines in the mammalian brain: when physiology meets pathology. Nat Rev Neurosci. 2012;13:465-477

73. Heyes MP, Saito K, Crowley JS. Quinolinic acid and

kynurenine pathway metabolism in and non-inflammatory neurological disease. Brain. 1992;115:1249–1273

74. Kita T, Morrison PF, Heyes MP. Effects of systemic and central nervous system localized inflammation on the contributions of metabolic precursors to the L-kynurenine and quinolinic acid pools in brain. J Neurochem. 2002;82:258–268
75. Schwarcz R, Pellicciari R. Manipulation of brain kynurenines: Glial targets, neuronal effects, and clinical opportunities. J Pharmacol Exp Ther. 2002;303:1–10
76. Owe-Young R, Webster NL, Mukhtar M. Kynurenine pathway metabolism in human blood-brain-barrier cells: implications for immune tolerance and neurotoxicity. J Neurochem. 2008;105:1346–1357
77. Wang Y, Liu H, McKenzie G. Kynurenine is an endothelium-derived relaxing factor produced during inflammation. Nat Med. 2010;16:279–285
78. Fazio F, Carrizzo A, Lionetto L. Vasorelaxing Action of the Kynurenine Metabolite, Xanthurenic Acid: The Missing Link in Endotoxin-Induced Hypotension? Front. Pharmacol. 2017;8:214
79. Cambiaghi A, Pinto BB, Brunelli L.Characterization of a metabolomic profile associated with responsiveness to therapy in the acute phase of septic shock. Sci Rep 2017;7:9748
80. Jung ID, Lee MG, Chang JH. Blockade of indoleamine2,3-dioxygenase protects mice against lipopolysaccharide-induced endotoxin shock. J Immunol, 2009, 182:3146–3154

Chapter 2. Cardio-Pulmonary Resuscitation Interventions: Hemodynamic Support.

"LUCAS Versus Manual Chest Compression During Ambulance Transport: A Hemodynamic Study in a Porcine Model of Cardiac Arrest"

Aurora Magliocca, Davide Olivari, Daria De Giorgio, Davide Zani, Martina Manfredi, Antonio Boccardo, Alberto Cucino, Giulia Sala, Giovanni Babini, Laura Ruggeri, Deborah Novelli, Markus B Skrifvars, MD, Bjarne Madsen Hardig, RN, Davide Pravettoni, Lidia Staszewsky, Roberto Latini, Angelo Belloli, Giuseppe Ristagno.

Published: J Am Heart Assoc. 2019;8:e011189. DOI: 10.1161/JAHA.118.011189.

Abstract

Background - Mechanical chest compression (CC) is currently suggested to deliver sustained high-quality CC in a moving ambulance. This study compared the hemodynamic support provided by a mechanical piston device or manual CC during ambulance transport in a porcine model of cardiopulmonary resuscitation.

Methods and Results - In a simulated urban ambulance transport, 16 pigs in cardiac arrest were randomized to 18 minutes of mechanical CC with the LUCAS (n=8) or manual CC (n=8). ECG, arterial and right atrial pressure, together with end-tidal CO2 and transthoracic impedance curve were continuously recorded. Arterial lactate was assessed during cardiopulmonary resuscitation and after resuscitation. During the initial 3 minutes of cardiopulmonary resuscitation, the ambulance was stationary, while then proceeded along a predefined itinerary. When the ambulance was stationary, CC-generated hemodynamics were equivalent in the 2 groups. However, during ambulance transport, arterial and coronary perfusion pressure, and end-tidal CO2 were significantly higher with mechanical CC compared with manual CC (coronary perfusion pressure: 434 versus 18±4 mmHg; end-tidal CO2: 31±2 versus 19±2 mmHg, $P<0.01$ at 18 minutes). During cardiopulmonary resuscitation, arterial lactate was lower with mechanical CC compared with manual CC (6.6±0.4 versus 8.2±0.5 mmol/L, $P<0.01$). During transport, mechanical CC showed greater constancy compared with the manual CC, as represented by a higher CC fraction and a lower transthoracic impedance curve

variability (P<0.01). All animals in the mechanical CC group and 6 (75%) in the manual one were successfully resuscitated.

Conclusions - This model adds evidence in favor of the use of mechanical devices to provide ongoing high-quality CC and tissue perfusion during ambulance transport.

Introduction

Out-of-hospital cardiac arrest is a leading cause of death worldwide (1,2). Despite major efforts to improve outcome, the most recent trials have provided dismal end results with only 3% to 10% of patients surviving to hospital discharge (3-6). Accordingly, prompt cardiopulmonary resuscitation (CPR) is the major determinant of successful resuscitation, (2,7) but its quality heterogeneity may contribute to the variable survival rates reported in different regions (8,9).

During CPR, provision of high-quality chest compression (CC) may re-establish systemic blood flow, achieving and maintaining threshold levels of coronary and cerebral perfusion (2,10,11). Nevertheless, ineffective and frequently interrupted manual CC is often provided even by well-trained rescuers, leading to unsuccessful resuscitative efforts (12-15). The challenge is even greater during transport, a condition characterized by the presence of acceleration, deceleration, and rotational forces that may affect the rescuers' performance (16–19). Thus, high-quality manual CC in the moving ambulance is physically demanding and impractical, and might compromise providers' safety (16,20). For this special circumstance, the use of a

mechanical CPR device, capable to deliver CC consistently, has been suggested as a reasonable alternative to manual CC (16).

However, the above suggestion has been supported only by manikin studies or clinical data on the quality of CPR metrics (18,19,21–24). Indeed, whether mechanical CPR is superior to manual CPR in special situations, such as the moving ambulance, has been highlighted as a knowledge gap in the 2015 International Consensus on Cardiopulmonary Resuscitation and Emergency Cardiovascular Care Science, underlying the urgency to focus research efforts on this field (16).

This experimental study, therefore, sought to directly investigate the hemodynamic support generated by a mechanical piston device or manual CC in a moving ambulance. The hypothesis on whether mechanical CC would improve systemic perfusion compared with manual CC was tested in a preclinical porcine model of out-of-hospital cardiac arrest. The primary aim of the study was to assess if mechanical CC would provide a higher coronary perfusion pressure (CPP) compared with manual CC during ambulance transport. The secondary aim was the comparison of CC quality between the 2 CPR strategies during transport.

Methods

All procedures involving animals and their care were in conformity with national and international laws and policies (Art. 31, D. Lgs n_ 26/2014). Approval of the study was obtained by the institutional review board committee and governmental institution (Ministry of

Health approval no. 979/2017-PR). The data that support the findings of this study are available from the corresponding author upon reasonable request.

Animal Preparation

Sixteen male domestic swine (34±0.5 kg) were fasted the night before the experiments except for free water access. Anesthesia was induced by intramuscular injection of ketamine (20 mg/kg) followed by intravenous administration of propofol (2 mg/kg) and sufentanyl (0.3 μg/kg) through an ear vein access. Anesthesia was maintained with a continuous intravenous infusion of propofol (4-8 mg/kg per hour) and sufentanyl (0.3 μg/kg per hour). A cuffed tracheal tube was placed, and animals were mechanically ventilated (Bellavista 1000, IMT Medical, Switzerland) with a tidal volume of 15 mL/kg, a fraction of inspired oxygen (FiO2) of 0.21, and a positive-end expiratory pressure of 5 cmH2O. Respiratory frequency was adjusted to maintain the end-tidal partial pressure of carbon dioxide (EtCO2) between 35 and 40 mmHg, monitored with an infrared capnometer (LIFEPAK 15 monitor/defibrillator, Physio-Control, WA) (25).

For measurement of aortic pressure, a fluid-filled 7F catheter was advanced from the right femoral artery into the thoracic aorta. For measurements of right atrial pressure, another fluid-filled 7F catheter was advanced from the right femoral vein into the right atrium. Conventional pressure transducers were used and connected to the monitor defibrillator (LIFEPAK 15) (25). For inducing ventricular fibrillation (VF), a 5F pacing catheter was advanced from the right

subclavian vein into the right ventricle (26). The position of all catheters was confirmed by characteristic pressure morphology and/or fluoroscopy. Frontal plane ECG was recorded.

Experimental Procedure

Before inducing cardiac arrest, animals were randomized by the sealed envelope method to receive either mechanical or manual CC. Animals were then placed in a standard clinical ambulance, in use at the veterinarian hospital where the experiments were performed. Baseline measurements were obtained, and VF was electrically induced with 1 to 2 mA alternating current delivered to the endocardium of the right ventricle (26). Mechanical ventilation was discontinued after onset of VF. After 2 minutes of untreated VF, continuous CC with 1 of the 2 strategies, mechanical or manual, was begun and performed for 18 minutes. Mechanical ventilation with a FiO2 of 1.0 (Oxylog, Dr€ager, L€ubeck, Germany) was resumed simultaneously to CC (tidal volume of 500 mL, respiratory rate of 10 breaths/min) (25). Every 5 minutes during CPR, epinephrine (1 mg) was administered via the right atrium, while arterial blood samples were obtained to assess lactate levels. The experimental protocol is summarized in Figure 1.

During the initial 3 minutes of CPR, the ambulance was stationary, and this allowed for a comparison of CC quality and hemodynamics during a basal static condition. In the following 15 minutes, the ambulance proceeded along a predefined itinerary inside the veterinarian university campus and in the surrounding area, simulating a typical urban transportation. The route of the ambulance journey,

together with the total distance traveled and the average speed, were recorded using a GPS-based tracker app (Endomondo Sports Tracker, vers. 18.6.2). Manual CC was provided in accordance to 2015 international CPR guidelines (2). A group composed by the same 4 qualified CPR providers was available for all experiments. During CPR, the rescuers could see the physiologic parameters on the defibrillator monitors, ie, arterial pressure, right atrial pressure, EtCO2, and were allowed to optimize the CPR quality accordingly, while CC rate was guided by the monitor/ defibrillator metronome. Mechanical CC was delivered by the LUCAS 3.0 chest compression system (Stryker/Jolife AB, Lund, Physio-Control, Sweden), which delivers continuous CC (rate: 102±2 per minute; depth: 53±2 mm; duty cycle: 50±5%). The mechanical compressor was already positioned on the animal chest before inducing VF.

Beside the driver and a copilot, the ambulance cabin crew consisted of 2 certified professional rescuers who alternated each other in performing manual CC every 2 minutes, and 1 operator responsible for drug administration and arterial blood sampling. A fourth investigator, seating at the head site, provided continuous timing information to the rescuers and assured compliance to the experimental protocol, without any direct intervention in the resuscitative maneuvers.

After the 18-minute interval of CPR, defibrillation was attempted with a single biphasic 200-joule shock, using a LIFEPAK 15 monitor/defibrillator. Return of spontaneous circulation (ROSC) was defined as the presence of sinus rhythm with a mean arterial pressure of >60 mmHg. If ROSC was not achieved, CPR was resumed and

continued for 1 minute before a subsequent defibrillation with an escalating energy strategy (300-360-j). If VF reoccurred after ROSC, an immediate defibrillation was delivered. The same resuscitation protocol was continued until successful resuscitation or for a maximum of 5 additional minutes.

At the end of the resuscitation maneuvers, a chest computerized tomography was performed with a 16-slices computerized tomography scanner (GE Brightspeed, GE Healthcare, Italy) to evaluate rib fractures and other major CPR-related injuries. Animals were then returned in the operating room, where they were monitored for an additional 3 hours, under anesthesia. Catheters were then removed, wounds were repaired, and the animals were extubated and returned to their cages. Analgesia with butorphanol (0.1 mg/kg) was administered by intramuscular injection. At the end of the 72-hour post resuscitation observation, animals were reanesthetized for echocardiographic examination and blood sample withdrawn. Animals were then euthanized painlessly with an intravenous injection of 150 mg/kg sodium thiopental.

Measurements

ECG, hemodynamics (arterial and right atrial pressures), EtCO2, and esophageal temperature were continuously recorded with 2 LIFEPAK 15 monitor/defibrillators. All data were then stored on CODE-STAT 9.0 (Physio-Control, WA) and subsequently exported as comma separated values (.csv) to LabChart 8.0 (ADInstruments, UK) for the analysis. The coronary perfusion pressure (CPP) was computed from

the differences in time-coincident diastolic aortic pressure and right atrial pressure (25,26).

Transthoracic echocardiography was performed using a phase-array multifrequency 2.5- to 5-MHz probe (CX50, Philips, The Netherlands). Two-dimensional apical 4 chamber view was acquired to determine left ventricular volumes and ejection fraction calculations were computed using the modified single-plane Simpson's rule (25). Cardiac output (CO) was determined as the product of the time-velocity integral of the outflow curves (VTI) obtained in 5-chamber apical view using pulsed wave Doppler, the cross sectional area of the left ventricular outflow tract (LVOT) obtained from 2-dimensional echocardiography image in parasternal long-axis view and heart rate (HR) [CO=VTIxLVOTxHR].

CC rate, CCs delivered per minute, and CC fraction (CCF) were calculated using the CODE-STAT 9.0 CPR quality assessment tool, which uses the information derived from the transthoracic impedance (TTI). CC quality was additionally evaluated measuring the total power from the power spectral density analysis of the TTI curve after Fast Fourier Transformation (LabChart 8.0, ADInstrumets, UK) (27). This served as a measure of variability in CC consistency (CC-generated thoracic impedance (Impcc) variability).

CC providers' fatigue at the end of the resuscitative maneuvers and their perception on the feasibility of CC provision during ambulance transport, intended as practicability and safety of the intervention, were evaluated using a score on a 10-point scale from 0 (no fatigue or intervention 100% feasible) to 10 (maximal physical effort or intervention 100% impractical).

Arterial blood gases were assessed with i-STAT System (Abbott Laboratories, Princeton, NJ). Plasma high-sensitivity cardiac troponin T and serum neuron-specific enolase (NSE) were measured with electrochemiluminescence assays (Roche Diagnostics, Italy) (25).
Functional recovery was evaluated before euthanasia according to overall performance categories as follows: 1=normal; 2=slight disability; 3=severe disability; 4=coma; and 5=brain death or death (25). Scores were assessed by veterinarian doctors masked to group treatment.

Statistical Analysis

Shapiro–Wilk test was used to confirm normal distribution of the data. Continuous variables are reported as mean±SEM or median with interquartiles [Q1–Q3], as appropriate. Categorical variables were described as count and proportion (%). For comparisons between time-based measurements within the 2 groups, repeated-measures analysis of variance was used. In the case of a significant test result, a post-hoc analysis was performed using the Fisher Least Significant Difference (LSD) test. For comparisons between groups at the given time points, 1-way analysis of variance was used. Non-parametric Mann-Whitney U test was used for variables not normally distributed. When the dependent variable was categorical, a Fisher exact test was used. A $P<0.05$ (2-tailed) was regarded as statistically significant. GraphPad Prism 7.0 (GraphPad Software Inc., La Jolla, CA) was used for statistical analyses.

The sample size was estimated on the mean CPP. Using CPP values from a previous study, (25) (38.5±13.7 mmHg after 5 minutes of mechanical CC), and assuming a 50% reduction in the manual CC group during transport compared with the mechanical CC, 8 animals per group would be needed to have a power=0.8 (a=0.05, 2-sided).

Results

No significant differences in body weight, hemodynamics, EtCO2, cardiac function, arterial blood gases, and temperature were observed between the 2 groups at baseline (Table 1). No differences in the total distance traveled and average speed were noted between the 2 groups, as detailed in Table 2.

Hemodynamics During CPR

During the initial 3 minutes of CC, performed in the static condition, CPP was equivalent in the 2 groups. However, coincident with the onset of the ambulance movement and throughout the whole transport period, CPP was significantly higher in the mechanical CC group compared with the manual one ($P<0.01$, Figure 2).

Similarly, EtCO2, systolic and diastolic arterial pressures were not different in the 2 groups during the static condition, while they were significantly higher in the mechanical CC compared with the manual one during ambulance transport ($P<0.01$, Figures 2 and 3). Right atrial pressure, instead, significantly increased in the manual CC group compared with the mechanical one during transport ($P<0.01$, Figure 3).

Arterial lactate showed a significantly greater increase in the manual CC group compared with mechanical one during the whole CPR period (P<0.01, Figure 2).

No differences in post-resuscitation hemodynamics and arterial lactate were observed between the 2 groups (Figures 2 and 3). CPR Quality and Feasibility During Transport

Data on CPR quality and feasibility are summarized in Table 2. CC rate was similar in the 2 groups during the overall duration of CPR and complied with current guidelines recommendations.2 Nevertheless, CC rate was constant at 102 per minute in the mechanical CC group, while it slightly varied in the manual one over time (P<0.01 versus LUCAS CC). The number of CCs delivered per minute and the CCF were overall significantly higher in the mechanical CC group compared with the manual one during ambulance transport. CC was more consistent in the mechanical CC group compared with the manual one during the whole period of CPR, as represented by a significantly lower variability in the CC-generated TTI curve with the use of LUCAS 3 (P<0.01 versus manual CC, Table 2). More specifically, Impcc variability was similar between the 2 groups during the static condition, while it was >4-fold greater in the manual CC group compared with the mechanical one during transport (P<0.01, Figure 4). CPR providers described the manual CC during ambulance transport as significantly more physically exhausting (P<0.01) and less feasible (P<0.01) compared with the mechanical CC (Table 2).

CPR Outcome and Survival

All 8 (100%) animals in the mechanical CC group and 6 (75%) in the manual one achieved ROSC (P=0.47, Table 3). Only a single defibrillation attempt was required before ROSC in the mechanical CC group compared with almost 2 in the manual one (P=0.06, Table 3).

No differences in body temperature at ROSC and after resuscitation and in the total number of fractured ribs were observed between the 2 groups (Table 3).

All the resuscitated animals survived for 72 hours with a complete neurological recovery, except 1 in the mechanical CC group, which died 4 hours after resuscitation as a consequence of a hypertensive pneumothorax occurring during the transfer back to the cage (Table 3). No differences in post-resuscitation arterial blood gases (Table 4), myocardial function, assessed by left ventricular ejection fraction and CO, and plasma levels of NSE and high-sensitivity cardiac troponin T were observed between the 2 groups (Table 3). Nevertheless, in the early post-resuscitation period, a consistently lower high-sensitivity cardiac troponin T accompanied by a better ejection fraction and a lesser increased left ventricular end-systolic volume was observed in animals subjected to mechanical CC compared with those that received manual CC (Table 3).

Discussion

To our knowledge, this is the first investigation describing and comparing the hemodynamic support generated by a piston- based mechanical CC versus manual CC during ambulance transport in an

experimental model of cardiac arrest and CPR. This randomized, animal study demonstrated that mechanical CC allowed for a significantly greater systemic perfusion during transport, as represented by higher CPP, EtCO2, arterial pressure, and better tissue oxygenation evident with lower arterial lactate, compared with manual CC. During ambulance transport, the use of a mechanical piston compression device also accounted for better CC quality, with a lesser rescuer's physical effort requirements, compared with manual compression.

Coronary perfusion pressure is the main determinant of myocardial blood flow and threshold levels of CPP have been identified as leading predictors of CPR success (7,10,28,29). Indeed, maintaining a CPP >20 mmHg has been shown to increase the likelihood of ROSC and survival in both preclinical and clinical studies (7,29–31). In the present study, a CPP % 20 mmHg was achieved in the manual CC group, but >2-fold greater values were observed during mechanical CC. CPP generated during CPR have been shown to be directly related to the quality of CC and more specifically to the depth (10,32). In this study, the quality of compression, derived from the TTI signal was suboptimal in the manual CC compared with the mechanical one during transport. This might have been likely associated with provision of CC with shallow depth, as previously reported in manikin studies (22,33). Moreover, right atrial pressure significantly increased during ambulance transport in the manual group compared with the mechanical one, accounting for the lower CPP. Higher right atrial pressure in the manual CC group might have been the consequence of the suboptimal CC quality provided, which produced low CO and

forward blood flow. A possible rescuers' leaning on the animal chest to warrant a stable position against the vehicle's movements might be another valid explanation (22,23,34).

Similarly, capnography is another valuable tool to monitor the physiological effects of CPR, as it reflects pulmonary blood flow and indirectly the CC-generated CO (7,10,35). During prolonged CPR, failure to achieve an EtCO2 >10-15 mmHg has shown a strong correlation with unsuccessful resuscitation (35–37). In this study, EtCO2 achieved the above thresholds, nevertheless, it was consistently higher in the mechanical CC group compared with the manual one during transport, anticipating a greater effectiveness of CC delivered mechanically (10,38,39). Somewhat surprising, during the static condition no differences in CPP, EtCO2, and hemodynamics were detected between the 2 groups, indicating a manual CC of high quality, comparable with that of the mechanical piston device. During transport, however, the use of the LUCAS provided a constant and reliable CC performance, which resulted in a higher perfusion and lesser increase in arterial lactate. The sharper increases in arterial pressure after each epinephrine administration in the mechanical CC group in contrast to the blunted response in the manual CC provides additional evidence of the better hemodynamic support generated by mechanical CC during transport (40).

Adequate CC rate and CCF during CPR have been demonstrated to be associated with greater likelihood of ROSC and survival after cardiac arrest (2,13,14). Thus, a CC rate between 100 and 120 per minute and a CCF of at least 60% 2 have been recommended. In this study, the mechanical piston device worked constantly, with a CC rate

consistently stable at 102 per minute, with no variance, both in static condition and during ambulance transport. In the manual group, the CC rate fully complied with current guidelines but showed a greater variance, similarly to what has been previously reported on manikins (22,23,41,42). In 4 pigs, mechanical CC needed to be interrupted immediately after onset of CPR to allow for LUCAS repositioning on the chest and this explains the unexpected lower CCF compared with the manual CC group noted during the static condition. The high CC quality, in terms of CC rate and fraction, in the manual group was likely achieved because of the presence of the metronome guide provided by the defibrillator. With this feedback, rescuers were able to compress the chest with the correct rate, even under the difficult condition created by the moving ambulance.

Deterioration of the manual CC consistency during transport has been recognized to be strongly influenced by the ambulance movements (23). Indeed, it has been reported that sudden changes in the ambulance speed may increase vibrations and induce rescuer's unnecessary movements that potentially impact on CC depth and rate, and on forces applied on the patient's chest (41). Moreover, the transport- generated external forces, ie, acceleration, deceleration, centrifugal forces in curves, have been shown to make manual CC physically more demanding and less effective (22). In a moving ambulance, maintaining the standard 2-handed CC technique has been also reported to be not feasible for the majority of the transport time, since providers are usually forced to perform CC with 1 hand, and the other to support themselves (43). Average speed in our study was similar in both groups as was the ambulance itinerary. However, in the

animals resuscitated manually, episodes of shallow CC, leaning, altered duty cycles and compression technique, 1-handed CC, and not correct hands position on the chest, were present. In contrast, transport seemed to have no effects on mechanical device performance, which remained stable and independent from motion influences throughout the whole ambulance journey.

Furthermore, delivery of manual CC in a moving ambulance has been described as physically exhausting, not easily reproducible, and potentially unsafe by the CPR team involved in this study. Indeed, CC performed during transport by an unrestrained provider has been considered as a hazardous situation, potentially dangerous for both the provider and the patient, and for this the mechanical devices have been suggested since they may allow providers to remain seated and restrained while CC is delivered (16,23,42,44). In our study, there were no injuries, however in several instances during the transport, the rescuer's stable position was compromised and falls or nearby falls occurred, worsening the CPR quality. Moreover, additional risks for the CC provider might come from the distraction attributable to focusing on CC, and unexpected movements of the ambulance (22). Besides providing consistent high-quality CC, mechanical compression devices might therefore significantly reduce the above described risks and improve ambulance safety practices.

This study has several strengths. The investigation provides evidence of hemodynamics generated and maintained in a moving vehicle by both a mechanical piston device and manual CC. A great effort was done to reproduce a real clinical scenario of ambulance transport with ongoing CPR in an urban area, ie, a clinical ambulance with human

medical equipment and professional rescuers were used. The study results add evidence to the current knowledge gap on mechanical CPR devices as claimed in the 2015 International Consensus on CPR (16).

Limitations

Some limitations deserve to be mentioned. The studies were conducted in healthy anesthetized animals and therefore in the absence of underlying diseases or injuries that are causative of cardiac arrest and with potential anesthesia- related effects. Secondly, the time of untreated VF was relatively short, ie, 2 minutes, to be comparable with a real out-of-hospital cardiac arrest scenario and to account for a relevant myocardial ischemia (45.) Nevertheless, the aim of the study was to investigate the hemodynamics during CPR in a moving ambulance, while effects on survival or long-term outcome will be assessed in future studies using more clinically relevant durations of no-flow (46). Thirdly, CC depth was not assessed, and thus the impact of transport on this CPR parameter can be only speculated based on the TTI signal and CPP. However, data on CC depth have been already reported in earlier studies performed on manikins, whereas no data on hemodynamics have been present yet. Fourthly, our rescuer team was well trained for the task requested by the experimental protocol and could optimize the CC performance based on the resulting arterial pressure and EtCO2 monitored on the defibrillators. Thus, it is likely that a CC with a quality superior than current standard has been delivered. Nevertheless, effects on hemodynamics were still not comparable with those from the LUCAS device during

transport. Moreover, in accordance to what was reported in the clinical scenario, (43) frequently CC providers had to perform 1-handed CC, using the other hand to support themselves and prevent accidental falls because of transport-generated external forces (22,41). In these instances, the 1-handed CC technique remains the only option to perform CC with minimal interruptions, in the absence of devices specifically designed to stabilize the provider in a moving ambulance (47). Accordingly, the efficacy of the 1-handed CC technique compared with the standard 2-handed approach needs future investigations. Finally, rescuers focused only on providing uninterrupted CC with no need for delivering bag ventilation because animals were mechanically ventilated. However, the use of a standardized mechanical ventilation in both groups allowed for an unbiased comparison of EtCO2 between the 2 CPR strategies.

Conclusions

In this preclinical model of CPR performed in a moving ambulance, a piston-based mechanical CC allowed for a significantly greater hemodynamic support and systemic perfusion, as represented by higher CPP, EtCO2, and arterial pressure, and lower arterial lactate, compared with manual CC. Mechanical CC accounted also for a better CC quality, with a lesser rescuer's physical effort requirements, compared with manual compression. This study provides evidence to suggest and encourage the use of mechanical devices during ambulance transport to assure ongoing high-quality CC, tissue perfusion, and rescuers' safety.

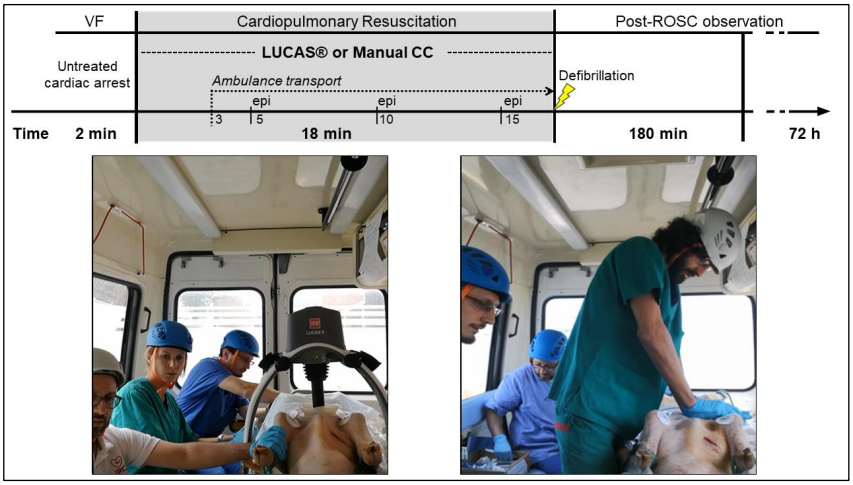

Figure 1. On the top: a flowchart of the study protocol. On the bottom: a view of the ambulance cabin with an ongoing mechanical chest compression (CC) on the left and manual CC on right. VF, ventricular fibrillation; ROSC, return of spontaneous circulation; epi, epinephrine administration.

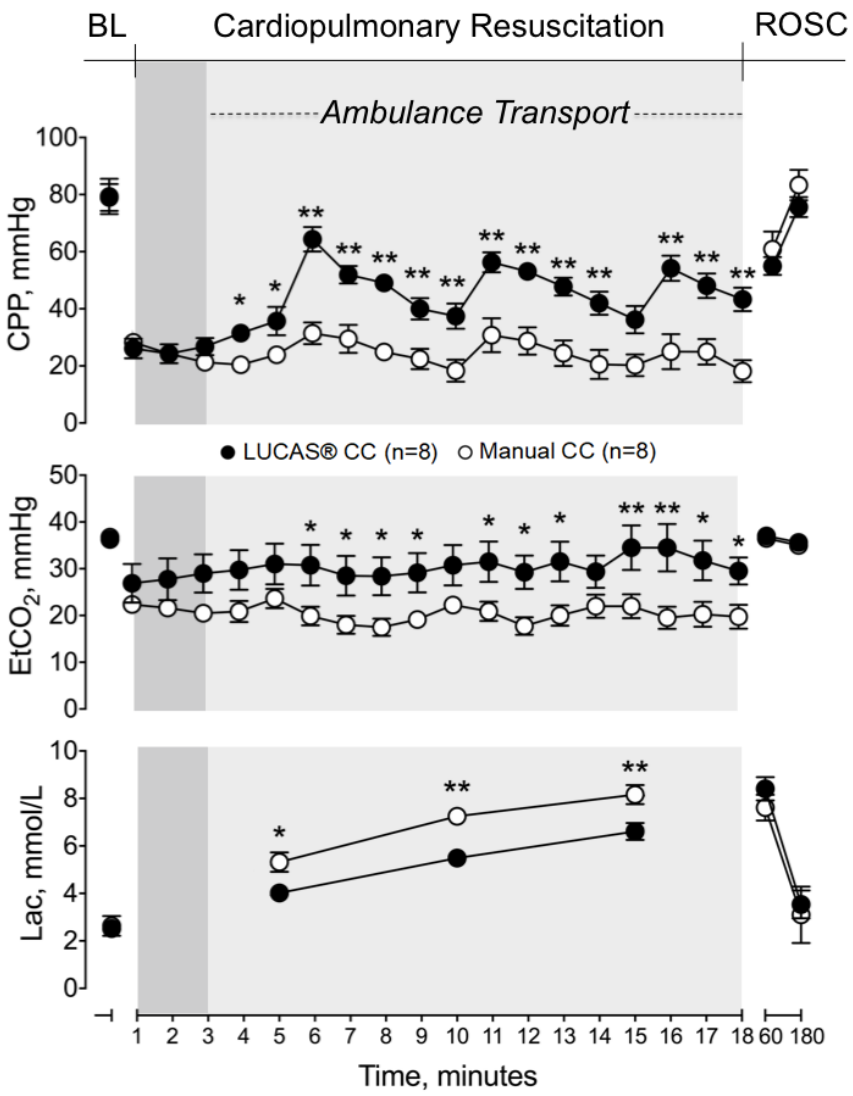

Figure 2. Coronary perfusion pressure (CPP), end tidal CO2 (EtCO2), and arterial lactate levels (Lac) at baseline (BL), during cardiopulmonary resuscitation, and after return of spontaneous circulation (ROSC).

* p<0.05, **p<0.01 versus manual chest compression.

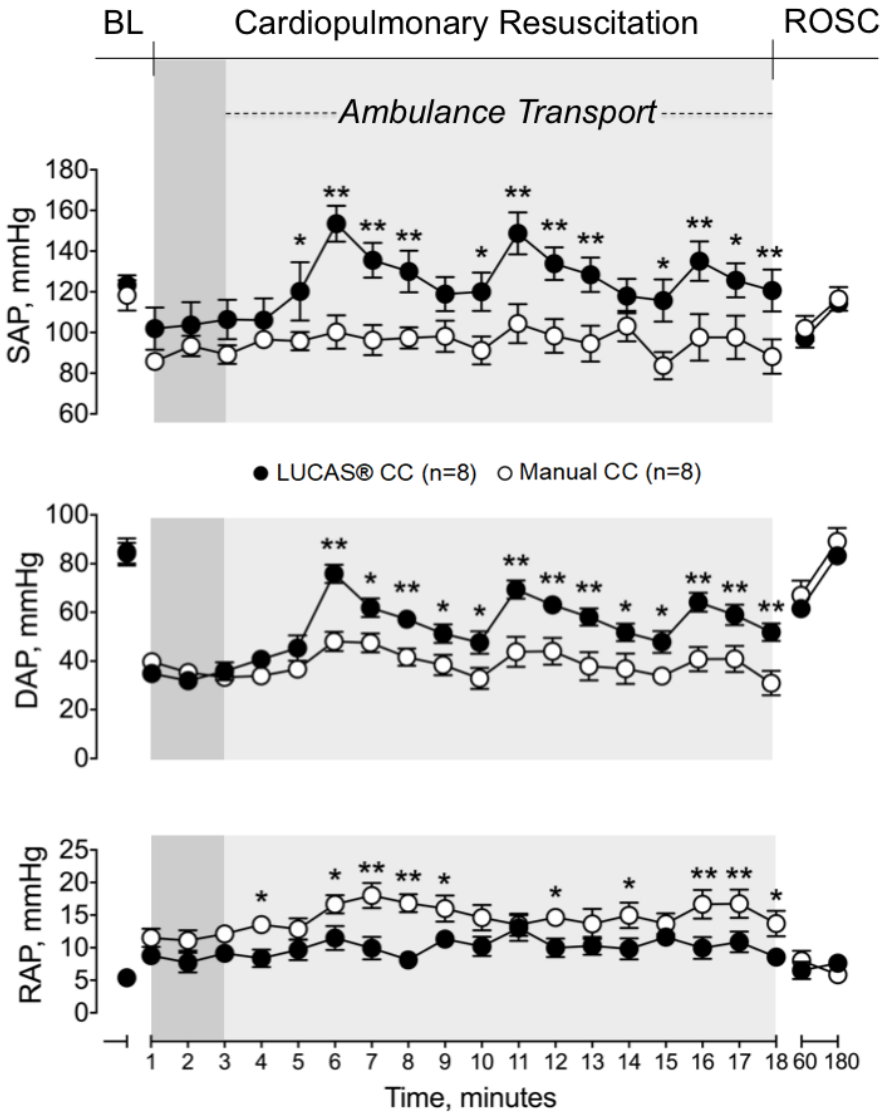

Figure 3. Systolic (SAP) and diastolic (DAP) arterial pressure, and right atrial pressure (RAP) at baseline (BL), during cardiopulmonary resuscitation, and after return of spontaneous circulation (ROSC). * $p<0.05$, **$p<0.01$ versus manual chest compression.

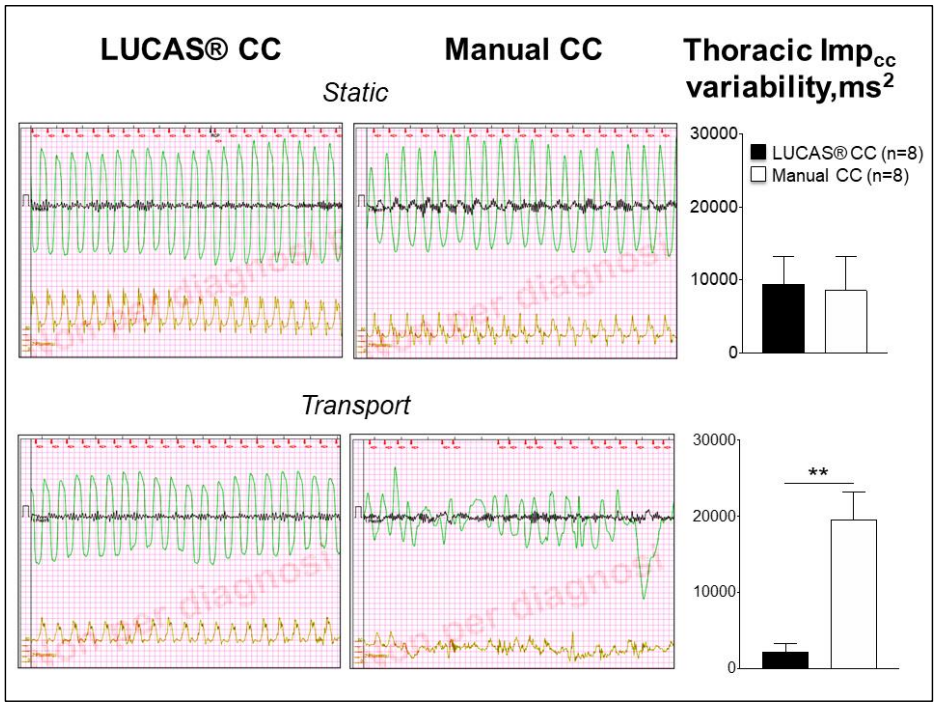

Figure 4. LUCAS® (on the left) and manual (on the right) chest compression-generated transthoracic impedance signal (in green) and corresponding arterial pressure (in orange) during cardiopulmonary resuscitation performed in static condition (on the top) and in the moving ambulance (on the bottom).

The graphs on the right represent the transthoracic impedance variability in the LUCAS® in the manual chest compression during the static condition (on the top) and the ambulance transport (on the bottom).

**$p<0.01$ versus manual chest compression.

Table 1. Baseline characteristics

	LUCAS (n=8)	Manual (n=8)
Body weight, Kg	35±1	34±1
Heart rate, bpm	79±6	83±8
Systolic arterial pressure, mmHg	123±5	118±8
Diastolic arterial pressure, mmHg	85±6	84±4
Right atrial pressure, mmHg	5±1	5±1
End-tidal CO_2, mmHg	36±1	37±1
pH	7.44±0.02	7.44±0.01
Arterial oxygen partial pressure, mmHg	86±4	80±3
Arterial carbon dioxide partial pressure, mmHg	36±1	37±1
Arterial oxygen saturation, %	97±1	96±1
Arterial bicarbonate, mmol/L	25±2	25±1
Arterial base excess, mmol/L	1±2	1±1
Left ventricular ejection fraction, %	67±3	69±4
Left ventricular end-diastolic volume, mL	30±3	27±2
Left ventricular end-systolic volume, mL	10±1	8±1
hs-cTnT, pg/mL	6 [3–8]	8 [6–9]
Temperature, °C	36.7±0.3	37.2±0.2

Data are reported in mean±SEM, except for hs-cTnT and NSE that are expressed as median [interquartile range]. hs-cTnT indicates highsensitivity cardiac troponin T; NSE, neuron-specific enolase.

Table 2. Ambulance Itinerary and Cardiopulmonary Resuscitation Quality

	LUCAS CC (n=8)	Manual CC (n=8)
Transport distance, km	7.8±0.4	8.6±0.5
Ambulance average speed, km/h	26.0±2	28.5±2
CC rate, n		
Total CPR duration	102 [102–102]	103 [101– 104]
Static	102 [102–102]*	101 [100–101]
Transport	102 [102–102]†	103 [102–105]
CC delivered per min, n		
Total CPR duration	101 [100–102]†	97 [93–99]
Static	97 [96–102]	100 [99–101]
Transport	102 [100–102]†	97 [92–99]
CCF, %		
Total CPR duration	99 [98–100]	98 [98–99]
Static	96 [95–100]†	100 [100–100]
Transport	100 [99–100]†	98 [97–99]
Imp_{cc} variability, ms^2	2854 [1035–4584]*	16 068 [13 240–19 446]
Fatigue, score	1.2±0.3*	8.8±0.3
Feasibility, score	9.1±0.3*	3.7±0.6

Data are reported as mean±SEM or median [interquartile range]. CC indicates chest compression; CCF, chest compression fraction; CPR, cardiopulmonary resuscitation; Imp, impedance. *P<0.01 vs manual; †P<0.05.

Table 3. CPR Outcomes

	LUCAS (n=8)	Manual (n=8)
ROSC, n (%)	8/8 (100)	6/8 (75)
Defibrillations to first ROSC, n	1±0	1.8±0.4
Defibrillations to final resuscitation, n	1.8±0.4	2.5±0.6
CPR duration, min	18±0	18.7±0.4
Rib fractures, n	5±1	5±1
72-h survival, n (%)	7/8 (88)	6/6 (100)
72-h OPC, score	1.5±0.5	1±0
HR, bpm		
PR 60 min	136±14	148±7
PR 120 min	125±14	114±8
PR 180 min	120±13	111±7
Temperature, °C		
ROSC	36.9±0.2	37.2±0.2
PR 60 min	36.4±0.3	36.6±0.4
PR 120 min	36.4±0.3	36.4±0.3
PR 180 min	36.4±0.3	36.3±0.3
CO, L/min		
PR 180 min	2.6±0.2	2.9±0.2
PR 72 h	4.1±0.4	3.6±0.5
EF, %		
PR 180 min	60±4	53±12
PR 72 h	76±2	77±2
EDV, mL		
PR 180 min	31±5	33±4
PR 72 h	38±5	37±2
ESV, mL		
PR 180 min	13±4	17±6
PR 72 h	9±2	9±1
hs-cTnT, pg/mL		
PR 180 min	210 [91–619]	562 [381–687]
PR 72 h	38 [21–80]	41 [12–144]
72-h NSE, ng/mL	0.18 [0.06–0.25]	0.16 [0.05–0.37]

Table 3. CPR Outcomes

Data are reported as mean±SEM, except for hs-cTnT and NSE that are expressed as median [interquartile range]. CO indicates cardiac output; CPR, cardiopulmonary resuscitation; EDV, left ventricular end-diastolic volume; EF, left ventricular ejection fraction; ESV, left ventricular end-systolic volume; HR, heart rate; hs-cTnT, high-sensitivity cardiac troponin T; NSE, neuron-specific enolase; OPC, overall performance category; PR, post resuscitation; ROSC, return of spontaneous circulation.

Table 4. Post-Resuscitation Arterial Blood Gas Analyses

	LUCAS (n=8)	Manual (n=8)
pH		
PR 60 min	7.27±0.02	7.28±0.01
PR 180 min	7.40±0.01	7.41±0.02
PaO_2, mmHg		
PR 60 min	99±12	126±6
PR 180 min	117±11	136±3
$PaCO_2$, mmHg		
PR 60 min	44±2	44±3
PR 180 min	43±1	42±2
SpO_2, %		
PR 60 min	94±2	98±0
PR 180 min	98±1	99±0
HCO_3, mmol/L		
PR 60 min	20±1	20±1
PR 180 min	26±0	27±1
BE, mmol/L		
PR 60 min	−7±1	−6±1
PR 180 min	2±1	2±1

Data are reported as mean±SEM. BE indicates base excess; HCO3, bicarbonate; PaCO2; arterial carbon dioxide partial pressure; PaO2; arterial oxygen partial pressure; PR, post- resuscitation; SpO2, arterial oxygen saturation.

References

1. Benjamin EJ, Virani SS, Callaway CW, Chamberlain AM, Chang AR, Cheng S, Chiuve SE, Cushman M, Delling FN, Deo R, de Ferranti SD, Ferguson JF, Fornage M, Gillespie C, Isasi CR, Jim_enez MC, Jordan LC, Judd SE, Lackland D, Lichtman JH, Lisabeth L, Liu S, Longenecker CT, Lutsey PL, Mackey JS, Matchar DB, Matsushita K, Mussolino ME, Nasir K, O'Flaherty M, Palaniappan LP, Pandey A, Pandey DK, Reeves MJ, Ritchey MD, Rodriguez CJ, Roth GA, Rosamond WD, Sampson UKA, Satou GM, Shah SH, Spartano NL, Tirschwell DL, Tsao CW, Voeks JH, Willey JZ, Wilkins JT, Wu JH, Alger HM, Wong SS, Muntner P; American Heart Association Council on Epidemiology and Prevention Statistics Committee and Stroke Statistics Subcommittee. Heart Disease and Stroke Statistics-2018 Update: a report from the American Heart Association. Circulation. 2018;137:e67–e492.
2. Perkins GD, Handley AJ, Koster RW, Castr_en M, Smyth MA, Olasveengen T, Monsieurs KG, Raffay V, Gr€asner JT, Wenzel V, Ristagno G, Soar J; Adult basic life support and automated external defibrillation section Collaborators. European Resuscitation Council Guidelines for Resuscitation 2015: Section 2. Adult basic life support and automated external defibrillation. Resuscitation. 2015;95:81–99.
3. Perkins GD, Ji C, Deakin CD, Quinn T, Nolan JP, Scomparin C, Regan S, Long J, Slowther A, Pocock H, Black JJM, Moore

F, Fothergill RT, Rees N, O'Shea L, Docherty M, Gunson I, Han K, Charlton K, Finn J, Petrou S, Stallard N, Gates S, Lall R; PARAMEDIC2 Collaborators. A randomized trial of epinephrine in out-of- hospital cardiac arrest. N Engl J Med. 2018;379:711–721.

4. Benger JR, Kirby K, Black S, Brett SJ, Clout M, Lazaroo MJ, Nolan JP, Reeves BC, Robinson M, Scott LJ, Smartt H, South A, Stokes EA, Taylor J, Thomas M, Voss S, Wordsworth S, Rogers CA. Effect of a strategy of a supraglottic airway device vs tracheal intubation during out-of-hospital cardiac arrest on functional outcome: the AIRWAYS-2 Randomized Clinical trial. JAMA. 2018;320:779– 791.
5. Wang HE, Schmicker RH, Daya MR, Stephens SW, Idris AH, Carlson JN, Colella MR, Herren H, Hansen M, Richmond NJ, Puyana JCJ, Aufderheide TP, Gray RE, Gray PC, Verkest M, Owens PC, Brienza AM, Sternig KJ, May SJ, Sopko GR, Weisfeldt ML, Nichol G. Effect of a strategy of initial laryngeal tube insertion vs endotracheal intubation on 72-hour survival in adults with out-of-hospital cardiac arrest: a randomized clinical trial. JAMA. 2018;320:769–778.
6. Soar J, Nolan JP, B€ottiger BW, Perkins GD, Lott C, Carli P, Pellis T, Sandroni C, Skrifvars MB, Smith GB, Sunde K, Deakin CD; Adult advanced life support section Collaborators. European resuscitation council guidelines for resusci- tation 2015 section 3. Adult advanced life support. Resuscitation. 2015;95:100–147.
7. Aufderheide TP, Frascone RJ, Wayne MA, Mahoney BD,

Swor RA, Domeier RM, Olinger ML, Holcomb RG, Tupper DE, Yannopoulos D, Lurie KG. Standard cardiopulmonary resuscitation versus active compression-decompression cardiopulmonary resuscitation with augmentation of negative intrathoracic pressure for out-of-hospital cardiac arrest: a randomised trial. Lancet. 2011;377:301–311.

8. Okubo M, Schmicker RH, Wallace DJ, Idris AH, Nichol G, Austin MA, Grunau B, Wittwer LK, Richmond N, Morrison LJ, Kurz MC, Cheskes S, Kudenchuk PJ, Zive DM, Aufderheide TP, Wang HE, Herren H, Vaillancourt C, Davis DP, Vilke GM, Scheuermeyer FX, Weisfeldt ML, Elmer J, Colella R, Callaway CW; Resuscitation Outcomes Consortium Investigators. Variation in survival after out-of-hospital cardiac arrest between emergency medical services agencies. JAMA Cardiol. 2018;3:989–999.
9. Grasner JT, Lefering R, Koster RW, Masterson S, B€ottiger BW, Herlitz J, Wnent J, Tjelmeland IB, Ortiz FR, Maurer H, Baubin M, Mols P, Hadzibegovi_c I, Ioannides M, Skulec R, Wissenberg M, Salo A, Hubert H, Nikolaou NI, L_oczi G, Svavarsd_ottir H, Semeraro F, Wright PJ, Clarens C, Pijls R, Cebula G, Correia VG, Cimpoesu D, Raffay V, Trenkler S, Markota A, Str€oms€oe A, Burkart R, Perkins GD, Bossaert LL; EuReCa ONE Collaborators. EuReCa ONE-27 Nations, ONE Europe, ONE Registry: a prospective one month analysis of out-of- hospital cardiac arrest outcomes in 27 countries in Europe. Resuscitation. 2016;105:188–195.
10. Ristagno G, Tang W, Chang YT, Jorgenson DB, Russell JK,

Huang L, Wang T, Sun S, Weil MH. The quality of chest compressions during cardiopulmonary resuscitation overrides importance of timing of defibrillation. Chest. 2007;132:70–75.

11. Klouche K, Weil MH, Sun S, Tang W, Povoas H, Bisera J. Stroke volumes generated by precordial compression during cardiac resuscitation. Crit Care Med. 2002;30:2626–2631.
12. Wik L, Kramer-Johansen J, Myklebust H, Sørebø H, Svensson L, Fellows B, Steen PA. Quality of cardiopulmonary resuscitation during out-of-hospital cardiac arrest. JAMA. 2005;293:299–304.
13. Idris AH, Guffey D, Aufderheide TP, Brown S, Morrison LJ, Nichols P, Powell J, Daya M, Bigham BL, Atkins DL, Berg R, Davis D, Stiell I, Sopko G, Nichol G; Resuscitation Outcomes Consortium (ROC) Investigators. Relationship between chest compression rates and outcomes from cardiac arrest. Circulation. 2012;125:3004–3012.
14. Christenson J, Andrusiek D, Everson-Stewart S, Kudenchuk P, Hostler D, Powell J, Callaway CW, Bishop D, Vaillancourt C, Davis D, Aufderheide TP, Idris A, Stouffer JA, Stiell I, Berg R; Resuscitation Outcomes Consortium Investi- gators. Chest compression fraction determines survival in patients with out-of- hospital ventricular fibrillation. Circulation. 2009;120:1241–1247.
15. Perkins GD, Travers AH, Berg RA, Castren M, Considine J, Escalante R, Gazmuri RJ, Koster RW, Lim SH, Nation KJ, Olasveengen TM, Sakamoto T, Sayre MR, Sierra A, Smyth MA, Stanton D, Vaillancourt C; Basic Life Support Chapter

Collaborators. Part 3: adult basic life support and automated external defibrillation 2015 International Consensus on Cardiopulmonary Resuscitation and Emergency Cardiovascular Care Science with Treatment Recommendations. Resuscitation. 2015;95:e43–e69.

16. Callaway CW, Soar J, Aibiki M, B€ottiger BW, Brooks SC, Deakin CD, Donnino MW, Drajer S, Kloeck W, Morley PT, Morrison LJ, Neumar RW, Nicholson TC, Nolan JP, Okada K, O'Neil BJ, Paiva EF, Parr MJ, Wang TL, Witt J; Advanced Life Support Chapter Collaborators. Part 4: advanced life support: 2015 interna- tional consensus on cardiopulmonary resuscitation and emergency cardio- vascular care science with treatment recommendations. Circulation. 2015;132:S84–S145.
17. Russi CS, Myers LA, Kolb LJ, Lohse CM, Hess EP, White RD. Comparison of chest compression quality delivered during on-scene and ground transport cardiopulmonary resuscitation. West J Emerg Med. 2016;17:634–639.
18. Olasveengen TM, Wik L, Steen PA. Quality of cardiopulmonary resuscitation before and during transport in out-of-hospital cardiac arrest. Resuscitation. 2008;76:185–190.
19. Sunde K, Wik L, Steen PA. Quality of mechanical, manual standard and active compression-decompression CPR on the arrest site and during transport in a manikin model. Resuscitation. 1997;34:235–242.
20. Lattery DE, Silver A. The hazards of providing care in emergency vehicles: an opportunity for reform. Prehospital Emerg Care. 2009;13:388–397.

21. Cheskes S, Byers A, Zhan C, Verbeek PR, Ko D, Drennan IR, Buick JE, Brooks SC, Lin S, Taher A, Morrison LJ; Rescu Epistry Investigators. CPR quality during out-of-hospital cardiac arrest transport. Resuscitation. 2017;114:34–39.
22. Fox J, Fiechter R, Gerstl P, Url A, Wagner H, L€uscher TF, Eriksson U, Wyss CA. Mechanical versus manual chest compression CPR under ground ambulance transport conditions. Acute Card Care. 2013;15:1–6.
23. Gassler H, Ventzke MM, Lampl L, Helm M. Transport with ongoing resuscitation: a comparison between manual and mechanical compression. Emerg Med J. 2013;30:589–592.
24. Kim TH, Shin SD, Song KJ, Hong KJ, Ro YS, Song SW, Kim CH. Chest compression fraction between mechanical compressions on a reducible stretcher and manual compressions on a standard stretcher during transport in out-of-hospital cardiac arrests: the Ambulance Stretcher Innovation of Asian Cardiopulmonary Resuscitation (ASIA-CPR) pilot trial. Prehosp Emerg Care. 2017;21:636–644.
25. Ristagno G, Fumagalli F, Russo I, Tantillo S, Zani DD, Locatelli V, De Maglie M, Novelli D, Staszewsky L, Vago T, Belloli A, Di Giancamillo M, Fries M, Masson S, Scanziani E, Latini R. Postresuscitation treatment with argon improves early neurological recovery in a porcine model of cardiac arrest. Shock. 2014;41:72–78.
26. Ristagno G, Castillo C, Tang W, Sun S, Bisera J, Weil MH. Miniaturized mechanical chest compressor: a new option for cardiopulmonary resuscita- tion. Resuscitation. 2008;76:191–

197.

27. Li Y, Ristagno G, Guan J, Barbut D, Bisera J, Weil MH, Tang W. Preserved heart rate variability during therapeutic hypothermia correlated to 96 hrs neurolog- ical outcomes and survival in a pig model of cardiac arrest. Crit Care Med. 2012;40:580–586.
28. Halperin HR, Tsitlik JE, Guerci AD, Mellits ED, Levin HR, Shi AY, Chandra N, Weisfeldt ML. Determinants of blood flow to vital organs during cardiopul- monary resuscitation in dogs. Circulation. 1986;73:539–550.
29. Paradis NA, Martin GB, Rivers EP, Goetting MG, Appleton TJ, Feingold M, Nowak RM. Coronary perfusion pressure and the return of spontaneous circulation in human cardiopulmonary resuscitation. JAMA. 1990;263:1106–1113.
30. Kern KB, Ewy GA, Voorhees WD, Babbs CF, Tacker WA. Myocardial perfusion pressure: a predictor of 24-hour survival during prolonged cardiac arrest in dogs. Resuscitation. 1988;16:241–250.
31. Naim MY, Sutton RM, Friess SH, Bratinov G, Bhalala U, Kilbaugh TJ, Lampe JW, Nadkarni VM, Becker LB, Berg RA. Blood pressure- and coronary perfusion pressure-targeted cardiopulmonary resuscitation improves 24-hour survival from ventricular fibrillation cardiac arrest. Crit Care Med. 2016;44:e1111–e1117.
32. Wik L, Naess PA, Ilebekk A, Nicolaysen G, Steen PA. Effects of various degrees of compression and active decompression on haemodynamics, end-tidal CO2, and ventilation during

cardiopulmonary resuscitation of pigs. Resuscitation. 1996;31:45–57.

33. Blair L, Kendal SP, Shaw GR, Byers S, Dew R, Norton M, Wilkes S, Wright G. Comparison of manual and mechanical cardiopulmonary resuscitation on the move using a manikin: a service evaluation. British Paramedic Journal. 2017;2:6–15.
34. Niles DE, Sutton RM, Nadkarni VM, Glatz A, Zuercher M, Maltese MR, Eilevstjønn J, Abella BS, Becker LB, Berg RA. Prevalence and hemodynamic effects of leaning during CPR. Resuscitation. 2011;82:S23–S26.
35. Weil MH, Bisera J, Trevino RP, Rackow EC. Cardiac output and end-tidal carbon dioxide. Crit Care Med. 1985;13:907–909.
36. Sanders AB, Kern KB, Otto CW, Milander MM, Ewy GA. End-tidal carbon dioxide monitoring during cardiopulmonary resuscitation: a prognostic indica- tor for survival. JAMA. 1989;262:1347–1351.
37. Cantineau JP, Lambert Y, Merckx P, Reynaud P, Porte F, Bertrand C, Duvaldestin P. End-tidal carbon dioxide during cardiopulmonary resuscitation in humans presenting mostly with asystole: a predictor of outcome. Crit Care Med. 1996;24:791–796.
38. Axelsson C, Karlsson T, Axelsson AB, Herlitz J. Mechanical active compres- sion-decompression cardiopulmonary resuscitation (ACD-CPR) versus manual CPR according to pressure of end tidal carbon dioxide (P(ET)CO2) during CPR in out-of-hospital cardiac arrest (OHCA). Resuscitation.

2009;80:1099– 1103.

39. Hamrick JL, Hamrick JT, Lee JK, Lee BH, Koehler RC, Shaffner DH. Efficacy of chest compressions directed by end-tidal CO2 feedback in a pediatric resuscitation model of basic life support. J Am Heart Assoc. 2014;3:e000450. DOI: 10.1161/JAHA.113.000450.
40. Pytte M, Kramer-Johansen J, Eilevstjønn J, Eriksen M, Strømme TA, Godang K, Wik L, Steen PA, Sunde K. Haemodynamic effects of adrenaline (epinephrine) depend on chest compression quality during cardiopulmonary resuscitation in pigs. Resuscitation. 2006;71:369–378.
41. Chung TN, Kim SW, Cho YS, Chung SP, Park I, Kim SH. Effect of vehicle speed on the quality of closed-chest compression during ambulance transport. Resuscitation. 2010;81:841–847.
42. Roosa JR, Vadeboncoeur TF, Dommer PB, Panchal AR, Venuti M, Smith G, Silver A, Mullins M, Spaite D, Bobrow BJ. CPR variability during ground ambulance transport of patients in cardiac arrest. Resuscitation. 2013;84:592–595.
43. Hung SC, Mou CY, Hung HC, Lin IH, Lai SW, Huang JY. Chest compression fraction in ambulance while transporting patients with out-of-hospital cardiac arrest to the hospital in rural Taiwan. Emerg Med J. 2017;34:398–401.
44. Stapleton ER. Comparing CPR during ambulance transport: manual vs. mechanical methods. JEMS. 1991;16:63–64.
45. Klouche K, Weil MH, Sun S, Tang W, Povoas HP, Kamohara T, Bisera J. Evolution of the stone heart after prolonged

cardiac arrest. Chest. 2002;122:1006–1011.

46. Babini G, Grassi L, Russo I, Novelli D, Boccardo A, Luciani A, Fumagalli F, Staszewsky L, Fiordaliso F, De Maglie M, Salio M, Zani DD, Letizia T, Masson S, Luini MV, Pravettoni D, Scanziani E, Latini R, Ristagno G. Duration of untreated cardiac arrest and clinical relevance of animal experiments: the relationship between the “No-Flow” duration and the severity of post-cardiac arrest syndrome in a porcine model. Shock. 2018;49:205–212.
47. Foo NP, Chang JH, Su SB, Lin HJ, Chen KT, Cheng CF, Lin TY, Chen PC, Guo HR. A stabilization device to improve the quality of cardiopulmonary resuscitation during ambulance transportation: a randomized crossover trial. Resuscitation. 2013;84:1579–1584.

Chapter 3. Cardio-Pulmonary Resuscitation Interventions: Lung damage.

"**Cardiopulmonary Resuscitation-Associated Lung Edema (CRALE) - A Translational Study."**

Aurora Magliocca, Emanuele Rezoagli, Davide Zani, Martina Manfredi, Daria De Giorgio, Davide Olivari, Francesca Fumagalli, Thomas Langer, Leonello Avalli, Giacomo Grasselli, Roberto Latini, Antonio Pesenti, Giacomo Bellani, Giuseppe Ristagno

Published: Am J Resp Crit Care Med 2020

Abstract

Rationale: Cardiopulmonary Resuscitation is the cornerstone of cardiac arrest (CA) treatment. However, lung injuries associated with it have been reported.

Objectives: To assess 1) the presence and characteristics of lung abnormalities induced by Cardiopulmonary Resuscitation and 2) the role of mechanical and manual chest compression (CC) in its development.

Methods: This translational study included : 1) a porcine model of CA and Cardiopulmonary Resuscitation (n=12), 2) a multicenter cohort of out-of-hospital CA patients undergoing mechanical or manual CC (n=52). Lung Computed Tomography performed after resuscitation was assessed qualitatively and quantitatively along with with respiratory mechanics and gas exchanges.

Measurements and Main Results: The lung weight in the mechanical CC group was higher compared to the manual CC group in the experimental (431±127 *vs* 273±66, p=0.022) and clinical study (1208±630*vs*837±306, p=0.006). The mechanical CC group showed significantly lower oxygenation (p=0.043) and respiratory system compliance (Cpl,rs) (p<0.001) compared to the manual CC group in the experimental study. The variation of right atrial pressure was significantly higher in the mechanical compared to the manual CC group (54±11*vs*31±6 mmHg, p=0.001) and significantly correlated with lung weight (r=0.686, p=0.026) and Cpl,rs (r=-0.634, p=0.027). Incidence of abnormal lung density was higher in patients treated with mechanical compared to manual CC (37% *vs* 8%, p=0.018).

Conclusions: This study demonstrated the presence of Cardiopulmonary Resuscitation Associated Lung Edema (CRALE) in

animals and in out-of-hospital CA patients, which is more pronounced after mechanical- as opposed to manual CC and correlates with higher variations of right atrial pressure during CC.

Introduction

Cardiac arrest (CA) is a leading cause of death worldwide (1). Despite early initiation of cardiopulmonary resuscitation (CPR) and prompt defibrillation have increased the rate of return of spontaneous circulation (ROSC), CA outcome remains poor. Only 12% of out-of-hospital CA patients survive to hospital discharge, and barely 8% of these survivors regain good neurological recovery (1).

The high mortality rate after successful resuscitation from CA is attributed to the "post-CA syndrome" (2-3); a post-reperfusion state characterized by systemic inflammation leading to multiple organ dysfunction. Recently, a non-negligible incidence of lung injury in the post-CA period has been demonstrated (4-5). Up to 50% CA survivors develop acute respiratory distress syndrome (ARDS) within 48h after hospital admission, and this early ARDS is associated with hospital mortality and poor neurological outcome (4). Indeed, a post-resuscitation lung protective ventilation strategy is suggested, as low tidal volume ventilation may improve neurocognitive outcome after CA. In a study comparing a tidal volume lower or higher than 8 ml kg^{-1} in out-of-hospital CA survivors, it was observed that a lower tidal volume in the first 48 h post-ROSC was associated with a favorable neurological outcome, more ventilator and shock-free days (5).

The different risk factors associated with lung injury after CA include pulmonary ischemia–reperfusion, aspiration of gastric content, pulmonary contusion from chest compression, and systemic inflammation (6-8). Autopsy-based comparison between manual and mechanical chest compression (CC) revealed that lung lesions are present respectively in 4% and 18.6% of patients undergoing manual and mechanical CCs respectively (9). Imaging studies using Computed Tomography (CT) showed that lung injuries may be detectable in up to 79% of patients undergoing CPR (10-11). Despite these observations, a radiological (qualitative and quantitative CT scan analysis) and functional description of lung abnormalities after CPR is lacking, especially after the introduction of mechanical CC. Furthermore, pressure applied to the respiratory system generated by different CC strategies (mechanical versus manual), has not been investigated so far. Accordingly, the aim of this study was to systematically assess the presence of lung abnormalities associated with cardiopulmonary resuscitation- and to evaluate whether mechanical and manual chest compression (CC) could play a different role in the development of these in a porcine model of CA. We then corroborated our observations in a retrospective multicenter observational cohort study including non-traumatic out-of-hospital CA patients with a lung CT scan at hospital admission.

Methods

This study encompassed two phases. Lung abnormalities were first investigated in a porcine model of CA and prolonged mechanical vs manual CPR and then in a cohort of out-of-hospital CA patients undergoing mechanical or manual CC with a lung CT scan performed after resuscitation.

Experimental study

This is a secondary analysis of a previous study (12). In an ambulance transport, pigs in CA were randomized to 18 min of mechanical or manual CC.

After 2 min of CA, continuous CC was started simultaneously to unsynchronized mechanical ventilation. Manual CC was provided in accordance to 2015 international CPR guidelines (13). Mechanical CC was delivered by the LUCAS® 3.0 chest compression system (Stryker/Jolife AB, Lund, Physio-Control, Sweden), delivering continuous CC (rate: 102±2 per min; depth: 53±2 mm; duty cycle: 50±5%). Every 5 min during CPR, epinephrine (1 mg) was administered.

Defibrillation was attempted with a biphasic 200-Joule shock. ROSC was defined as the presence of sinus rhythm with a mean arterial pressure of more than 60 mmHg.

Measurements

ECG, hemodynamics, $EtCO_2$, were continuously recorded. For each minute of CPR the minimum, the maximum and the swing in right atrial pressure were computed. The variation of right atrial pressure (Δ RAP) was reported as surrogate of intrathoracic pressure (ITP).

Dynamic compliance of the respiratory system (Cpl,rs) was assessed. Arterial blood gas analyses were obtained. Plasma high-sensitivity cardiac troponin T (hs-cTNT), N-Terminal Pro-Atrial Natriuretic Peptide (NTpro-ANP), receptor for advanced glycation end product (RAGE) and pulmonary surfactant associated protein D (SPD) were measured with ELISA assays.

CT scanning and morphological analysis

All successfully resuscitated animals underwent lung CT scan at the end of resuscitation maneuvers (n=12, mechanical n=6 or manual n=6), performed during breath holding at end-expiration. Two veterinary radiologists, blind to study groups, assessed lung CT scans in order to describe the morphological lung alterations (14).

Clinical study

This was a multicenter observational, retrospective cohort study. The Ethical Committee of each enrolling hospital approved the study (Ethical Committee N° 3070). Informed consent was waived from the Ethical Committee due to the retrospective observational nature of the investigation and CA patients admitted from 2011 to 2019 in the intensive care units (ICU) of three hospitals were enrolled.

Inclusion criteria were adult out-of-hospital non-traumatic CA who received manual or mechanical CC with a lung CT scan performed within 24h. Exclusion criteria were aspiration pneumonia and/or pulmonary embolism.

Since CT scan was performed as part of the diagnostic work-up of the patients, scans occurred during uninterrupted ventilation, as per clinical practice.

The following clinical data were retrieved from patient electronic medical records:

sex, age, weight, CA characteristics, physiological data including gas exchanges and ventilator setting, ICU and hospital length-of-stay and hospital mortality.

Lung CT quantitative analysis

Quantitative analysis of lung CT scans of experimental CAs and out-of-hospital CA patients were performed using manual segmentation in blind and published methods for volume and weight measurements (15-17).

A threshold of 500 HU (17) of mean lung CT was used in order to define average lung density as normal (mean lung CT<-500) or below normal (mean lung CT ≥-500).

Statistical analysis

Continuous and categorical data were expressed as mean±standard deviation or frequency (percentage), respectively. Differences among groups were assessed with parametric or non-parametric tests as appropriate. Fisher's exact test was used for categorical data. In the morphological analysis of the CT scan findings, the presence of ground glass attenuation (GGA) and airspace consolidation (AC) were evaluated in each of the six lung lobes of each animal. In order to adjust the model for the within animal correlation, difference among

groups in the proportion of GGA and AC was calculated using an adjusted logistic regression analysis with robust clustering, where GGA and AC were considered as outcome variable, the type of chest compressions as exposure variable, and the pigs were considered as cluster variable. Correlations between continuous data were explored using linear regression analyses. Statistical significance was set at p-value<0.05 (two-tailed).

Please refer to the online data supplement for detailed methods.

Results

Experimental study

Figure 1 shows a representative CT image of pigs receiving mechanical or manual CC; the graph below shows that the mean lung weight was significantly higher when a mechanical CC device was used. Table 1 shows the morphological analysis of animals' lung CTs. The ground glass attenuation was present in both groups, affecting a significantly higher fraction of lobes with diffuse pattern in the mechanical CC compared to the manual CC group (83% vs 25%, p<0.001). The airspace consolidations were detected more frequently in the mechanical CC group compared to the manual CC one (72% vs 42%, p=0.012). Peribronchovascular thickening, interlobular thickening, air bronchogram, pleural effusion and rib fractures were not significantly different between the two groups. The proportion of animals affected by ground glass attenuation and airspace

consolidation stratified by lung lobes is illustrated in Table E1 and Figure 2.

Data regarding the main quantitative CT variables in animals are summarized in Table 2. The lung volume was higher in the mechanical CC group compared to the manual group (p=0.043). The lung weight was higher in the mechanical CC group compared to the manual one (p=0.022). The poorly inflated tissue was higher in the mechanical CC group compared to the manual one (p=0.023) and accordingly the well-inflated tissue was less represented in the mechanical CC group (p=0.029).

The lung density shows a gravitational gradient in both the mechanical and manual CC group. The lung density is higher in the mechanical versus manual CC group at each gravitational level (treatment effect p=0.018, Figure 3, panel A). Furthermore, the mechanical CC group shows a higher ventro-dorsal gradient compared to the manual one ($p<0.05$, Figure 3, panel B).

The PaO_2/FiO_2 was significantly lower in the mechanical CC group compared to the manual group overtime (group-by-time interaction p=0.043) (Figure 4A) with return to baseline values 3h after ROSC. The $PaCO_2$ was higher in the mechanical CC group compared to the manual one (group-by-time interaction $p<0.001$) (Figure 4B). Cpl,rs decreased significantly after CPR, with a more severe decline in the mechanical CC group compared to the manual one (group-by-time interaction $p<0.001$) (Figure 4C). Furthermore, the Cpl,rs was negatively associated with both total lung weight (r=-0.723, p=0.008) (Figure E1A) and total lung volume (r=-0.691, p=0.013) (Figure E1B).

The variation of right atrial pressure (Δ RAP) generated by CCs is represented in Figure 5A. Higher Δ RAP during CC was observed in the mechanical CC group compared to the manual CC group (54±11 vs 31±6 mmHg, p=0.001). Δ RAP was positively correlated to the lung weight (r=0.686, p=0.026) (Figure 5B) and negatively correlated to the Cpl,rs (r=-0.634, p=0.027) (Figure 5C). A representative image of the RAP waveform during CC is reported in Figure E2; differences in ΔRAP between the two groups over 18 min CPR is reported in Figure E3. Hemodynamics and plasmatic levels of biomarkers over time together with lung histology at 72 hours after ROSC did not show significant changes among groups (Table E2, Figure E4-E5).

Clinical study

During the observation period, 52 patients received a lung CT scan within 24h from CA. Patients' demographic and outcome data are reported in Table 3. CA patients undergoing mechanical CC were significantly younger (p=0.009) and with a 2-fold higher low-flow time (p<0.001) compared to the group receiving manual CC. Ten out of 16 patients receiving mechanical CC underwent veno-arterial extracorporeal membrane oxygenation (v-a ECMO) while none of the patients in the manual CC group was treated with v-a ECMO (p<0.001).

Quantitative analysis of CT scans revealed that mean lung weight was significantly higher in the mechanical CC group compared to manual group (p=0.006) (Table 4). The lung volume and the lung gas volume did not differ among the two groups. The amount of not inflated lung

tissue was significantly higher in the mechanical CC group compared to the manual one (p=0.025), the poorly inflated lung tissue was higher in the mechanical CC group (p=0.007) while the well inflated lung tissue was less represented in the mechanical compared to manual group (p=0.006).

Table 5 shows the first arterial blood gas analysis and ventilator setting of CA patients at ICU admission and after 24 h. pH, base excess and lactate level were significantly higher in the mechanical CC group compared to the manual one. Mechanical CC treated patients showed a lower PaO_2/FiO_2 compared to the manual CC group at ICU admission (p=0.013) and at 24 h (p=0.027). Hemodynamics at ICU admission are represented in table E4.

Exploratory incidence of abnormal lung density in the preclinical and clinical investigation

In the experimental study we observed a higher incidence of abnormal lung density in the mechanical compared to the manual CC group, despite a non statistical significance (4/6 versus 1/6, 67% versus 17%, p=0.242).

In the clinical study, we confirmed a significantly higher proportion of abnormal lung density in the mechanical CC group (6/16 versus 3/36, 37% versus 8%, p=0.018). We explored the role of age and low-flow time on abnormal lung density as they differ between mechanical versus manual CC group (Table 3). We observed that mechanical CC (OR 6.6; 95%CI, 1.39–31.28; p=0.017) and a trend to a prolonged low flow time (OR 4.42; 95%CI, 0.82–23.79; p=0.083) were associated to a higher risk of abnormal lung density (Table E4A). These findings

were confirmed using mean lung CT as outcome variable (Table E4B).

We further investigated in 4 independent linear regression models (Model A-D) the association between low-flow time and type of CC with the mean lung CT (Table E5). To include interdependency among the 4 groups of patients, we performed a non-parametric analysis. Patients undergoing mechanical CC with a prolonged CPR showed a significantly higher mean lung density than patients undergoing manual CC with a shorter low-flow time ($p<0.01$), and a trend to a higher mean lung density compared to patients undergoing manual CC with a prolonged low-flow time ($p=0.080$) (Figure 6).

Discussion

In this translational study we provide a comprehensive description of lung abnormalities following cardiopulmonary resuscitation, with similar techniques, in both pigs and humans. The consistent clinical and experimental findings allow us to introduce the concept of "Cardiopulmonary-Resuscitation Associated Lung Edema" (CRALE), as detailed in the following paragraphs. In a preclinical model of CA in pigs, CPR caused lung abnormalities that were more prominent after mechanical CC compared to manual CC. Mechanical CC led to increased lung weight, reduced lung aeration, and reduced oxygenation and compliance compared to the manual CC strategy. The intensity of intrathoracic pressure swings generated by mechanical CC (assessed by variation in right atrial pressure) was associated with higher lung weight and reduced Cpl,rs. The clinical

study confirmed that presence of increased lung density was more frequent after mechanical versus manual CC (37% versus 8%, respectively) in keeping with what observed in the animals (67% versus 17%, respectively). Moreover, the lung weight and the amount of not aerated lung tissue were markedly increased when a mechanical CC strategy was used. This was accompanied by a lower PaO_2/FiO_2, even with a higher PEEP level.

Comparison with existing literature

In CA patients lung damage related to CPR has been described since the 80's (18). Lung injuries detected by CT scan seem frequent complication in CA patients who undergo CPR (11-12). An autopsy-based study demonstrated that mechanical CC leads more often to lung lesions compared to manual CC (10). However, these findings are not unanimously reported (19-22). Moreover, the only randomized non-inferiority safety study comparing mechanical or manual CC, revealed that LUCAS did not cause significantly more serious or life-threatening visceral damage than manual CC (23). Indeed, also in this study mechanical CC did not cause lifethreating injuries in both animals and humans.

Liu and colleagues described the radiological finding of ground-glass attenuation in pigs 6h after manual resuscitation from either 5 or 10 min of CA (7). Moreover, the authors described the presence of histopathological changes resembled as alveolar flooding, inflammatory cells (i.e. neutrophils), and alveolar barrier disruption suggested by the presence of erythrocytes in the alveolar spaces proportional with the duration of CA (7,8). These experimental

studies, however, did not address the effect of mechanical or manual CC.

Characterization of CRALE

In our model, 18 min of CPR led to increased airspace consolidation and ground-glass attenuation in pigs treated with mechanical CC compared to the manual CC group. Further quantitative CT scan analyses were performed after the qualitative ones: these showed that the aeration loss was accompanied by increased lung weight and gravitational gradient, suggesting the presence of lung edema as opposed to sole atelectasis.

In line with the morphological and quantitative lung alterations, gas exchange and respiratory mechanics were impaired during CPR and early after ROSC especially in the mechanical CC treated animals. The compliance of the respiratory system has been reported to decrease after CC, regardless of the technique used (24-26). The aetiology of changes in lung compliance is multifactorial. In our experimental model of CA, mechanical CC treated pigs showed a greater reduction in Cpl,rs 10 min after ROSC together with a higher lung weight and lung volume compared to the manual CC group. These observations suggest an increase in the total amount of fluid in the lung. In addition, a lower PaO_2/FiO_2 was observed in the mechanical CC group compared to the manual one during CPR, at ROSC and up to one hour later, to then recover in the subsequent two hours of observation.

The findings in the cohort of out-of-hospital CA patients were consistent with the animal results. A higher lung weight and amount

of not inflated and poorly inflated lung tissue was detected in the mechanical CC group by the quantitative lung CT scan.

Etiology of CRALE

Several possible mechanisms might explain the genesis of CRALE and the greater severity of lung abnormalities in mechanical CC treated animals.

At first, a reduction in lung volume occurs during CC, indeed lung volume during CC is between Functional Residual Capacity (FRC) and residual volume (27), possibly causing alveolar decrecruitment, atelectrauma and hence aeration and compliance loss.

However, the fundamental role of transmural vascular pressures generated by mechanical CC, in contrast to manual CC, must be taken into account (28-30). In fact ΔRAP during CPR was positively correlated with lung weight and negatively correlated with compliance. This association could also explain the difference among the study groups in lung weight, which is majorly exposed to high pressure swings and negative pressures during the CCs using a mechanical device for CPR. The better hemodynamics generated by the piston-based device might reflect also on the pulmonary blood flow, leading to vascular congestion, as shown in a different setting by Katira et al (31). Pulmonary edema in patients generated by negative intrathoracic pressure has been previously reported (32-34). When the interstitial pressures become negative the hydrostatic pressure gradient increases leading to transcapillary flow with alveolar flooding (35) and inflammation (36). Interestingly, Scharf et al demonstrated that negative-pressure pulmonary edema is more pronounced in patients

with myocardial dysfunction (37). The transient nature of CRALE and the lack of difference in biochemical or histological markers of epithelial lung injury favours the hypothesis of an hydrostatic nature of the edema as opposed to increased permeabilty.

Recently, the concept of patient-self inflicted lung injury has highlighted the possible harmful role of the spontaneous patient effort on the development of lung injury. In the presence of acute respiratory failure, the patient's effort leads to extremely low intrathoracic pressure to correct impaired gas exchanges. Although in a different clinical scenario, we believe that CRALE and P-SILI may share the pathophysiological pathway of the negative intrathoracic pressure (38).

Given that the exact mechanisms are still to be identified and that potential confounders exist (e.g. ischemia/reperfusion (39) and hyperoxia (40) inducing lung injury and atelectasis (41)) it appears more appropriate to consider the edema "associated to-" as opposed to "induced by-" CPR .

Streghts and limitations

The experimental study was performed in a scenario simulating a real clinical challenge such as the management of CPR after CA during ambulance transportation, increasing the translation to humans of the experimental findings. Another point of strength is represented by the novelty, since to our knowledge this is the first report describing a comprehensive assessment of lung CT scan with qualitative and quantitative analyses after experimental and clinical CPR.

Several limitations must also be achnowledged. Firstly, it represents a secondary analysis of a randomized preclinical study aimed to compare the hemodynamic effect of mechanical and manual CC strategy, where the pleural pressure was not directly measured; however, CT scan were prospectively obtained with the aim of assess lung aeration and weight. Moreover, biological assessment of lung edema fluid was not available, in order to assess alveolar permeability and inflammation. Secondly, only one ventilation strategy was tested. Whether the role of unsynchronized ventilation is prevalent over CC itself in causing lung injury cannot be excluded and need further studies. Future work is necessary to identify the optimal ventilation strategy and PEEP setting during mechanical CC. Thirdly, we cannot also exclude that the ventilator used accounted for the generation of a closed circuit with the animals airway, similarly to the impedance threshold device (41), ultimately decreasing ITP during CC release and the subsequent lung edema.

The main limitation of the clinical study is the retrospective observational design, which accounted for a great heterogeneity of the out-of-hospital CA population studied. Patients undergoing mechanical CC were subjected to a significantly longer CPR time and showed a significantly higher proportion of extracorporeal life support. Based on local clinical protocols, mechanical CC is used mainly in CA patients candidate for extracorporeal life support, which is applied in the instance of refractory CA after an interval of at least 15 min of CPR. The presence of both factors was associated with CRALE, but the contribution of each factor has yet to be elucidated.

Moreover, in these patient data on how ventilation during CC was provided are missing. Heterogeneous clinical practice has been reported in ventilator setting and monitoring during CPR, with significant divergence from international recommendations (42). The importance of mechanical ventilation during CPR is suggested to play a key role on outcomes after out-of-hospital CA (43).

Another limitation of the clinical study is that the majority of patients undergoing mechanical CC were candidate for venous-arterial (V-A) ECMO. Lung CT scan was performed when V-A ECMO was already placed. V-A ECMO significantly reduces pulmonary perfusion of the lung with a relative increase of the ventilation perfusion ratio and the potential risk of alveolar alkalosis which could decrease the alveolar fluid reabsorption (44).

Conclusion

In conclusion, our observations highlight the presence of lung abnormalities, likely representing a Cardiopulmonary-Associated Lung Edema (CRALE) which were more pronounced after mechanical versus manual CC, with a derangement in mechanical properties and gas exchange. These alterations are transient and appear related with the intensity of intratoracic pressure swings during CC. Further reasarch should be focused on the identification of the optimal ventilation strategy in order to prevent or reduce the occurence of CRALE.

Acknowledgments

The authors want to thank Fabiana Madotto (University of Milan-Bicocca, Monza, Italy) for statistical support; Vanessa Zambelli, Silvia Villa, Valentina Ciceri (University of Milan-Bicocca, Monza, Italy), Carlo Perego (Istituto di Ricerche Farmacologiche Mario Negri IRCCS, Milan, Italy), Alberto Cucino, Giovanni Babini (University of Milan, Milan, Italy) for their valuable support.

Table 1. Lung morphological CT-scan analysis in the experimental study

	Manual CC (n=6)	**Mechanical CC (n=6)**	**p-value**
Ground Glass Attenuation	***36 lung lobes***	***36 lung lobes***	
Presence, n (%)	28/36 (78)	34/36 (94)	0.144
• Local, n (%)	19/36 (53)	4/36 (11)	<0.001
• Diffuse, n (%)	9/36 (25)	30/36 (83)	<0.001
Airspace consolidation	***36 lung lobes***	***36 lung lobes***	
Presence, n (%)	15/36 (42)	26/36 (72)	0.012
• Local, n (%)	7/36 (19)	11/36 (30)	0.342
• Diffuse, n (%)	8/36 (22)	15/36 (42)	0.147
Peribronchovascular thickening, n (%)	4/6 (67)	4/6 (67)	1.000
Interlobular septal thickening, n (%)	1/6 (17)	5/6 (83)	0.080
Air bronchogram, n (%)	3/6 (50)	6/6 (100)	0.182
Pleural effusion, n (%)			
• Right	0/6 (0)	1/6 (17)	1.000
• Left	0/6 (0)	0/6 (0)	/
• Bilateral	0/6 (0)	0/6 (0)	/

Bone fractures and dislocations, n (%)			
Rib fractures			
• Incomplete	4/6 (67)	5/6 (83)	1.000
• Complete			
- Compound	3/6 (50)	5/6 (83)	0.545
- Dislodged	4/6 (67)	2/6 (33)	0.567
Sterno-costal dislocation	1/6 (17)	1/6 (17)	1.000

Table 2. Lung CT-scan quantitative analysis in the experimental study

	Manual CC (n=6)	**Mechanical CC (n=6)**	**p-value**
Lung density, HU	-548±45	-457±74	0.028
Lung volume, mL	601±111	782±157	0.043
Lung gas Volume, mL	327±55	352±65	0.498
Lung weight, g	273±66	431±127	0.022
Not inflated lung tissue, %	2±3	9±9	0.100
Poorly inflated lung tissue, %	32±11	49±11	0.023
Well inflated lung tissue, %	66±13	41±20	0.029

Data expressed as mean±SD.

Table 3. Baseline characteristics and outcomes of out-of-hospital CA patients.

	Manual CC (n=36)	**Mechanical CC (n=16)**	**p-value**
Demographic Characteristics			
Age, years (mean±SD)	63±13	52±17	0.009
Gender, M/F, %	22/14 (61/39)	10/6 (63/37)	1.000
Weight, kg	74±18	78±16	0.223
Cardiac Arrest Characteristics			
Bystander-performed CPR, n (%)	22 (61)	12 (75)	0.528
No-flow time, min (mean±SD)	5±4	3±4	0.123
Low-flow time, min (mean±SD)	22±11	55±26	<0.001
First monitored rhythm, n (%) • Shockable • Non-shockable	 17/36 (47) 19/36 (53)	 6/16 (38) 10/16 (62)	0.560
Hospital procedures			
ECMO v-a, n (%)	0 (0)	10 (62)	<0.001
IABP, n (%)	0 (0)	1 (6)	0.300
Coronary angiography, n (%)	19 (53)	8 (50)	1.000
Cardiac surgery, n (%)	0 (0)	1 (6)	0.300
Targeted temperature management, n (%)	23 (64)	16 (100)	0.709
Outcomes			

ICU-Length of Stay, n	6±8	10±26	0.120
Hospital length of stay,	16±23	14±36	0.010
Survival to hospital discharge, n (%)	13 (36)	2 (13)	0.106
Cerebral Performance Category at 6-month follow-up, n (%)			0.106
• 1	13 (36)	2 (13)	
• 2	0 (0)	0 (0)	
• 3	0 (0)	0 (0)	
• 4	0 (0)	0 (0)	
• 5	21 (58)	14 (87)	

M=male; F=female; CPR=cardiopulmonary resuscitation; ECMO=extracorporeal membrane oxygenation; IABP=intra-aortic balloon pump; ICU=intensive care unit.

Table 4. Lung CT-scan quantitative analysis in out-of-hospital cardiac arrest patients.

	Manual CC (n=36)	**Mechanical CC (n=16)**	**p-value**
Lung density, HU	-663±97	-541±171	0.002
Lung volume, mL	2534±917	2613±812	0.617
Lung gas volume, mL	1698±733	1405±631	0.172
Lung weight, g	837±306	1208±630	0.006
Not inflated lung tissue, %	1±4	9±15	0.025
Poorly inflated lung tissue, %	10±13	21±15	0.007
Well inflated lung tissue, %	89±15	69±28	0.006

Data expressed as mean±SD.

Table 5. Arterial blood gas analyses and respiratory variables of out-of-hospital cardiac arrest patients.

	Manual CC (n=36)	**Mechanical CC (n=16)**	**p**
Arterial blood gas analysis at ICU admission			
pH	7.336±0.11	7.214±0.21	0.025
$PaCO_2$, mmHg	38±8	43±12	0.060
PaO_2/FiO_2	328±132	232±103	0.013
BE, mmol/L	-5.3±5.6	-9.6±7	0.028
Lactate, mmol/L	3.9±4	7.7±6	0.015
Ventilatory setting at ICU admission			
Tidal volume, ml	509±77	527±56	0.197
Peak inspiratory pressure, cmH_2O	23±5	26±7	0.214
Respiratory rate	15±3	9±7	<0.001
FiO_2, %	48±14	71±20	0.028
PEEP, cmH_2O	6.1±1.5	7.5±3.0	<0.001
Arterial blood gas analysis 24h after ICU admission			
pH	7.42±0.06	7.404±0.06	0.403
$PaCO_2$, mmHg	37±6	39±5	0.352
PaO_2/FiO_2	344±95	263±106	0.027
BE, mmol/L	-0.5±3.6	-0.44±3.7	0.825
Lactate, mmol/L	2±1.9	2.6±2.3	0.126
Ventilatory setting 24			

h after ICU admission			
Tidal volume, ml	496±102	532±93	0.367
Peak inspiratory pressure, cmH_2O	20±7	22±4	0.368
Respiratory rate	14±4	8±4	<0.001
PEEP, cmH_2O	7.0±2.0	9±3.2	0.021
FiO_2, %	40±16	58±21	<0.001

Data expressed as mean±SD. FiO_2 of the natural lung (equal or lower that the FiO_2 of the membrane lung) was used to calculate the PaO_2/FiO_2 in patients with ECMO in the mechanical CC group.

Figure legends

Figure 1. Representative CT images of cranial (A) and caudal (B) lung lobes in the mechanical CC (right panels) and in the manual CC (left panels) treated pigs. In the bottom graph (C), differences in the lung weight estimated by CT scan analysis among the experimental groups. L=left lung side.

Figure 2. Morphological distribution of the lung abnormailties stratified by lung lobes and reported as proportion of animals with ground glass attenuation (GGA) and airspace consolidation (AC). In A, lung lobe anatomy in pigs. In B and C, GGA in manual and mechanical CC group, respectively. In D and E, AC in manual and mechanical CC group, respectively.

Figure 3. Differences of lung tissue density among groups at each gravitational level expressed as thirds of the lung sterno-costal height from the ventral to the dorsal lung areas (A). Difference in the gradient of lung density from the ventral to the dorsal regions among groups (B). The gradient of lung density was calculates as (Ventral HU-Dorsal HU)/(ventral HU)*100. *, $p<0.05$; **, $p<0.01$.

Figure 4. Differences of PaO_2/FiO_2 (A) and $PaCO_2$ (B) between the groups at baseline, during CPR and within 3 hours after ROSC. Differences of dynamic respiratory compliance (Cpl,rs) between the groups at baseline and at 3 hours after ROSC (C). In A and B data are expressed as whisker plots. In C data are represented as mean±SD.

Group-by-time interaction p-value of the repeated measurements two-way ANOVA was reported. In A, at 5 minutes post-ROSC there was a trend in the difference of PaO_2/FiO_2 between the study groups (p=0.068). *p<0.05, **p<0.01, and ***p<0.001 versus Manual group.

Figure 5. A) Differences of right atrial pressure variation (ΔRAP) between the two animal groups. Association of ΔRAP with lung weight (B) and dynamic compliance of the respiratory system (C). In A data are expressed as mean ± SD. Duration of exposure to ΔRAP is the same for both experimental groups. In B and C the continuous line represents the best fit line of the linear regression with the 95% CI represented with dashed lines.

Figure 6. Differences of mean lung CT between 4 groups of out-of-hospital cardiac arrest patients stratified by type of CPR and length of low-flow time. Overall difference among groups was tested using a Kruskal-Wallis test. Post-hoc pairwise comparisons among groups were tested using Mann-Whitney U test. CT, computed tomography; HU, Hounsfield unit; CC, chest compression. **, p<0.01.

Figure 1

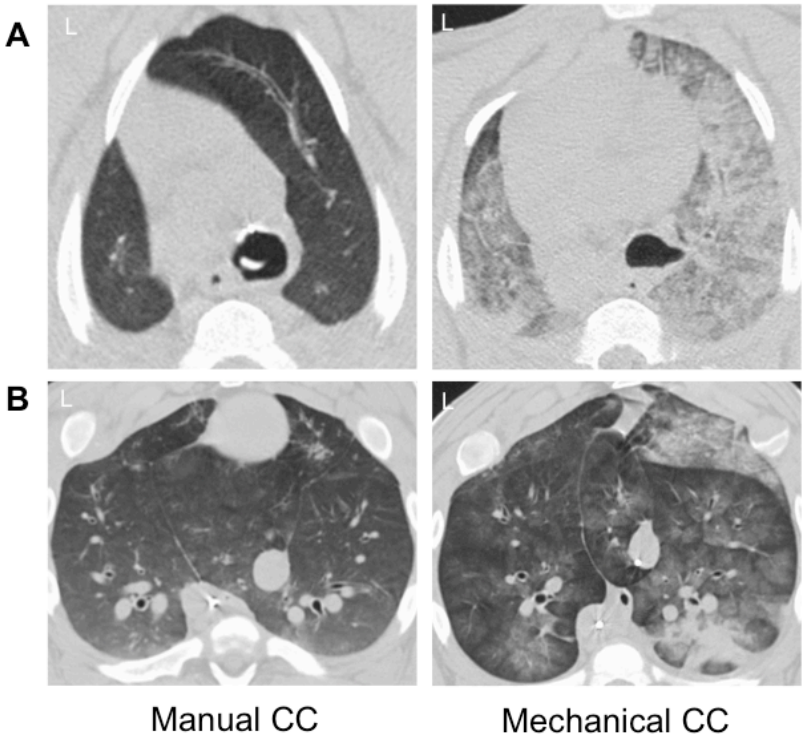

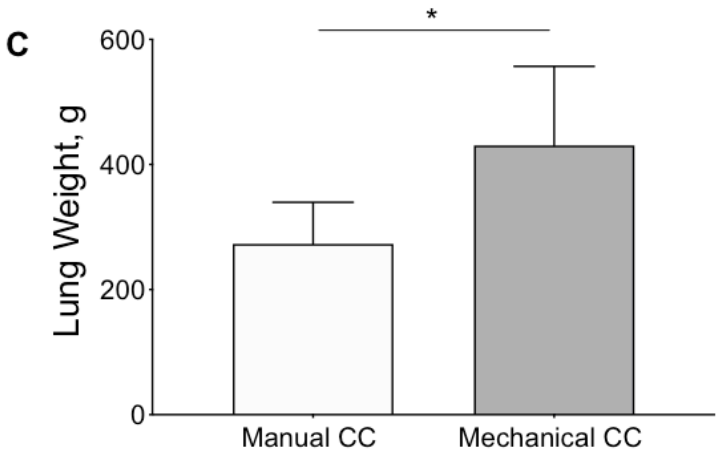

Figure 2

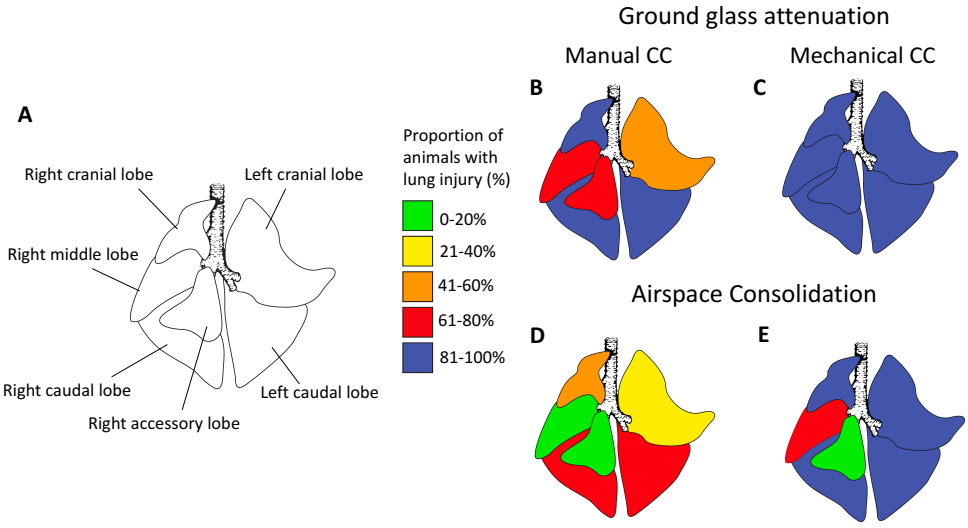
Ground glass attenuation
Manual CC
Mechanical CC
A
B
C
Right cranial lobe
Left cranial lobe
Right middle lobe
Right caudal lobe
Left caudal lobe
Right accessory lobe
Proportion of animals with lung injury (%)
0-20%
21-40%
41-60%
61-80%
81-100%
Airspace Consolidation
D
E

Figure 3

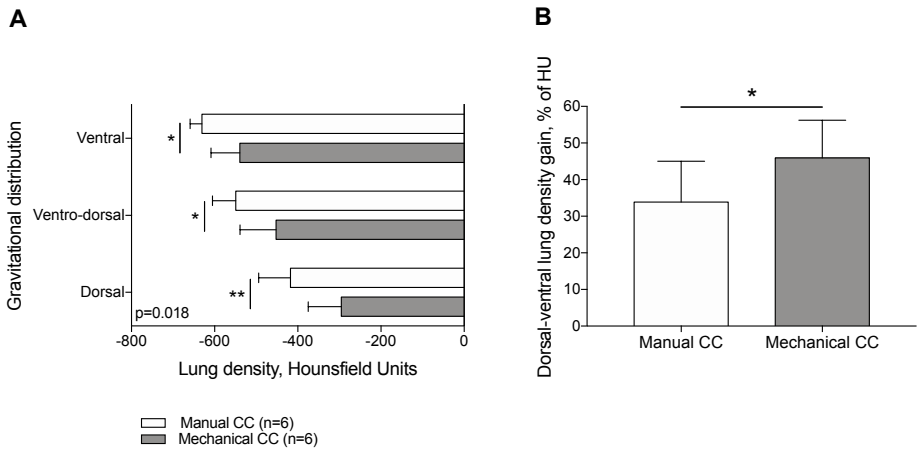

Figure 4

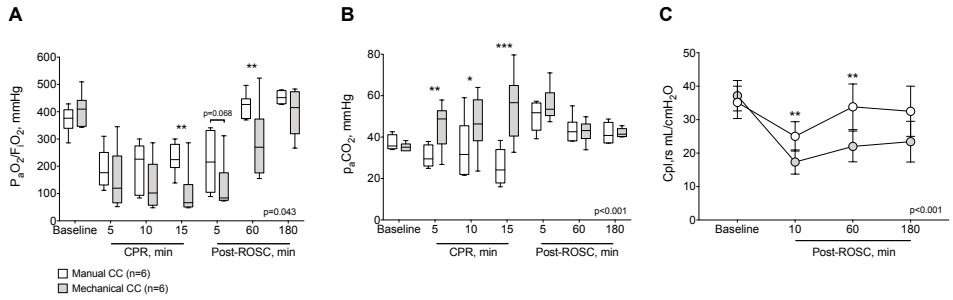

Figure 5

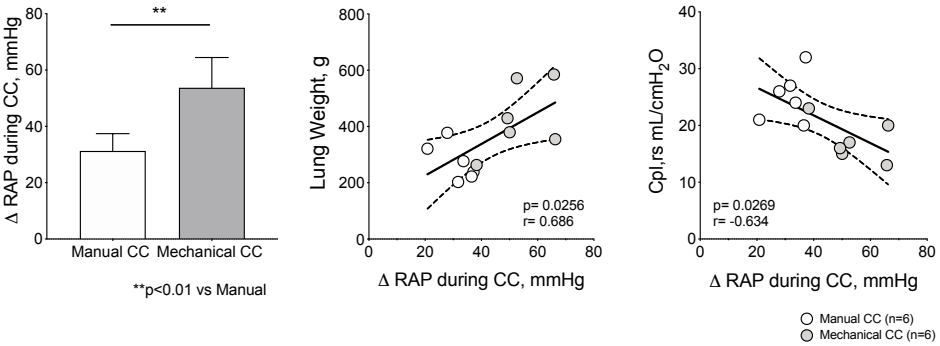

Figure 6

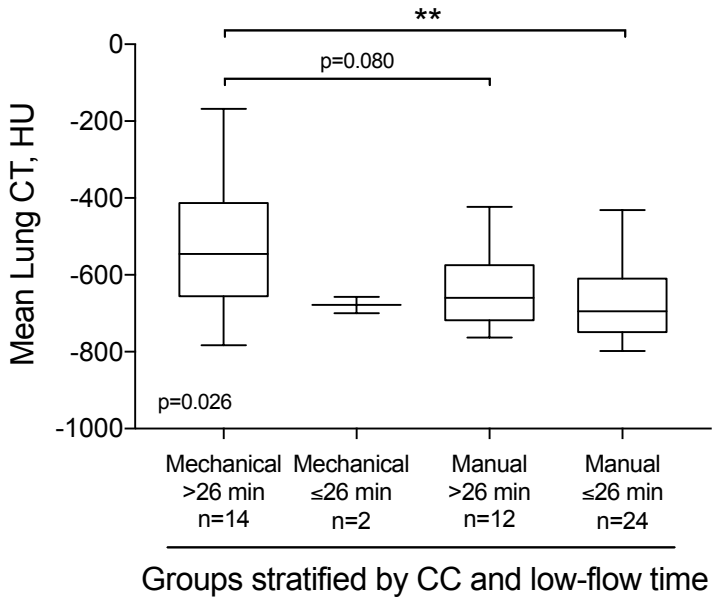

References

1. Benjamin EJ, Muntner P, Alonso A, Bittencourt MS, Callaway CW, Carson AP, Chamberlain AM, Chang AR, Cheng S, Das SR, Delling FN, Djousse L, Elkind MSV, Ferguson JF, Fornage M, Jordan LC, Khan SS, Kissela BM, Knutson KL, Kwan TW, Lackland DT, Lewis TT, Lichtman JH, Longenecker CT, Loop MS, Lutsey PL, Martin SS, Matsushita K, Moran AE, Mussolino ME, O'Flaherty M, Pandey A, Perak AM, Rosamond WD, Roth GA, Sampson UKA, Satou GM, Schroeder EB, Shah SH, Spartano NL, Stokes A, Tirschwell DL, Tsao CW, Turakhia MP, VanWagner LB, Wilkins JT, Wong SS, Virani SS; American Heart Association Council on Epidemiology and Prevention Statistics Committee and Stroke Statistics Subcommittee. Heart Disease and Stroke Statistics-2019 Update: A Report From the American Heart Association. Circulation. 2019;139(10):e56-e528.
2. Adrie C, Adib-Conquy M, Laurent I, Monchi M, Vinsonneau C, Fitting C, Fraisse F, Dinh-Xuan AT, Carli P, Spaulding C, Dhainaut JF, Cavaillon JM. Successful cardiopulmonary resuscitation after cardiac arrest as a "sepsis-like" syndrome. Circulation. 2002;106(5):562-8.
3. Neumar RW, Nolan JP, Adrie C, Aibiki M, Berg RA, Böttiger BW, Callaway C, Clark RS, Geocadin RG, Jauch EC, Kern KB, Laurent I, Longstreth WT Jr, Merchant RM, Morley P, Morrison LJ, Nadkarni V, Peberdy MA, Rivers EP, Rodriguez-Nunez A, Sellke FW, Spaulding C, Sunde K, Vanden Hoek T. Post-cardiac arrest syndrome: epidemiology, pathophysiology,

treatment, and prognostication. A consensus statement from the International Liaison Committee on Resuscitation (American Heart Association, Australian and New Zealand Council on Resuscitation, European Resuscitation Council, Heart and Stroke Foundation of Canada, InterAmerican Heart Foundation, Resuscitation Council of Asia, and the Resuscitation Council of Southern Africa); the American Heart Association Emergency Cardiovascular Care Committee; the Council on Cardiovascular Surgery and Anesthesia; the Council on Cardiopulmonary, Perioperative, and Critical Care; the Council on Clinical Cardiology; and the Stroke Council. Circulation. 2008;118(23):2452-83.

4. Johnson NJ, Caldwell E, Carlbom DJ, Gaieski DF, Prekker ME, Rea TD, Sayre M, Hough CL. The acute respiratory distress syndrome after out-of-hospital cardiac arrest: Incidence, risk factors, and outcomes. Resuscitation. 2019;135:37-44.
5. Beitler JR, Ghafouri TB, Jinadasa SP, Mueller A, Hsu L, Anderson RJ, Joshua J, Tyagi S, Malhotra A, Sell RE, Talmor D. Favorable Neurocognitive Outcome with Low Tidal Volume Ventilation after Cardiac Arrest. Am J Respir Crit Care Med. 2017;195(9):1198-1206.
6. Johnson NJ, Carlbom DJ, Gaieski DF. Ventilator Management and Respiratory Care After Cardiac Arrest: Oxygenation, Ventilation, Infection, and Injury. Chest. 2018;153(6):1466-1477

7. Liu Z, Liu Q, Wu G, Li H, Wang Y, Chen R, Wen C, Ling Q, Yang Z, Tang W. Quantitative CT assessment of lung injury after successful cardiopulmonary resuscitation in a porcine cardiac arrest model of different downtimes. Quant Imaging Med Surg. 2018;8(9):946-956.
8. Yang Z, Zheng H, Lin L, Hou J, Wen C, Wang Y, Ling Q, Jiang L, Tang W, Chen R. Alterations in Respiratory Mechanics and Neural Respiratory Drive After Restoration of Spontaneous Circulation in a Porcine Model Subjected to Different Downtimes of Cardiac Arrest. J Am Heart Assoc. 2019;8(19):e012441.
9. Ondruschka B, Baier C, Bayer R, Hammer N, Dreßler J, Bernhard M. Chest compression-associated injuries in cardiac arrest patients treated with manual chest compressions versus automated chest compression devices (LUCAS II) - a forensic autopsy-based comparison. Forensic Sci Med Pathol. 2018;14(4):515-525.
10. Cho SH, Kim EY, Choi SJ, Kim YK, Sung YM, Choi HY, Cho J, Yang HJ. Multidetector CT and radiographic findings of lung injuries secondary to cardiopulmonary resuscitation. Injury. 2013;44(9):1204-7.
11. Cha KC, Kim YW, Kim HI, Kim OH, Cha YS, Kim H, Lee KH, Hwang SO. Parenchymal lung injuries related to standard cardiopulmonary resuscitation. Am J Emerg Med. 2017;35(1):117-121.
12. Magliocca A, Olivari D, De Giorgio D, Zani D, Manfredi M, Boccardo A, Cucino A, Sala G, Babini G, Ruggeri L, Novelli

D, Skrifvars MB, Hardig BM, Pravettoni D, Staszewsky L, Latini R, Belloli A, Ristagno G. LUCAS Versus Manual Chest Compression During Ambulance Transport: A Hemodynamic Study in a Porcine Model of Cardiac Arrest. J Am Heart Assoc. 2019;8(1):e011189.

13. Perkins GD, Handley AJ, Koster RW, Castrén M, Smyth MA, Olasveengen T, Monsieurs KG, Raffay V, Gräsner JT, Wenzel V, Ristagno G, Soar J. Adult basic life support and automated external defibrillation section Collaborators. European Resuscitation Council Guidelines for Resuscitation 2015: Section 2. Adult basic life support and automated external defibrillation. Resuscitation. 2015;95:81-99.
14. Judge EP, Hughes JM, Egan JJ, Maguire M, Molloy EL, O'Dea S. Anatomy and bronchoscopy of the porcine lung. A model for translational respiratory medicine. Am J Respir Cell Mol Biol. 2014 Sep;51(3):334-43.
15. Chiumello D, Marino A, Brioni M, Cigada I, Menga F, Colombo A, Crimella F, Algieri I, Cressoni M, Carlesso E, Gattinoni L. Lung Recruitment Assessed by Respiratory Mechanics and Computed Tomography in Patients with Acute Respiratory Distress Syndrome. What Is the Relationship? Am J Respir Crit Care Med 2016;193:1254–1263.
16. Reske AW, Reske AP, Gast HA, Seiwerts M, Beda A, Gottschaldt U, Josten C, Schreiter D, Heller N, Wrigge H, Amato MB. Extrapolation from ten sections can make CT-based quantification of lung aeration more practicable. Intensive Care Med. 2010;36(11):1836-44.

17. Gattinoni L, Pesenti A, Avalli L, Rossi F, Bombino M. Pressure-volume curve of total respiratory system in acute respiratory failure. Computed tomographic scan study. Am Rev Respir Dis. 1987;136:730–736.
18. Hillman K, Albin M. Pulmonary barotrauma during cardiopulmonary resuscitation. Crit Care Med. 1986;14(7):606-9.31.
19. Smekal D, Lindgren E, Sanderl H, Johansson J, Rubertsson S. CPR-related injuries after manual or mechanical chest compres- sions with the LUCASTM device: a multicenter study of victims after unsuccessful resuscitation. Resuscitation. 2014;85:1708–12.
20. Smekal D, Johansson J, Huzevka T, Rubertsson S. No difference in autopsy detected injuries in cardiac arrest patients treated with manual chest compressions compared with mechanical compressions with the LUCAS device--a pilot study. Resuscitation. 2009;80(10):1104-7.
21. Pinto DC, Haden-Pinneri K, Love JC. Manual and automated cardiopulmonary resuscitation (CPR): a comparison of associated injury patterns. J Forensic Sci. 2013;58:904–909.
22. Lardi C, Egger C, Larribau R, Niquille M, Mangin P, Fracasso T. Traumatic injuries after mechanical cardiopulmonary resuscitation (LUCAS2): a forensic autopsy study. Int J Legal Med. 2015;129(5):1035-42.
23. Koster RW, Beenen LF, van der Boom EB, Spijkerboer AM, Tepaske R, van der Wal AC, Beesems SG, Tijssen JG.Safety of mechanical chest compression devices AutoPulse and

LUCAS in cardiac arrest: a randomized clinical trial for non-inferiority. Eur Heart J. 2017;38(40):3006-3013.

24. Ornato JP, Bryson BL, Donovan PJ, Farquharson RR, Jaeger C. Measurement of ventilation during cardiopulmonary resuscitation. Crit Care Med. 1983;11:79–82.
25. Wenzel V, Idris AH, Banner MJ, Kubilis PS, Band R, Williams JL Jr, Lindner KH, Davis KJ, Johannigman JA, Johnson RCJ, Branson RD. Lung compliance following cardiac arrest. Acad Emerg Med 1995;2:874–8.
26. Wenzel V, Idris AH, Banner MJ, Kubilis PS, Band R, Williams JL Jr, Lindner KH. Respiratory system compliance decreases after cardiopulmonary resuscitation and stomach inflation: impact of large and small tidal volumes on calculated peak airway pressure. Resuscitation. 1998;38(2):113-8.
27. Idris AH, Banner MJ, Wenzel V, Fuerst RS, Becker LB, Melker RJ. Ventilation caused by external chest compression is unable to sustain effective gas exchange during CPR: a comparison with mechanical ventilation. Resuscitation 1994;28:143–150.
28. Magder S, Guerard B. Heart-lung Interactions and Pulmonary Buffering: Lessons From a Computational Modeling Study. Respir Physiol Neurobiol. 2012;182(2-3):60-70.
29. Broccard AF, Hotchkiss JR, Kuwayama N, Olson DA, Jamal S, Wangensteen DO, Marini JJ. Consequences of vascular flow on lung injury induced by mechanical ventilation. Am J Respir Crit Care Med. 1998 Jun;157:1935-42.

30. Katira BH, Giesinger RE, Engelberts D, Zabini D, Kornecki A, Otulakowski G, Yoshida T, Kuebler WM, McNamara PJ, Connelly KA, Kavanagh BP. Adverse Heart-Lung Interactions in Ventilator-induced Lung Injury. Am J Respir Crit Care Med. 2017;196(11):1411-1421.
31. Katira BH, Engelberts D, Otulakowski G, Giesinger RE, Yoshida T, Post M, Kuebler WM, Connelly KA, Kavanagh BP.
Abrupt Deflation after Sustained Inflation Causes Lung Injury. Am J Respir Crit Care Med. 2018;198:1165-1176.
32. Capitanio MA, Kirkpatrick JA. Obstructions of the upper airway in children as reflected on the chest radiograph. Radiology. 1973;107(1): 159-161.
33. Oswalt CE, Gates GA, Homstrom MG. Pulmonary edema as a complication of acute airway obstruction. JAMA. 1977;238(17): 1833-1835.
34. Bhattacharya M, Kallet RH, Ware LB, Matthay MA. Negative-Pressure Pulmonary Edema. Chest 2016;150(4):927-933.
35. Loyd JE, Nolop KB, Parker RE, Roselli RJ, Brigham KL. Effects of inspiratory resistance loading on lung fluid balance in awake sheep. J Appl Physiol. 1986;60:198-203.
36. Toumpanakis D, Kastis GA, Zacharatos P, Sigala I, Michailidou T, Kouvela M, Glynos C, Divangahi M, Roussos C, Theocharis SE, Vassilakopoulos T. Inspiratory resistive breathing induces acute lung injury. Am J Respir Crit Care Med. 2010;182:1129-36

37. Scharf SM, Woods BO, Brown R, Parisi A, Miller MM, Tow DE. Effects of the Mueller maneuver on global and regional left ventricular function in angina pectoris with or without previous myocardial infarction. Am J Cardiol. 1987;59(15):1305-1309.
38. Brochard L, Slutsky A, Pesenti. Mechanical Ventilation to Minimize Progression of Lung Injury in Acute Respiratory Failure. Am J Respir Crit Care Med. 2017;195(4):438-442.
39. De Perrot M, Liu M, Waddell TK , Keshavjee S. Ischemia–Reperfusion–induced Lung Injury. Am J Respir Crit Care Med. 2003 Feb 15;167(4):490-511.
40. Markstaller K, Rudolph A, Karmrodt J, Gervais HW, Goetz R, Becher A, David M, Kempski OS, Kauczor HU, Dick WF, Eberle B. Effect of chest compressions only during experimental basic life support on alveolar collapse and recruitment. Resuscitation. 2008;79:125-32.
41. Budinger GRS, Mutlu GM, Urich D, Soberanes S, Buccellato LJ, Hawkins K, Chiarella SE, Radigan KA, Eisenbart J, Agrawal H, Berkelhamer S, Hekimi S, Zhang J, Perlman H, Shumacker PT, Jain M, Chandel NS. Epithelial cell death is an important contributor to oxidant-mediated acute lung injury. Am J Respir Crit Care Med 2011;183:1043–1054.
42. Kwon Y, Debaty G, Puertas L, Metzger A, Rees J, McKnite S, Yannopoulos D, Lurie K. Effect of regulating airway pressure on intrathoracic pressure and vital organ perfusion pressure during cardiopulmonary resuscitation: a non-randomized

interventional cross-over study. Scand J Trauma Resusc Emerg Med. 2015;23:83.

43. Cordioli RL, Brochard L, Suppan L, Lyazidi A, Templier F, Khoury A, Delisle S, Savary D, Richard JC. How Ventilation Is Delivered During Cardiopulmonary Resuscitation: An International Survey. Respir Care. 2018;63(10):1293-1301.
44. Chang MP, Lu Y, Leroux B, Aramendi Ecenarro E, Owens P, Wang HE, Idris AH. Association of ventilation with outcomes from out-of-hospital cardiac arrest. Resuscitation. 2019;141:174-181.
45. Myrianthefs PM, Briva A, Lecuona E, Dumasius V, Rutschman DH, Ridge KM, Baltopoulos GJ, Sznajder JI. Hypocapnic but not metabolic alkalosis impairs alveolar fluid reabsorption. Am J Respir Crit Care Med. 2005;171(11):1267-71.

Online Data Supplement

Methods

This translational study was conducted 1) in a porcine model of CA and prolonged CPR; 2) in a cohort of out-of-hospital CA patients undergoing manual or mechanical CC with a lung CT scan performed after resuscitation.

Experimental study

This is a secondary analysis of a previously published preclinical study (E1) comparing the hemodynamic effect of mechanical versus manual CC during ambulance transportation. We studied twelve successfully resuscitated pigs randomized to mechanical (n=6) or manual (n=6) CC with a thoracic CT scan performed at the end of resuscitation maneuvers.

Ethic statement

Procedures involving animals and their care were conducted in conformity with the institutional guidelines at the Istituto di Ricerche Farmacologiche Mario Negri IRCCS (IRFMN) and Azienda Polo Veterinario di Lodi, Università degli studi di Milano which adheres to the principles set out in the following laws, regulations, and policies governing the care and use of laboratory animals: Italian Governing Law (D.lgs 26/2014; Authorization n.19/2008-A issued March 6, 2008 by Ministry of Health); Mario Negri Institutional Regulations and Policies providing internal authorization for persons conducting

animal experiments (Quality Management System Certificate – UNI EN ISO 9001:2008 – Reg. N° 6121); the EU directives and guidelines (EEC Council Directive 2010/63/UE). They were reviewed and approved by the Mario Negri and Università di Milano Institute of Animal Care and Use Committee, which includes ad hoc members for ethical issues, and by the Italian Ministry of Health (Decreto no. 26/2014, authorization no. 979/2017-PR). Animal facilities meet international standards and are regularly checked by a certified veterinarian who is responsible for health monitoring, animal welfare supervision, experimental protocols and review of procedures.

Animal preparation

Twelve male domestic swine (34.0 ± 1.4 kg) were fasted with free water access the night before the experiments. Anesthesia was induced by intramuscular injection of ketamine (20 mg/kg) followed by intravenous administration of propofol (2 mg/kg) and sufentanyl (0.3 μg/kg) through an ear vein access. Anesthesia was maintained with a continuous intravenous infusion of propofol (4-8 mg/kg/h) and sufentanyl (0.3 μg/kg/h). A cuffed endotracheal tube was placed, and animals were mechanically ventilated in volume-controlled mode with a tidal volume of 15 mL/kg, a fraction of inspired oxygen (FiO_2) of 0.21, and a positive-end expiratory pressure of 5 cmH_2O, I:E 1:2 at baseline (Bellavista 1000, IMT Medical, Switzerland). Respiratory rate was adjusted to maintain the end-tidal partial pressure of carbon dioxide ($EtCO_2$) between 35 and 40 mmHg, using an infrared capnometer (LIFEPAK® 15 monitor/defibrillator, Physio-Control, WA, USA). For measurements of aortic pressure and right atrial

pressure fluid-filled 7F catheters were used. Frontal plane electrocardiogram (ECG) was recorded.

Experimental procedure

Animals were randomized by the sealed envelope method to receive mechanical or manual CC, before the induction of cardiac arrest. 1-2 mA alternating current delivered to the endocardium of the right ventricle was used to induce ventricular fibrillation (VF). Mechanical ventilation was discontinued after onset of VF and the endotracheal tube was left open to room air. After 2 min of untreated VF, continuous CC with one of the two strategies (mechanical or manual) was started and performed for 18 min during ambulance transportation. Unsynchronized mechanical ventilation was resumed simultaneously to CC, with the following parameters: volume-controlled mode with tidal volume of 15 mL/kg, respiratory rate of 10 breaths/min, inspiratory to expiratory ratio (I:E) 1 to 1.5, FiO_2 of 1.0 and zero positive end-expiratory pressure (ZEEP) (Oxylog 1000, Dräger, Lübeck, Germany). Every 5 min during CPR, epinephrine (1 mg) was administered via the right atrium, while arterial blood samples were obtained. Manual CC was provided in accordance to 2015 international CPR guidelines (E2). Mechanical CC was delivered by the LUCAS® 3.0 chest compression system (Stryker/Jolife AB, Lund, Physio-Control, Sweden), which delivers continuous CC (rate: 102±2 per min; depth: 53±2 mm; duty cycle: 50±5%). In the first 3 min of CPR the ambulance was stationary, for the following 15 min the ambulance moved along a predefined itinerary inside the veterinary campus.

After the 18-min interval of CPR, defibrillation was attempted with a single biphasic 200-Joule shock, using a LIFEPAK® 15 monitor/defibrillator. Return of spontaneous circulation (ROSC) was defined as the presence of sinus rhythm with a mean arterial pressure (MAP) of more than 60 mmHg. If ROSC was not achieved, CPR was resumed and continued for 1 min prior to a subsequent defibrillation with an escalating energy strategy (300-360-J). If VF reoccurred after ROSC, an immediate defibrillation was delivered. The same resuscitation protocol was continued until successful resuscitation or for a maximum of 5 additional min. 10 min after ROSC a lung computed tomography (CT) was performed and then animals were monitored for additional 3 h, under anesthesia. A continuous infusion of propofol (4-8 mg/kg/h) and sufentanyl (0.3 μg/kg/h) was provided through an ear vein access. Post ROSC mechanical ventilation was provided using volume-controlled mode with the following parameters: tidal volume 15 mL/kg, positive-end expiratory pressure of 5 cmH_2O, I:E 1:2, a fraction of inspired oxygen (FiO_2) of 0.21-0.4 (Bellavista 1000, IMT Medical, Switzerland).

Measurements

ECG, hemodynamics (arterial and right atrial pressures), $EtCO_2$, and esophageal temperature were continuously recorded with two LIFEPAK® 15 monitor/defibrillators. All data were then stored on CODE-STAT 9.0 (Physio-Control, WA, USA) and exported as comma separated values (.csv) to LabChart 8.0 (ADInstruments, UK) for the analysis. For each minute of CPR the minimum, the maximum and the swing in right atrial pressure were computed. The variation of

right atrial pressure (Δ RAP) was reported as surrogate of intrathoracic pressure (ITP). Compliance of the respiratory system (Cpl,rs) was assessed at baseline and up to 3h after ROSC using dynamic compliance calculated using recursive least square algorithm, with a sample rate of 200Hz by the ventilator (Bellavista 1000, IMT Medical, Switzerland). Arterial blood gas analyses were assessed with i-STAT System (Abbott Laboratories, Princeton, NJ).

When blood was withdrawn from the animals, it was immediately centrifuged, and plasma was aliquoted (200 µl) and stored at -70°C for biomarker assays. Hs-cTnT was measured with an electrochemiluminescence assay (Cobas, Roche Diagnostics, Rotkreuz, CH). NT-proANP was assayed with a validated ELISA kit (Biomedica BI-20892, Wien, Austria) following the manufacturer's recommendations. Porcine Receptor for advanced glycation end products (RAGE) and Porcine Pulmonary Surfactant Associated Protein D (SPD) were measured with quantitative competitive immunoassay (ABclonal, Cliniscience, Rome, Italy).

Autopsy

At the end of the 72-hour post resuscitation observation, animals were anesthetized for echocardiographic examination and blood sample withdrawn. Animals were then euthanized painlessly with an intravenous injection of 150 mg/kg sodium thiopental. Lung tissue samples were excised from the ventral portion of the caudal left lobe, with careful dissection from surrounding tissues. Lung tissues were fixed by immersion in 10% formalin for at least 24 h then embedded in paraffin. Five-µm thick sections were obtained and stained with

hematoxylin-eosin. The extent of histologic lung damage (i.e. lung tissue versus alveolar airspace) was determined using quantitative stereological techniques as previously reported (E3).

CT scanning

At the end of the resuscitation maneuvers, a chest computerized tomography (CT) was performed with a 16-slices helical CT scanner (GE Brightspeed Elite®, GE Healthcare, Italy) using the following parameters: 1.25 slice thickness, tube current 220 mA, tube voltage 120 kV, scan speed 1 s/rotation, 0.938:1 pitch, 18.75 mm/rot. The images were reconstructed with a window setting for the evaluation of the lung parenchyma (level -700 HU; width: 1500 HU) and bone tissue (level: 600 HU; width: 3000 HU).

Lung CT scans were performed during breath holding at end-expiration at 5 cmH_2O, with subjects in dorsal recumbency and no contrast media was used. The OsiriX 10.0 software (Pixmeo, Switzerland) was used to perform the morphological analysis of the lung parenchyma.

Lung CT morphological analysis

Two veterinary radiologists, blind to study group assessed lung CT scans in order to describe the presence of the following lung findings: ground-glass attenuation, airspace consolidation, peribronchovascular thickening, interlobular septal thickening, air-bronchogram, and pleural effusion. Ground-glass attenuation and airspace consolidation were defined as an increased attenuation respectively without or with obscuration of the underlying vasculature. An air-bronchogram was

defined as an air-filled bronchus, which could be visualized in the parenchymal opacity (E4). Ground-glass attenuation and airspace consolidation were described in a scale from 0 to 2 as 0=absent, 1=local, 2=diffuse. Rib and sternal fractures were described.

Clinical study

This was a multicenter observational, retrospective cohort study conducted according to the Declaration of Helsinki and followed the Italian guidelines of good clinical practice and Data Protection Code. We recorded patient personal information anonymously using an alpha-numeric code and we filed patient data electronically.

We collected the clinical records of out-of-hospital CA patients admitted from 2011-01-01 to 2019-12-01 in the Intensive Care Units (ICU) of three different Italian hospitals (University Hospital San Gerardo, Monza; University Hospital IRCCS Ospedale Maggiore Policlinico, Milano; and University Hospital ASST Grande Ospedale Metropolitano Niguarda, Milano). The promoting center of the study was University Hospital San Gerardo in Monza.

The Ethical Committee Monza-Brianza Province, ASST Monza–Ospedale San Gerardo–Anestesia e Rianimazione, Monza, Italy (promoting center, Ethical Committee Monza N° 3070) and the Ethical Committee of the two collaborating centers (University Hospital IRCCS Ospedale Maggiore Policlinico, Milano Ethical Committee N° 935_2019, and University Hospital ASST Grande Ospedale Metropolitano Niguarda, Milano Ethical Committee N° 181-15042020) approved this study. Informed consent was waived based

on the retrospective observational nature of the investigation and as per approval of internal Ethical Committee.

The inclusion criteria were adult patients with out-of-hospital CA of non-traumatic origin who received CPR with either manual or mechanical CCs and underwent a lung CT scan within 24h from the cardiac arrest. Exclusion criteria were presence of aspiration pneumonia, pulmonary thromboembolism, lung cancer, chronic pulmonary diseases and lung CT scan performed after 24 hours of CA.

The following clinical data were retrieved from patient electronic medical records:

sex, age, weight, CA characteristics, physiological data including hemodynamics, gas exchanges and ventilator setting, ICU and hospital length-of-stay, hospital mortality.

Patients CT scanning

We analyzed lung CT scan performed at three different institutions. Each CT had been requested by the treating physicians as part of the diagnostic work-up of the patient.

Two helical multislice CT-scanners were used: Philips Tomoscan SR 7000 (Philips Medical Systems, Hamburg, Germany: 120 kV tube voltage, 165 mA/s tube current) and Somatom Definition Flash (Siemens, Munich, Germany: 120 kV voltage 110 mA/second tube current).

Different reconstruction methods were used during routine clinical imaging. Contiguous images were reconstructed with both 2 and 3 mm slice thickness. In patients who received contrast material, only baseline CT scan images without contrast were analysed.

Mechanically ventilated patients were scanned during uninterrupted ventilation, as per current clinical practice.

Lung CT quantitative analysis

Quantitative analysis of lung CT scans of experimental CAs and out-of-hospital CA patients were performed using manual segmentation in blind and published methods for volume and weight measurements (E5-E10).

The manual segmentation of lung parenchyma was performed with manual delineation of each lung (from the internal rib border and the external border of the mediastinum) using the mediastinal window (CT min = -250 HU, CT max = +150 HU). The full CT – scale window (CT min = -1000 HU, CT max = +1000 HU) was used instead to view bronchi, bronchioles, blood vessels, and pleural effusion allowing a more accurate identification of these structures, in order to exclude main vessels/bronchi from the segmentation (E9). Pleural effusion was also excluded from the segmentation.

Ten slices were selected: the most cranial and caudal CT-sections and eight evenly spaced CT-sections between them were analyzed. Each of these ten CT-sections was analyzed using the standard segmentation described above. Previously described densitometry method was used to assess four differently aerated lung compartments in the 10 sections (E5-E8). The results were extrapolated to the entire lung, according to the method described by Reske et al. (E10).

In each slice the lungs were divided into three sterno-vertebral areas of equal height (i.e. ventral, ventro-dorsal and dorsal) in which we

computed the number of voxels within each attenuation range: hyper-aerated (-1000 to -901 Hounsfield units [HU]), normally-aerated (-900 to -501 HU), poorly-aerated (-500 to -101 HU) and non-aerated lung parenchyma (-100 to +100 HU). Overall lung density was calculated as the average densitiy of all lung slices normalized by the areas of the lung slices. The gradient of lung density was calculates as (Ventral HU-Dorsal HU)/(ventral HU)*100. Increased lung density was defined in the presence of a mean lung density ≥ -500 HU, as this threshold is known to discriminate the presence of loss versus presence of aereation (E11-E12).

Statistical analysis

Continuous and categorical data were expressed as mean±standard deviation and frequency (percentage), respectively. Normality of distribution of continuous variables was assessed using D'Agostino-Pearson omnibus normality test. Difference among groups for continuous data was assessed using unpaired Student's t-test or Mann-Whitney U test, according to data distribution. Differences in categorical data among groups were assessed using the Fisher's exact test. Differences between the study groups (treatment effect) was evaluated using a two-way analysis of variance for repeated measurements over time (group-by-time interaction). In the presence of a significant test result, a post-hoc analysis was performed by controlling the false discovery rate using a two-stage step-up method of Benjamini, Krieger and Yekutieli for multiple comparisons.

In the morphological analysis of the CT scan findings, the presence of ground glass attenuation (GGA) and airspace consolidation (AC) were

evaluated in each of the six lung lobes of each animal. In order to adjust the model for the within animal correlation, difference among groups in the proportion of GGA and AC was calculated using an adjusted logistic regression analysis with robust clustering, where GGA and AC were considered as outcome variable, the type of chest compressions as exposure variable, and the pigs were considered as cluster variable. Graphs were represented using mean±standard deviation or whisker plots. Correlations between continuous data were explored using linear regression analysis. The degree of association was reported using the Pearson's correlation coefficient (r) ranging between -1; +1. In the clinical study, univariate logistic regression analysis was used to evaluate the association of different variables between the manual versus mechanical CC group (i.e. age and low-flow time in Table 3) with the presence of increased lung density. Prolonged or shorter low-flow time was defined for value above or below/equal to the median value (i.e. 26 minutes). As the number of cases of increased lung density was low (n=9), and the 95%CI was quite wide for both the exposure variable (type of CC) and the confounder (low-flow time) we investigate the role of low-flow time as confounder/effect modifier using as outcome variable – in place of the dichotomic variable increased/normal lung density– the mean lung CT expressed as a continuous variable by HU.

Accordingly, we explored the association of low-flow time and type of CC in a univariate linear regression model. To investigate the association between all possible combinations of type of low-flow time and type of CC with the mean lung CT and avoid the use of unstable multivariate models in a limited sample size (n=52), we

further explored the associations of the 4 groups of patients with outcome in 4 independent linear regression models (i.e. model A-D). As last, to include the interdependency among the 4 groups of patients that could not be taken into account in model A-D – in which the comparison was always between a single group against all 3 other groups of patients - we performed a non-parametric analysis among the 4 groups of patients using the Kruskal-Wallis test. We then performed post-hoc pairwise comparisons among all possible combinations using a Mann-Whitney U test.

Statistical significance was reached when the p-value <0.05 (two-tailed). Statistical analyses were performed using STATA-14/MP (StataCorp LP, College Station, TX, USA), GraphPad Prism 8.3.0 (GraphPad Software, San Diego, CA, USA) and Microsoft Excel for Mac 2017, Version 15.32.

	Mechanical CC (n=6)	Manual CC (n=6)	p-value
Ground glass attenuation			
Left lobe, n (%)			
• Cranial	5/6 (83)	3/6 (50)	0.545
• Caudal	6/6 (100)	6/6 (100)	/
Right lobe, n (%)			
• Cranial	6/6 (100)	5/6 (83)	1.000
• Middle	6/6 (100)	4/6 (67)	0.455
• Accessory	5/6 (83)	4/6 (67)	1.000
• Caudal	6/6 (100)	6/6 (100)	/
Overall cranial lobes, n (%)*	11/12 (92)	8/12 (67)	0.177
• Local	1/12 (8)	4/12 (33)	0.133
• Diffuse	10/12 (83)	4/12 (33)	0.024
Overall lower lobes, n (%)*	23/24 (96)	20/24 (83)	0.149
• Local	3/24 (12.5)	15/24 (63)	<0.001
• Diffuse	20/24 (83)	5/24 (21)	<0.001
All lobes	34/36 (94)	28/36 (78)	0.144
• Local	4/36 (11)	19/36 (53)	<0.001
• Diffuse	30/36 (83)	9/36 (25)	<0.001
Airspace consolidation			
Left lobe, n (%)			
• Cranial	5/6 (83)	2/6 (33)	0.242
• Caudal	6/6 (100)	4/6 (67)	0.455
Right lobe, n (%)			
• Cranial	5/6 (83)	3/6 (50)	0.545
• Middle	4/6 (67)	1/6 (17)	0.242
• Accessory	0/6 (0)	1/6 (17)	1.000
• Caudal	6/6 (100)	4/6 (67)	0.455
Overall cranial lobes, n (%)*	10/12 (83)	5/12 (42)	0.132
• Local	3/12 (25)	2/12 (17)	0.651
• Diffuse	7/12 (58)	3/12 (25)	0.139
Overall lower lobes, n (%)*	16/24 (67)	10/24 (42)	0.029
• Local	8/24 (33)	5/24 (21)	0.383
• Diffuse	8/24 (33)	5/24 (21)	0.346

All lobes	26/36 (72)	15/36 (42)	0.012
• Local	11/36 (30)	7/36 (19)	0.342
• Diffuse	15/36 (42)	8/36 (22)	0.147

Table E1. Lung morphological CT-scan analysis in the experimental study stratified by lung lobe location.

*According to swine lung anatomy lower lobes include middle, accessory and caudal lobes (E13). Overall cranial lobes include both cranial lobes of the left and right lung. Overall lower lobes include both lower lobes of the left and right lung.

Differences among groups were tested by the Fisher's exact test. Differences of ground glass consolidation and airspace consolidation among the groups for overall cranial and lower, and all lobes were adjusted for the within animal correlation by robust clustering. Significant p-values are reported in bold.

Table E2. Hemodynamic and echocardiographic variables in the experimental study.

	Manual CC (n=6)	**Mechanical CC (n=6)**	**p**
Systolic arterial pressure, mmHg			
Baseline	117±25	118±10	0.810
Post-ROSC, 10 min	103±9	113±24	
Post-ROSC, 120 min	107±13	104±7	
Post-ROSC, 180 min	117±14	115±10	
Diastolic arterial pressure, mmHg			
Baseline	84±14	80±13	0.889
Post-ROSC, 10 min	72±11	83±22	
Post-ROSC, 120 min	75±7	70±8	
Post-ROSC, 180 min	89±14	84±9	
Mean arterial pressure, mmHg			
Baseline	103±14	97±12	0.961
Post-ROSC, 10 min	82±10	93±22	
Post-ROSC, 120 min	89±9	85±8	
Post-ROSC, 180 min	98±16	97±12	
Right atrial pressure, mmHg			
Baseline	5±3	5±2	0.340
Post-ROSC, 10 min	8±2	9±2	
Post-ROSC, 120 min	5±2	6±3	
Post-ROSC, 180 min	6±3	7±3	
Heart rate, bpm			
Baseline	77±19	77±15	0.165
Post-ROSC, 10 min	124±24	159±50	
Post-ROSC, 120 min	114±24	121±36	
Post-ROSC, 180 min	111±19	110±29	
CO, L/min			
Baseline	2.9±0.4	3.4±0.4	0.408
Post-ROSC, 180 min	2.9±0.5	2.7±0.5	
Post-ROSC, 72 h	3.6±1.4	3.9±0.8	
LVEF, %			
Baseline	71±8	68±8	0.912
Post-ROSC, 180 min	53±24	57±12	

	Manual CC (n=36)	Mechanical CC (n=16)	p
Post-ROSC, 72 h	77±5	77±4	
EDV, mL			
Baseline	27±6	29±5	0.571
Post-ROSC, 180 min	33±9	36±9	
Post-ROSC, 72 h	37±4	39±14	
ESV, mL			
Baseline	7±2	9±3	0.795
Post-ROSC, 180 min	17±11	16±9	
Post-ROSC, 72 h	9±3	9±5	

ROSC=return of spontaneous consciousness; CO=cardiac output; EDV=end diastolic volume; ESV=end systolic volume; LVEF=left ventricle ejection fraction. Data expressed as mean±SD. Two-tailed p-value of treatment in a repeated measurements two-way analysis of variance.

Table E3. Hemodynamic characteristics of out of hospital cardiac arrest patients at ICU admission.

Hemodynamic variables			
Systolic arterial pressure, mmHg	120±15	102±28	0.005
Diastolic arterial pressure, mmHg	73±13	69±13	0.283
Mean arterial pressure, mmHg	89±12	80±14	0.026
Heart rate, bpm	76±19	94±23	0.008
Central venous pressure, mmHg	8±3	11±4	0.023
$ScVO_2$, %	74±9	73±10	0.801
SOFA Cardiovascular	2.0±1.5	3.3±0.8	0.045

$ScVO_2$=central venous oxygen saturation; SOFA=sequential organ failure assessment score.

Table E4.

A) Univariate analyses of association among the type of chest compressions (CC) and significantly different variables between the 2 groups (mechanical versus manual CC, see Table 3) with increased

lung density (number of events=9), defined as a lung mean CT HU within the whole lung ≥500 (categorical binomial data).

Variable	OR	95% CI	p
Age	0.97	0.93 – 1.02	0.236
Low flow time>26 minutes (Ref. Low Flow time≤26 minutes)	4.42	0.82 – 23.79	0.083
Mechanical CC (Ref. Manual CC)	6.6	1.39 – 31.28	0.017

B) Univariate analysis of association among the type of chest compressions (CC) and significantly different variables between the 2 groups (mechanical versus manual CC, see Table 3) with a higher lung CT density expressed as mean HU within the whole lung (continuous data).

Variable	β Coefficient	95% CI	p
Age	-1.55	-4.00 – 0.91	0.211
Low flow time>26 minutes (Ref. Low Flow time≤26 minutes)	96.31	25.25 – 167.36	0.009
Mechanical CC (Ref. Manual CC)	122.18	47.35 – 197.01	0.002

Table E5. Possible combinations of type of low-flow time and type of CC in patients with the mean lung CT of patients with out-of-hospital CA by 4 independent linear regression models.

Variable	β Coefficient	95% CI	p
Mechanical CC by Low flow time>26 minutes (Ref. Other patients) (14 versus 38 patients)	142.68	67.02 – 218.34	<0.001
Mechanical CC with Low flow time≤26 minutes (Ref. Other patients) (2 versus 50 patients)	-55.28	-252.63 – 142.06	0.576
Manual CC with Low flow time>26 minutes (Ref. Other patients) (12 versus 40 patients)	-22.50	-112.63 – 67.63	0.618

Manual CC with Low flow time≤26 minutes (Ref. Other patients) (24 versus 28 patients)	-88.65	-160.75 – -16.56	0.017

We investigated in 4 independent linear regression models (Model A-D) the association between low-flow time and type of CC with the mean lung CT. Patients undergoing mechanical CC and a prolonged low flow time (Model A) showed a strong positive correlation with mean lung density; in contrast, patients undergoing manual CC and with a shorter low flow time (model D) showed a negative correlation with mean lung density.

Supplemental figures

Figure E1. Correlation between lung weight (A) and lung volume (B) with compliance of the respiratory system (Cpl,rs).

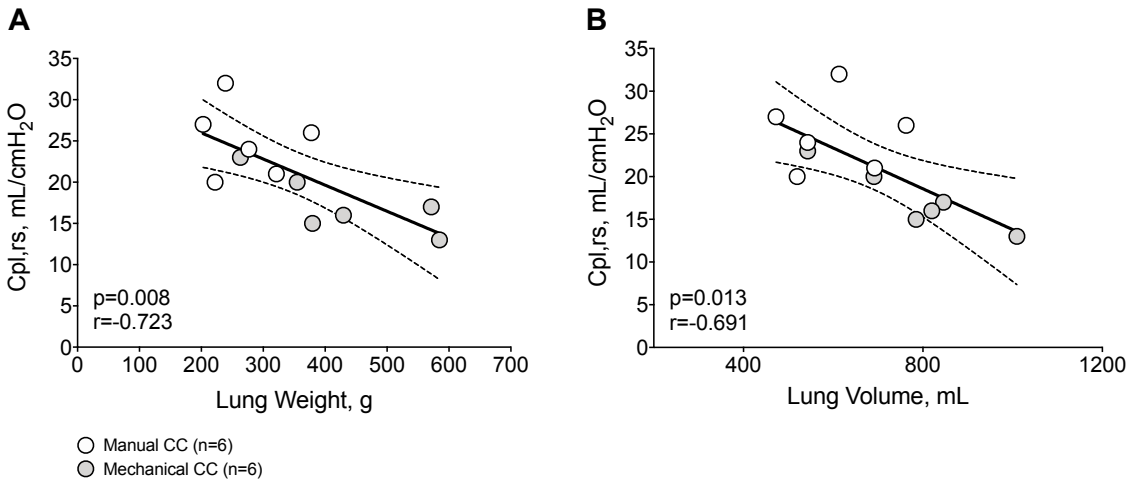
A
B
Cpl,rs, mL/cmH2O
Lung Weight, g
Lung Volume, mL
p=0.008
r=-0.723
p=0.013
r=-0.691
Manual CC (n=6)
Mechanical CC (n=6)

Figure E2. Representative image of in right atrial pressure variation (Δ RAP) during manual and mechanical CC.

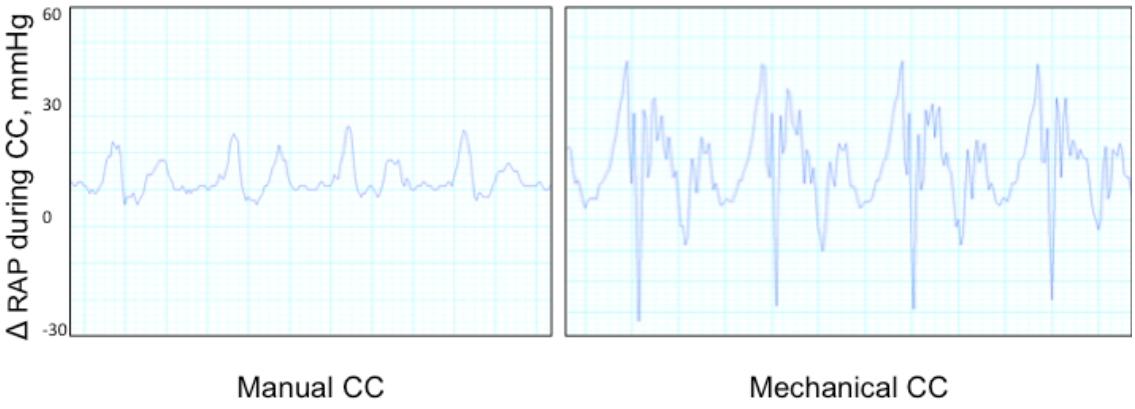

Figure E3. Differences in right atrial pressure variation (Δ RAP) among experimental groups over 18 minutes of cardiopulmonary resuscitation. Two tailed p-value of the difference among groups in a repeated measurements two-way analysis of variance.

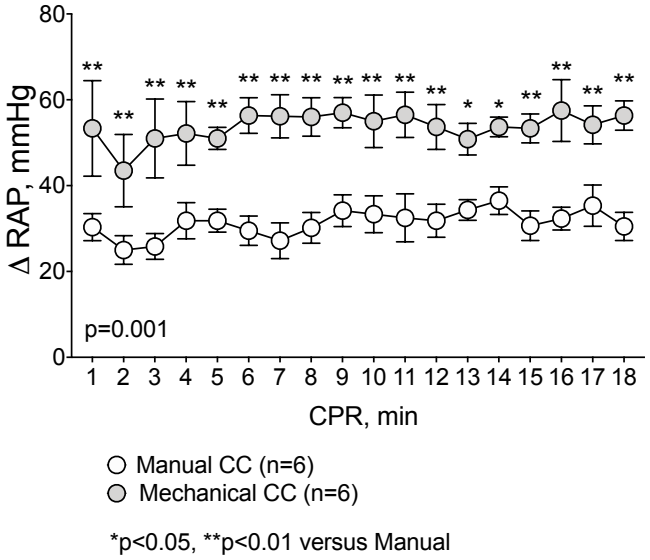

Figure E4. Differences in biomarkers of hemodynamic impairment (NT-proANP and TnT, A and B respectively) and lung injury (RAGE and SPD, C and D respectively) in plasma between experimental groups over 3-day follow-up. Two tailed p-value of the difference among groups in a repeated measurements two-way analysis of variance.

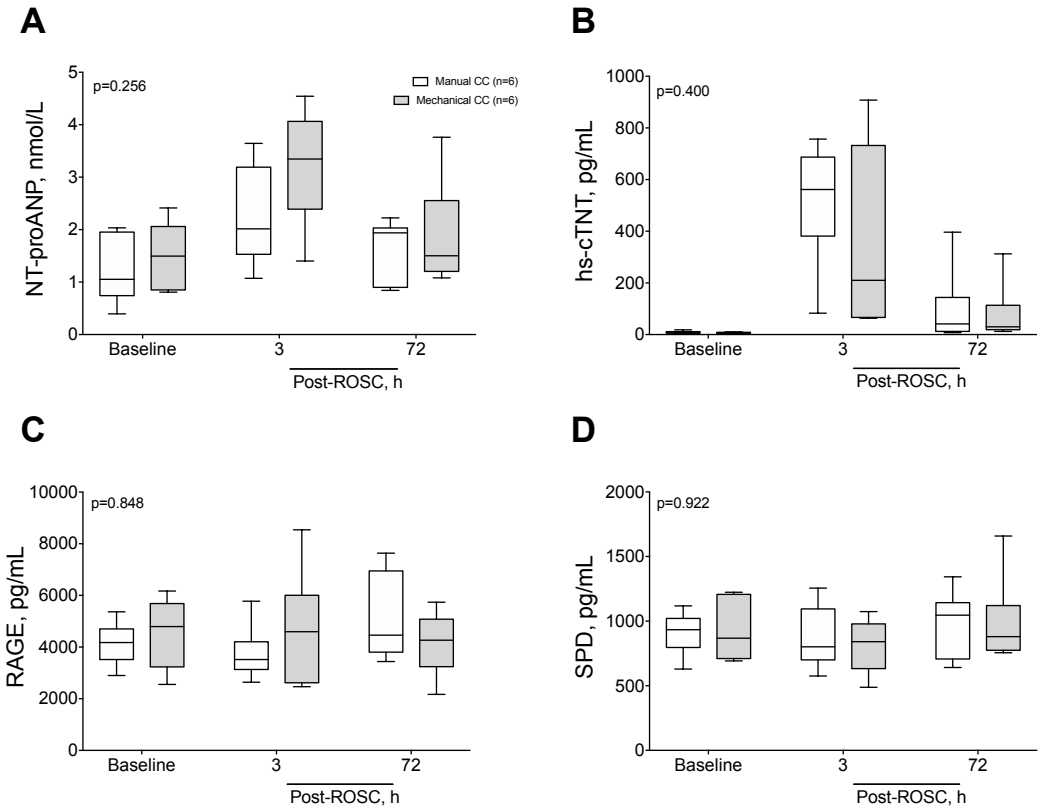

Figure E5. Histology of lung tissue at animal necropsy. Differences of alveolar lung tissue and alveolar airspace among experimental groups. Two tailed p-value of the difference among groups in a repeated measurements two-way analysis of variance.

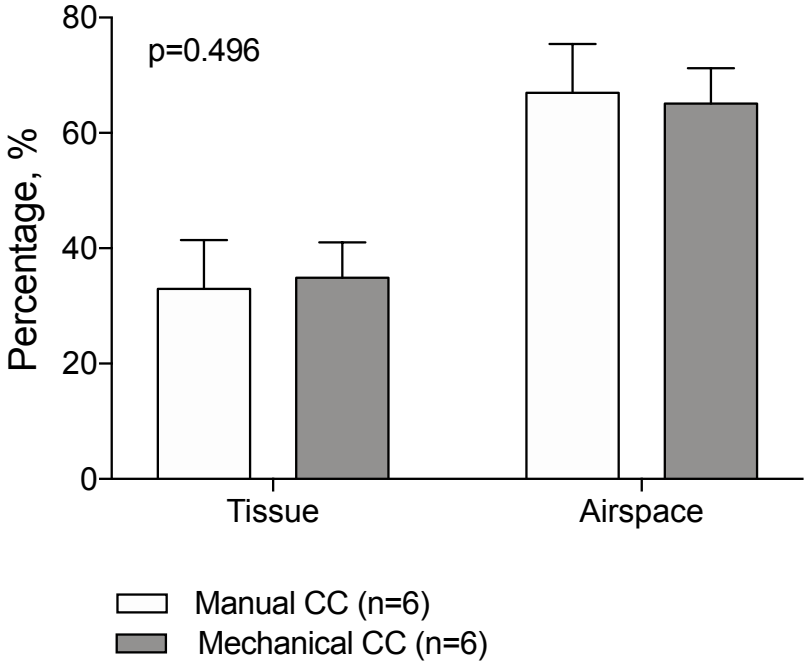

References:

1. Magliocca A, Olivari D, De Giorgio D, Zani D, Manfredi M, Boccardo A, Cucino A, Sala G, Babini G, Ruggeri L, Novelli D, Skrifvars MB, Hardig BM, Pravettoni D, Staszewsky L, Latini R, Belloli A, Ristagno G. LUCAS Versus Manual Chest Compression During Ambulance Transport: A Hemodynamic Study in a Porcine Model of Cardiac Arrest. J Am Heart Assoc. 2019;8(1):e011189.
2. Perkins GD, Handley AJ, Koster RW, Castrén M, Smyth MA, Olasveengen T, Monsieurs KG, Raffay V, Gräsner JT, Wenzel V, Ristagno G, Soar J. Adult basic life support and automated external defibrillation section Collaborators. European Resuscitation Council Guidelines for Resuscitation 2015: Section 2. Adult basic life support and automated external defibrillation. Resuscitation. 2015;95:81-99.
3. Hopkins N, Cadogan E, Giles S, et al: Chronic airway infection leads to angiogenesis in the pulmonary circulation. J Appl Physiol (1985) 2001; 91:919–928
4. E4. Komiya K, Ishii H, Murakami J, Yamamoto H, Okada F, Satoh K, Takahashi O, Tobino K, Ichikado K, Johkoh T, Kadota J. Comparison of chest computed tomography features in the acute phase of cardiogenic pulmonary edema and acute respiratory distress syndrome on arrival at the emergency department. J Thorac Imaging. 2013;28(5):322-8.
5. Puybasset L, Cluzel P, Gusman P, Grenier P, Preteux F, Rouby JJ Regional distribution of gas and tissue in acute respiratory distress syndrome. I. Consequences for lung morphology. CT

Scan ARDS Study Group. Intensive Care Med. 2000;26:857–869.

6. Gattinoni L, Caironi P, Pelosi P, Goodman LR. What has computed tomography taught us about the acute respiratory distress syndrome? Am J Respir Crit Care Med. 2001;164:1701–1711.
7. Rouby JJ, Puybasset L, Nieszkowska A, Lu Q. Acute respiratory distress syndrome: lessons from computed tomography of the whole lung. Crit Care Med. 2003;31(Suppl):S285-295.
8. Borges JB, Okamoto VN, Matos GF, Caramez MP, Arantes PR, Barros F, Souza CE, Victorino JA, Kacmarek RM, Barbas CS, Carvalho CR, Amato MB. Reversibility of lung collapse and hypoxemia in early acute respiratory distress syndrome. Am J Respir Crit Care Med. 2006;174:268-278.
9. Chiumello D, Marino A, Brioni M, Cigada I, Menga F, Colombo A, Crimella F, Algieri I, Cressoni M, Carlesso E, Gattinoni L. Lung Recruitment Assessed by Respiratory Mechanics and Computed Tomography in Patients with Acute Respiratory Distress Syndrome. What Is the Relationship? Am J Respir Crit Care Med 2016;193:1254–1263.
10. Reske AW, Reske AP, Gast HA, Seiwerts M, Beda A, Gottschaldt U, Josten C, Schreiter D, Heller N, Wrigge H, Amato MB.Extrapolation from ten sections can make CT-based quantification of lung aeration more practicable. Intensive Care Med. 2010;36(11):1836-44.
11. Gattinoni L, Pesenti A, Avalli L, Rossi F, Bombino M.

Pressure-volume Curve of Total Respiratory System in Acute Respiratory Failure. Computed Tomographic Scan Study Am Rev Respir Dis. 1987 Sep;136(3):730-6.

12. Gattinoni L, Caironi P, Pelosi P, Goodman LR. What Has Computed Tomography Taught Us About the Acute Respiratory Distress Syndrome? Am J Respir Crit Care Med. 2001 Nov 1;164(9):1701-11.
13. Judge EP, Hughes JM, Egan JJ, Maguire M, Molloy EL, O'Dea S. Anatomy and bronchoscopy of the porcine lung. A model for translational respiratory medicine. Am J Respir Cell Mol Biol. 2014 Sep;51(3):334-43.

Chapter 4. Post Resuscitation Care: Modulation of Kynurenine Pathway To Prevent Brain Injury After Cardiac Arrest.

Manuscript in preparation

Introduction

Cardiac arrest (CA) is a leading cause of death worldwide. (1) Despite efforts to improve cardiopulmonary resuscitation (CPR) interventions and post-resuscitation care, CA outcomes still remain poor. Only 12% of out-of-hospital CA patients survive to hospital discharge, and less than 10% of these survivors show good neurological recovery (1). The high mortality rate after successful resuscitation from CA can be due to the "post-CA syndrome", a distinctive pathophysiological process that includes neurological and cardiovascular dysfunction, together with systemic inflammatory reaction (2-4). The severity of post-cardiac arrest brain injury determines survival and neurological outcome. Indeed, hypoxic-ischemic brain injury accounts for 68% of hospital deaths after intensive care unit (ICU) admission in patients resuscitated from out-of-hospital CA (5).

Metabolism of the essential aminoacid tryptophan (TRP) to kynurenine, namely kynurenine (KYN) pathway (KP) (Figure 1), is emerging as one of the potential key components affecting cardiac arrest survival and neurological injury (6-8). Specifically, TRP is metabolized into KYN mainly by the enzyme indoleamine 2,3-dioxygenase (IDO). Inflammation can induce IDO expression in a variety of tissues, as well as in macrophages and dendritic cells via IFNγ or TNF (9-10). KYN has been identified as an endothelium-dependent relaxing factor contributing to the regulation of blood pressure in systemic inflammation (11). Downstream metabolites of KP include the neurotoxic 3-hydroxyanthranilic acid (3-HAA) and its derivatives, quinolinic acid (QA) and picolinic acid (PA). 3-HAA exerts its neurotoxic actions by inducing both cerebral oxidative stress

and excito-toxicity through activation of N-methyl-D-aspartate (NMDA) receptors by QA and PA (12-15). QA-induced neurotoxicity includes multiple mechanisms, such as generation of reactive oxygen species (16), inhibition of glutamate uptake (17) and excessive activation of NMDA-receptors (18). KYNA has neuroprotective properties acting as NMDA antagonist.

In a study including both small and large animals, it has been observed that KP is activated early after experimental CA (6). Thus, plasmatic reduction of TRP together with increased levels of KYN, KYNA and 3-HAA was consistently observed in all species, from the first hours following resuscitation, up to 3-5 days after CA. Of particular interest, an early activation of the KP has been highlighted in out-of-hospital CA patients and higher plasmatic levels of KP metabolites predicted 12-month poor neurological outcome (7). Indeed, in a prospective, multi-centre, observational study involving 21 intensive care units in Finland, higher levels of KP metabolites at ICU admission were associated with hypotension during the first 24 hours after resuscitation and with ICU mortality in out-of-hospital CA patients.

Although KP activation has been associated with poor outcome, the causative role of the pathway activation on neurological injury and survival after CA/CPR still remains to be elucidated. To date no studies have tested interventions that may inhibit the rate-limiting enzyme of KP after CA/CPR. This could represent a novel therapeutic target to reduce post-CA brain injury and improve outcomes.

Therefore, the aim of this study is to elucidate the impact of KP inhibition on outcome after CA/CPR in mice. More specifically, we

evaluated the effects of genetic deletion of the rate-limiting enzyme of the KP, indoleamine-2,3-dyoxygenase (IDO) on survival (aim 1) and neurological outcome (aim 2) after CA/CPR.

To further confirm the specific pathophysiological involvement of KP in brain injury, an additional positive control group of IDO knockout mice ($IDO^{-/-}$) received administration of L-kynurenine before induction of CA.

Methods

This is an experimental randomized animal study. The study experiments took place at the Istituto di Ricerche Farmacologiche Mario Negri (IRFMN), Istituto di Ricovero e Cura a Carattere Scientifico, Milan, Italy. Approval of the IRCCS-IRFMN on Animal Care together with Governmental Institutions clearance was obtained in order to perform the experiments. All procedures involving animals were conducted in conformity with national and international laws on animal care.

Animal preparation

Two strains of mice were used for this study: 8 to 12-week-old, weight-matched male C57BL/6 wild-type (WT) mice, and $IDO^{-/-}$ mice (19) on a C57BL/6 background. $IDO^{-/-}$ mice were purchased from the Jackson laboratories and then a colony was created at our institution. Mice were intubated, mechanically ventilated (rodent ventilator 28025, Ugo Basile, Italy), and instrumented under

anesthesia with isoflurane as previously described (20-23). Animals were ventilated with a respiratory rate of 110-120 breaths per minute (bpm) and a tidal volume of 10 μg/g of body weight. Anesthesia was maintained with isoflurane 1.5-2 vol% in an N2O/O2 (70%/ 30%). Fluid-filled microcatheters (PE-10, Becton Dickinson, Franklin Lakes, NJ) were inserted in the left femoral artery and vein, respectively, for monitoring blood pressure and for drug administration. Blood pressure and needle-probe electrocardiogram were recorded and analysed with the use of a PC-based data acquisition system (Labchart 8.0, Powerlab ADInstruments).

Mouse model of cardiac arrest and CPR

Experimental cardiac arrest and CPR in mice were performed using an established model (24). Briefly, mice were subjected to CA induced by potassium chloride (0.08 mg/g I.V.). After 8 min of untreated CA, finger chest compressions were delivered at a rate of 300 per minute. Mechanical ventilation with 100% oxygen was performed with a TV of 10 μg/g at a rate of 100 bpm. Infusion of 0.6 μg min^{-1} epinephrine was initiated 30 s before starting CPR. Chest compressions were delivered until return of spontaneous circulation (ROSC) was achieved. ROSC was defined as the return of sinus rhythm associated with MAP > 40 mm Hg lasting for at least 10 s. Mice were weaned from mechanical ventilation and extubated 60 min after CPR. Core body temperature was monitored by a rectal temperature probe and maintained at 37°C by a warming lamp after ROSC for 50 min. The survival times were recorded up to 7 days. For surgical pain relief during the recovery period, 2 mg/kg of 0.25% bupivacaine were

infiltrated around incisional wound after CPR. For pain relief, 0.1 mg/kg of buprenorphine I.P. before and 12 h after the procedure were administrated.

Assessment of Neurological Function

Neurological function score (NFS) was blinded assessed every 24 h for the 7 days of observation after CA/CPR. Neurological function scoring system previously described was used with minor modifications (25-26). Five parameters were assessed and scored: level of consciousness (no reaction to pinching of tail=0, poor response to tail pinch=1, normal response to tail pinch=2), corneal reflex (no blinking=0, sluggish blinking=1, normal blinking=2), respirations (irregular breathing pattern=0, decreased breathing frequency with normal pattern=1, normal breathing frequency and pattern=2), coordination (no movement=0, moderate ataxia=1, normal coordination=2), and movement/activity (no spontaneous movement=0, sluggish movement=1, normal movement=2). Total score was reported as the neurological function score (total possible score=10), dead mice were scored 0.

Continuous locomotor activity

Spontaneous locomotor activity was measured continuously through Digital Ventilated Cage (DVC®) system manufactured by Techniplast SpA (Buguggiate, Italy). Activity metric, as total distance walked, was recorded continuously in individually-housed mice after CA up to 7 days after ROSC. The system consists of a standard individual ventilated cage and an electronic sensing board underneath each cage.

The sensing board is composed by 12 electrodes connected to an integrated circuit that continuously measures their electrical capacitance. The electromagnetic field generated registered the effect of the presence of a mouse over an electrode that modifies the electromagnetic field causing a drop of the electrode signal, due to the change in electrical capacitance. The electrical capacitance sensing technology allows non-intrusive and continuous monitoring of the activity of the animals (27). Total distance travelled by each animal was computed for each day and dark/light cycles were reported up to 7 days post ROSC. Total distance was also measured in sham-operated animals, as a negative control group. Sham-operated mice received anesthesia, surgery and ventilation without CA.

Brain Magnetic Resonance Imaging acquisitions and analysis

To characterize the degree of ischemic brain injury after CA/CPR, diffusion-weighted imaging (DWI) was performed 24 hours after CA. The apparent diffusion coefficient (ADC) was used as a quantitative measurement of water diffusion changes in the brain. Intracerebral cytotoxic edema reduces water diffusivity and this corresponded to a reduction in ADC values. Brain imaging was performed on a 7 T small-bore animal scanner (Bruker Biospec, Germany) running ParaVision 6.01 and equipped with a quadrature 1H cryo probe surface coil as transmitter and receiver. Anesthetized mice (isoflurane 1.5-2% in a N_2O/O_2 (70/30%)) were positioned into the magnet. Respiratory frequency was monitored throughout the experiment and the body temperature maintained at 37°C with a water-heating pad.

Structural MRI: images were obtained with a 3D fast low angle shot magnetic resonance imaging (FLASH) sequence (TR/TE= 250/3ms; Flip angle 15°; image resolution of 100 × 100 × 100 μm3; FOV = 3 × 0.8 × 1.1 cm^2; acquisition matrix 300 × 80 × 110; total acquisition time=27min). The hypointense volumes were segmented manually following the Paxinos atlas by a trained expert using freely available ITK-SNAP software (28). Diffusion weighted echo-planar images (TR/TE=2000/48.5 ms) were adopted to obtain the apparent diffusion coefficient (ADC)-maps. Diffusion-encoding was applied in 3 orthogonal directions with b values of 200, 600 and 900 ms, respectively. ADC-maps were calculated on a pixel-by-pixel basis with an in-house MATLAB script using the model function: $\ln(S(b)/S0) = -b \cdot ADC$, where S(b) is the measured signal intensity at a specific b value (b) and S0 the signal intensity in the absence of a diffusion gradient (b = 0). The hypontense region was manually traced by an expert operator blind to experimental condition in three regions of interest: frontal cortex, caudoputamen and hippocampus. The average ADC value within each region of interest was computed for each animal. Group average ADC values were reported for each region of interest and the mean of the three analysed regions was reported as total. The lesion volume of each hypointense region was computed for each animal and group average was reported. The mean of the three analysed regions was reported as total.

Histological Brain Injury

Tissue processing for histological analysis

Twenty four hours after CA, mice were deeply anaesthetized with Ketamine 20 mg + Medetomidine 0.3 mg (ip) and transcardially perfused with 20 ml of PBS, 0.1 mol/l, pH 7.4, followed by 50 ml of chilled paraformaldehyde (4%) in PBS. The brains were carefully removed from the skull and post-fixed for 6 h at 4 °C, and then transferred to 30% sucrose in 0.1 mol/l PBS for 24 h until equilibration. The brains were frozen by immersion in isopentane at −45 °C for 3 minutes before being sealed into vials and stored at −80 °C until use. Coronal brain cryosections 20 μm thick were cut serially at -20°C at 320 μm intervals and stored at 4 °C in a solution of glycerol:PBS (1:1).

Slice selection and image acquisition

Four brain coronal sections per mouse at +2.58, +0.74, – 2.06, –3.20 mm from bregma, were used to quantify degenerating neurons and neuronal cell loss. The entire brain sections were acquired at 20X by an Olympus BX-61 Virtual Stage microscope, with a pixel size of 0.346 mm. Acquisition was done over 10 mm thick stacks, with a step size of 2 mm. The different focal planes were merged into a single stack by mean intensity projection to ensure consistent focus throughout the sample.

Quantification of degenerating neurons and neuronal cell loss

Degenerating neurons were identified by Fluoro Jade (Sigma-Aldrich, St. Louis, MO) labeling and counted as previously described (29).

Briefly, sections were dried in ethanol (100%, 75% and 50%) and rehydrated in distilled water. Sections were then incubated in 0.06% potassium permanganate, washed in distilled water and transferred to 0.001% FJ staining solution. Sections were rinsed in distilled water, dried, immersed in xylene and coverslipped. High-power fields (20X magnification; Olympus) along the frontal cortices, the caudate putamen, the CA1 and CA3 pyramidal cell layers, the hilus, were acquired. FJ-positive neurons were marked and an automated cell count was generated using Image J software. Cresyl Violet staining (Sigma-Aldrich, St. Louis, MO) was used to quantify neuronal cell. Neuronal count was performed by segmentating cells and excluding the round-shaped signal sized below the area threshold of 25 mm^2 that is known to be associated with glial cells as reported previously (30-32) and expressed as density of cells/mm^2 within each side. The CA1, CA3, CA4 pyramidal cell layers and hilus neurons were manually quantified using Image J software. Data obtained in each slice/area/brain were averaged providing a single value per mouse used for statistical analysis.

Administration of L-Kynurenine

L-Kynurenine (Sigma-Aldrich) was administered as described previously (33-34). Briefly, L-Kyn was dissolved in 0.1M HCl and brought to a final concentration of 2 mg/mL in phosphate-buffered saline (PBS) after adjusting pH to 6.5 to 7.0. Mice were injected with L-Kyn (20 mg/kg i.v.) 15 minutes before the induction of CA. For the experiments #2 WT and $IDO^{-/-}$ mice received the same volume of PBS intravenously 15 min before CA.

Statistical Analysis

Normality of data distribution was assessed using D'Agostino-Pearson omnibus normality test. Continuous and categorical data variables were described as mean±standard deviation of mean (SD) or median (interquartiles) as appropriate. Animals were randomized on 1:1 or 1:1:1 basis with a list randomizer (https://www.random.org/lists/) according to the treatment group in 2 independent experiments.

In aim 1, we wished to test the effect of genetic deletion of the enzyme (IDO knockout mice, $IDO^{-/-}$) on survival up to 7 days after CA. The following groups were compared:

1. Treatment group, IDO knockout mice ($IDO^{-/-}$) versus control group, wild type mice (WT).

In aim 2, we wished to determine the ability of genetic deletion of the enzyme to prevent brain injury, and to preserve neurological function up to 24 h after CA. The following groups were compared:

2. Treatment group, IDO knockout mice ($IDO^{-/-}$) versus control group, wild type mice (WT) versus a positive control group, $IDO^{-/-}$ + L-kynurenine ($IDO^{-/-}$ + L-kyn).

Difference among groups for continuous data was assessed using unpaired Student's t-test or Mann-Whitney U test, according to data distribution. Differences in categorical data among groups were assessed using the Fisher's exact test. Differences between the study groups (treatment effect) was evaluated using a two-way analysis of variance for repeated measurements over time (group-by-time interaction). In the presence of a significant test result, a post-hoc analysis was performed by controlling the false discovery rate using a

two-stage step-up method of Benjamini, Krieger and Yekutieli for multiple comparisons.

The Kaplan–Meier analysis and log-rank test were used to calculate the survival rates (primary outcome). Significance was considered at the level of $p<0.05$. GraphPad Prism 7.0 (GraphPad Software Inc., La Jolla, CA, USA) and STATA-14/MP (StataCorp LP, College Station, TX, USA) was used for statistical analyses.

Sample size justification

As the mean survival rate at 7 days after CA was expected to be 40% in WT mice, as showed in previous study by Minimashida et al. (23), and 80% in $IDO^{-/-}$ mice (expected effect size on mortality, HR=0.25), we anticipate that 16 mice per group were required for the survival study ($\alpha=0.05$, $\beta=0.8$, two-sided). For the secondary outcome of the study, the apparent diffusion coefficient (ADC) of DWI sequences of the brain at 24h after resuscitation was used. As the mean cortical ADC value was expected to be 0.47 ± 0.07 mm^2/ms at 24h after CA (23) and considering a 25% increase in the mean value in $IDO^{-/-}$ mice, we anticipate that 6 mice per group were required for the MRI study ($\alpha=0.05$, $\beta=0.8$, two-sided).

RESULTS

IDO-Deletion Improved Survival, Neurological Function and Locomotor Activity After Cardiac Arrest

No significant differences in body weight, temperature, total dose of epinephrine and CPR time to ROSC were observed between WT and $IDO^{-/-}$ mice. At baseline, hemodynamic parameters including heart rate and mean arterial pressure did not differ among groups (Table 1).

The survival rate was 37.5% (6 of 16) in WT mice at 7 days after CA/CPR. $IDO^{-/-}$ mice showed higher survival of 68.75% (11 of 16; log rank *P*=0.0361 versus WT, Figure 2). Neurological function was higher in $IDO^{-/-}$ mice than in the WT animals throughout the 7 days following CA (treatment p value: p=0.0124, figure 3).

Heart rate did not differ significantly overtime between the two groups (treatment p value: p=0.73). Mean arterial pressure (MAP) at baseline did not differ between groups, at the time of ROSC, 30 and 60 min after resuscitation MAP was significantly higher in $IDO^{-/-}$ mice compared to WT mice (treatment p value: p=0.0005) (Table1).

The total distance travelled by sham-operated animals in the 7 days after surgery was 1659±141 m. After CA, WT mice exhibited a significant decline in spontaneous locomotor activity compared to sham animals (WT 649±319 m, p=0.027 *vs* sham). IDO-deleted animals showed an improved locomotor function compared to WT mice (total distance travelled: 1403±279 m, p=0.037, Figure 4D). The cumulative distance covered by WT (Figure 4A) and $IDO^{-/-}$ mice (Figure 4B) during the dark/light periods up to 7 days after CA is

shown in Figure 4. As shown, spontaneous locomotor activity was higher in $IDO^{-/-}$ animals compared to WT after CA.

Kynurenine Pathway inhibition Prevents Brain Water Diffusion Abnormality 24 Hours After CA and CPR

No significant differences in body weight, temperature, total dose of epinephrine, CPR time to ROSC were observed between WT, $IDO^{-/-}$ and $IDO^{-/-}$ +Lkyn mice (Table 2).

Magnetic resonance imaging acquired 24 hours after CA/CPR showed areas of hyperintense signal in DWI sequences of the brain of WT mice. The ADC maps reported the same areas of restricted diffusion as hypointense signal. In Figure 5 is represented an ADC map of a WT mouse 24 hours after resuscitation.

Intracerebral cytotoxic edema reduces water diffusivity and this corresponded to a reduction in ADC values. The degree of abnormal water diffusion was quantified by calculating the average ADC in several regions of interest, including the frontal cortex, hippocampus and caudoputamen.

Twenty four hours after CA, WT mice showed a restriction in water diffusion in each region of interest and across the whole brain compared to sham-operated animals (Figure 6). $IDO^{-/-}$ mice showed a protection against the development of ischemia-induced brain edema (Figure 6A). Specifically, ADC values were higher in the frontal cortex and caudoputamen in the $IDO^{-/-}$ group compared to the WT group (Figure 6B-C). This beneficial effect was reverted by the administration of L-kynurenine before the induction of CA in the frontal cortex, caudoputamen and across the whole brain. A trend

towards a protective effect of IDO-deletion was observed also in the hippocampus (Figure 6D).

Neurological function significantly improved in $IDO^{-/-}$ mice compared to WT animals (p=0.005, Figure 7A). At 24h after CA, the ADC of the total brain positively correlated with the neurological function score (r=0.71, p=0.005, Figure 7B). A strong positive correlation is also observed between the ADC of each region of interest and the NFS (Figure 8A-C).

The volumes of the hypointense regions in ADC maps were computed for each region of interest (Figure 9). No significant differences were detected in lesion volumes between WT, $IDO^{-/-}$ and $IDO^{-/-}$+L Kyn mice in the hippocampus and caudoputamen (Kruskal-Wallis test, respectively p=0.48 and p=0.32, Figure 9C-D). A trend toward a reduction in cortical lesion volumes was observed in the $IDO^{-/-}$ group compared to WT and $IDO^{-/-}$+L Kyn groups (Kruskal-Wallis test, p=0.052, Figure 9B). When considering the lesion volumes of the total brain we found a significant reduction in the $IDO^{-/-}$ group compared to the $IDO^{-/-}$+L Kyn group (Kruskal-Wallis test, p=0.009, Figure 9A).

IDO-deletion Prevents Neuronal degeneration After CA and CPR

Histological studies revealed that the number of degenerating neurons, represented as Fluoro-Jade B positive cells, in the frontal cortex, caudoputamen and in different regions of the hippocampus (CA1 and hilus) was increased at 24 hours after CA compared to sham-operated mice (Figure 10). A trend towards prevention of neuronal degeneration in IDO-deleted mice was observed in frontal cortex (p=0.057, Figure 10A), while the administration of L-kyn dampened

the reduction in degenerating cells. No significant differences were observed in the number of Fluoro-Jade B positive cells among regions of the hippocampus including CA1 and CA3, while in the hilus a significant reduction in neuronal degeneration was observed in the $IDO^{-/-}$ group compared to $IDO^{-/-}$+L Kyn group (figure 10E).

Neuronal cells loss was observed in the caudoputamen and hilus in WT mice compared to sham operated animals at 24 hours after resuscitation (Figure 11B and 12D). IDO-deleted animals were protected from neuronal cell loss only in the caudoputamen (Figure 10B). Among all the regions of the hippocampus analyzed no differences in cell count was reported (figure 12).

Discussion

In this study we provide evidence that kynurenine pathway inhibition through IDO-deletion markedly improves survival and neurological outcome after experimental CA. The neuroprotective effects of IDO-deletion were associated with attenuation of CA-induced abnormality in water diffusion detected with brain magnetic resonance imaging at 24 hours after resuscitation and with prevention of neuronal degeneration in the hilus and in the frontal cortex. The protective effect of IDO-deletion was also associated with reduced neuronal cell loss in the caudoputamen. Moreover, IDO-deletion accelerated the recovery of spontaneous locomotor function up to 7 days after CA. Finally, administration of L-Kyn in $IDO^{-/-}$ mice abrogated the protective effects of IDO-deletion on neurological function, ischemic brain edema and neuronal degeneration after CA.

Taken together these observations suggest that inhibition of KP could represent a novel target to improve neurological outcomes after resuscitation.

Hypoxic-ischemic brain injury following CA has been increasingly recognized as the primary determinant of neurologic outcome after CA (4, 35). The unique vulnerability of the brain to ischemia and hypoxia provide the basis to understand the pivotal role of brain protection in post-resuscitation care. Neurological injury after CA is attributed to the primary ischemic injury during circulatory arrest and the suboptimal flow that depends on the quality of CPR; and the secondary injury following return of spontaneous circulation. Post-CA secondary injury accounts for several pathogenetic pathways including excitotoxicity, neuroinflammation, disrupted ion channel homeostasis, and membrane failure, as well as pathological activation of proteases and cell death signaling (4, 35).

Among different neurobiological cascades implicated in the pathophysiology of post-cardiac arrest brain injury**,** the role of KP activation has recently emerged (6-8). The KP has been recognized as a key player in the mechanisms of neuronal damage in several neurodegenerative disorders (36-38). Indeed, traumatic brain injury induces a striking activation of the KP pathway with sustained increase of the neurotoxic metabolite QA (36). Activation of the KP is also associated with acute brain dysfunction and mortality in intensive care unit patients (37) and correlates with infarct volume in stroke patients (38).

Along these lines, we previously characterized the role of KP activation after CA observing that: 1) KP is early activated after

experimental CA and KP metabolites increased from 2 hours following resuscitation up to 3-5 days after CA (6); 2) Higher levels of KP metabolites are associated with ICU mortality and 12-month poor neurological outcome in patients after CA (7); 3) inhibition of the KP improves neurological recovery in a rat model of cardiac arrest (39).

In the current study a marked improvement in survival and neurological function was observed in IDO-deleted mice after experimental CA. The neuroprotective effect of KP inhibition is supported by several lines of evidence both in long-term (7 days) and short-term (24h) observation. A higher neurological function score was observed in $IDO^{-/-}$ animals throughout the observation period up to 7 days post ROSC, indicating a better neurological performance compared to WT mice.

Previous report showed a significant decline of spontaneous activity after 8 min of CA in mice (40). IDO-deleted mice showed a higher spontaneous locomotor activity and a significant increase in the total distance travelled was observed up to 7 days after ROSC compared to WT animals. Notably, in this study the locomotor activity was recorded automatically and continuously 24/7, thus reducing the bias from the operator performing the tests and adding insights on the impact of CA on behavior throughout the light/dark cycles. As previously reported, $IDO^{-/-}$ mice did not show any behavioral abnormalities under normal conditions (41). Interestingly, a breakdown of the circadian rhythms was observed in WT animals after CA, whereas IDO-deletion seemed to preserve the circadian system.

In the present study, WT mice that were successfully resuscitated from 8 minutes of CA exhibited a marked abnormality in water diffusion in the cortex, caudoputamen and hippocampus 24 hours after CPR. The presence of restricted diffusion, corresponding to a low ADC value, in the vulnerable regions of the brain 24h after CA strongly correlated with neurological function. In contrast, IDO-deletion markedly attenuated the development of abnormalities in water diffusion in the brain and improved neurological outcomes. These observations are consistent with clinical studies showing that diffuse abnormalities in DWI are associated with poor outcomes in patients resuscitated from CA (42-47). However, the sensitivity and specificity of DWI abnormalities in outcome prediction varied widely, mostly due to the inconsistence definition of DWI alterations across studies. ADC enables a quantitative measurement of water diffusion changes (47-50). Consistently with clinical findings, in this study the ADC value positively correlated with neurological function score.

Restricted water diffusion indicates the presence of brain edema presumably resulting from disruption of ion pump function and membrane failure. The present observations therefore suggest that IDO-deletion can preserve ion pump homeostasis and membrane integrity early after CA. The administration of L-Kyn in genetic deleted mice abolishes the protective effect on brain edema after CA. Accordingly, previous studies showed that L-Kyn administration exacerbates acute neuronal damage after experimental stroke (51-52).

It has been previously reported that the inhibition of the first step in the KP has neuroprotective effects. Indeed, $IDO^{-/-}$ mice show

decreased levels of 3-hydroxykynurenine in the striatum and are less sensitive to QA-induced striatal neurotoxicity (53).

Inhibition of KP has been demonstrated to have beneficial effects also in the setting of systemic inflammation (11,41-42). Endotoxemia increased IDO expression in endothelial cells, leading to activation of KP and increase in KYN concentration causing hypotension. In mice injected with LPS, IDO-deletion attenuated the endotoxemia-induced hypotension suggesting that IDO activation plays a key role in regulation of vascular tone (11).

The protective effect of the blockade of IDO has been also demonstrated in endotoxin shock in mice. Specifically, the authors showed that IDO-deletion increases survival after LPS-induced endotoxin shock and reduces serum cytokine levels in mice (41). IDO inhibition reduces mortality from experimental polimicrobial peritonitis and sepsis via recruitment of neutrophils and mononuclear cells by chemokine production in peritoneal CD11b(+) cells (42). Consistent with these observations, we report that $IDO^{-/-}$ mice exhibited a protection against post resuscitation hypotension. Indeed, deletion of IDO1 attenuated the drop in mean arterial pressure after ROSC (~22 mmHg WT *vs* ~8 mmHg $IDO^{-/-}$). L-Kyn administration led to hypotension with a reduction in MAP of ~35 mmHg at 60 min after resuscitation compared to baseline values.

The main limitation of this study is represented by the absence of a group subjected to pharmacological inhibition of KP after CA. From the viewpoint of translating the present results into clinical benefit, the pharmacological inhibition of KP after resuscitation would add relevance to the present findings.

Different IDO inhibitors have been developed in the last years (56), in preclinical settings the most used IDO inhibitor is represented by 1-methyl-tryptophan (1MT). In clinical settings various compounds have been studied, in the field of oncology they have been used as immunometabolic adjuvants since 2008 (57); and phase I-II clinical trials are still ongoing (58).

In conclusion, the current study revealed protective effects of IDO-deletion on neurological and survival outcomes after CA in mice. Our observations suggest that inhibition of KP may prevent ischemic brain injury after CA by reducing brain edema. Administration of L-Kyn in $IDO^{-/-}$ mice abolishes the protective effects on brain edema. Further studies are warranted to elucidate the role of pharmacological inhibition of KP after CA, in order to explore the translability of these experimental findings into a clinical setting.

Table 1. Group characteristics before cardiac arrest and in the first hour after resuscitation

	WT (n=16)	IDO$^{-/-}$ (n=16)	p
Body weight, g	27±1.5	27±1.4	0.68
Total dose of epinephrine, μg	1.14±0.3	1.29±0.4	0.41
CPR time to ROSC, sec	84±30	99±39	0.41
HR before CA, bpm	402±47	394±52	0.73
HR at ROSC, bpm	449±45	375±49	-
HR PR 30, bpm	431±63	458±48	-
HR PR 60, bpm	386±76	457±59	-
MAP before CA, mmHg	76±7	77±135	0.75
MAP at ROSC, mmHg	100±16	112±11	0.004
MAP 30 PR, mmHg	57±13	69±14	0.005
MAP 60 PR, mmHg	53±12	70±14	0.0001

CA=cardiac arrest, ROSC=return of spontaneous circulation, CPR=cardiopulmonary resuscitation, HR=heart rate, MAP=mean arterial pressure.

Table 2. Group characteristics before cardiac arrest and in the first hour after resuscitation

	WT (n=6)	IDO$^{-/-}$ (n=5)	IDO$^{-/-}$ +L kyn (n=4)	p
Survival to 24h PR, n	6/9	5/7	4/8	0.76
Body weight, g	31±6	32±4	30±5	0.68
Total dose of epinephrine, μg	0.98±0.17	0.99±0.11	0.95±0.18	0.41
CPR time to ROSC, sec	68±17	69±11	65±16	0.41
HR before CA, bpm	458±59	455±42	456±35	0.45
HR at ROSC, bpm	445±66	436±44	476±19	-
HR PR 30, bpm	475±68	451±62	457±55	-
HR PR 60, bpm	443±87	484±38	347±34	-
MAP before CA, mmHg	79±4	82±9	79±10	0.19
MAP at ROSC, mmHg	112±13	113±8	99±26	-
MAP 30 PR, mmHg	66±14	76±19	61±24	-
MAP 60 PR, mmHg	56±16	72±23	44±13	-

CA=cardiac arrest, ROSC=return of spontaneous circulation, CPR=cardiopulmonary resuscitation, HR=heart rate, MAP=mean arterial pressure.

Table 3. Brain MRI characteristics

	WT (n=6)	IDO$^{-/-}$ (n=5)	IDO$^{-/-}$ +L kyn (n=4)	p
Total brain ADC, mm^2/ms	0.48±0.07	0.6±0.02	0.47±0.07	0.01
Cortex ADC, mm^2/ms	0.47±0.09	0.60±0.03	0.48±0.07	0.01
Caudoputamen ADC, mm^2/ms	0.45±0.06	0.56±0.03	0.45±0.04	0.003
Hippocampus ADC, mm^2/ms	0.56±0.07	0.62±0.03	0.52±0.08	0.053
Total brain volume of lesion, mm^3	0.36 (0 – 3.08)	0 (0 – 0)	1.1 (0 – 1.8)	0.009
Cortex volume of lesion, mm^3	2.6 (0 – 7.9)	0 (0 – 0.7)	1.8 (1.3 – 3.6)	0.052
Caudoputamen volume of lesion, mm^3	0.52 (0 – 3.8)	0 (0 – 0.77)	1.18 (0.27 – 1.7)	0.32
Hippocampus volume of lesion, mm^3	0 (0 – 0.97)	0 (0 – 0)	0 (0 – 0.45)	0.48

ADC=apparent diffusion coefficient, data are represented as mean and SD or median and interquartile range. p value of 1-way ANOVA is reported

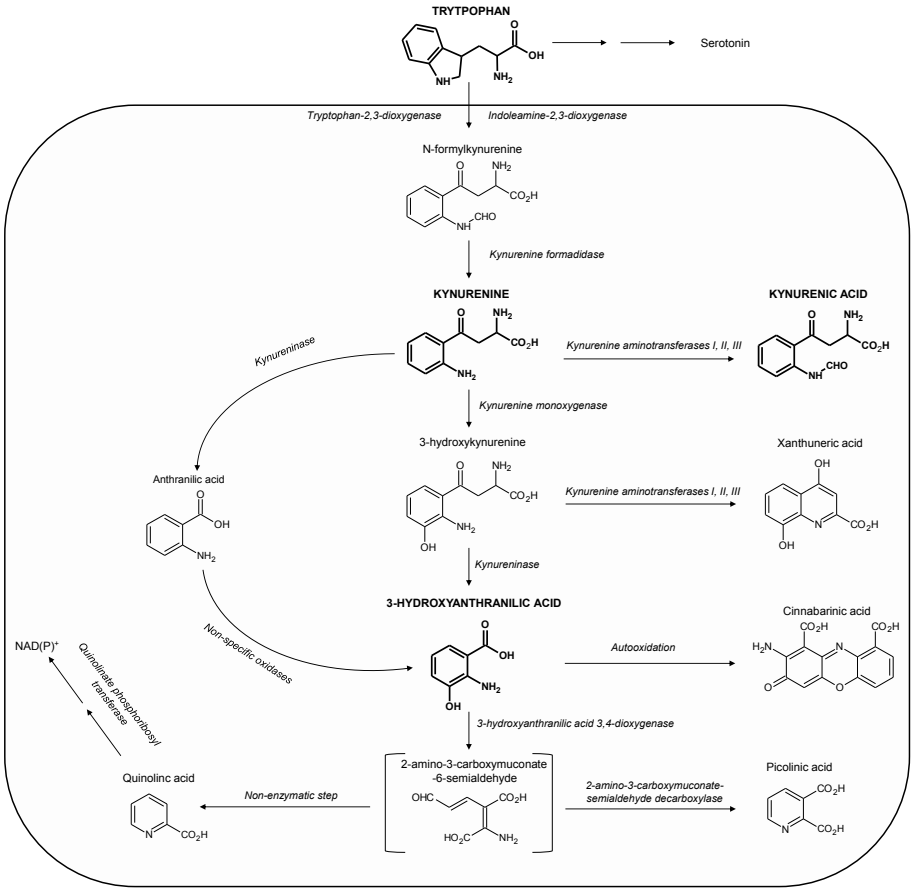

Figure 1. Overview of the kynurenine pathway.

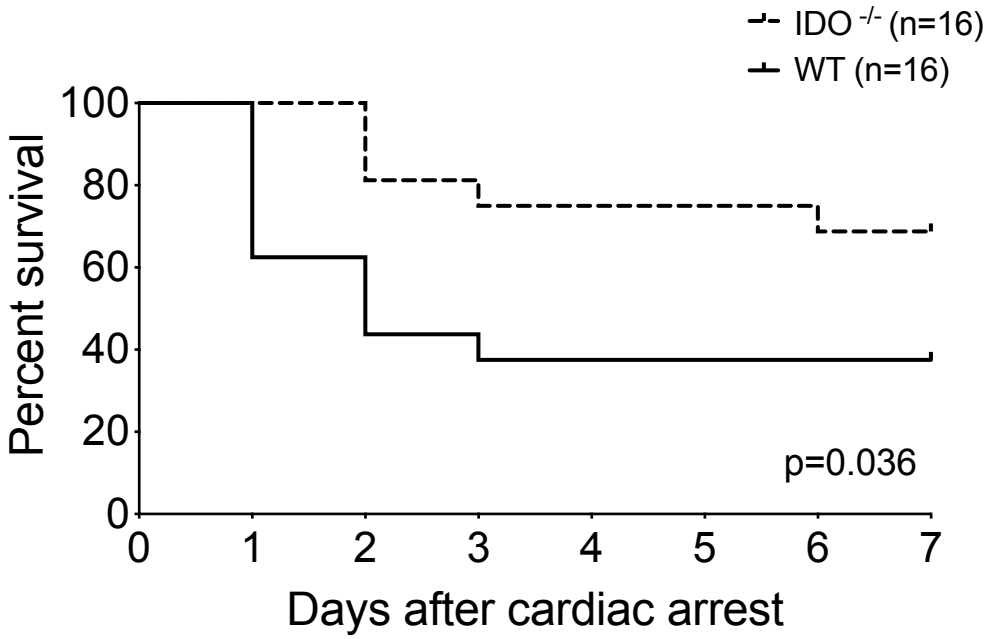

Figure 2. Survival rate of wild-type mice during the first 7 days after cardiac arrest (CA) and cardiopulmonary resuscitation (CPR). $IDO^{-/-}$ indicates knock-out mice for Indoleamine 2,3-deoxygenase (IDO). p=0.036 vs WT by log-rank test.

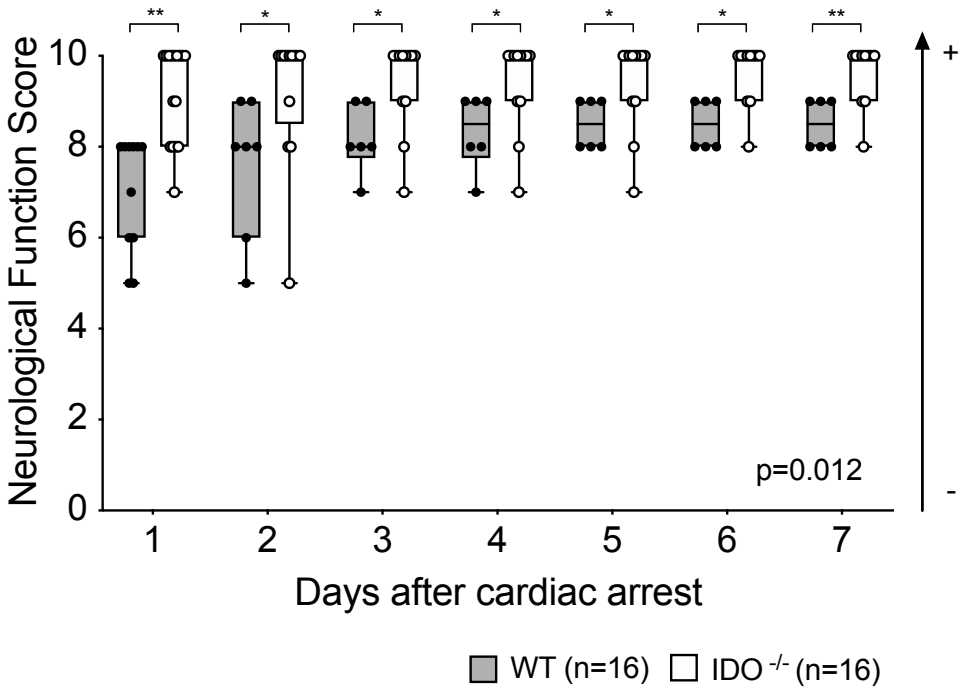

Figure 3. Neurological function score in surviving mice in the 7 days after cardiac arrest/cardiopulmonary resuscitation (CA/CPR).

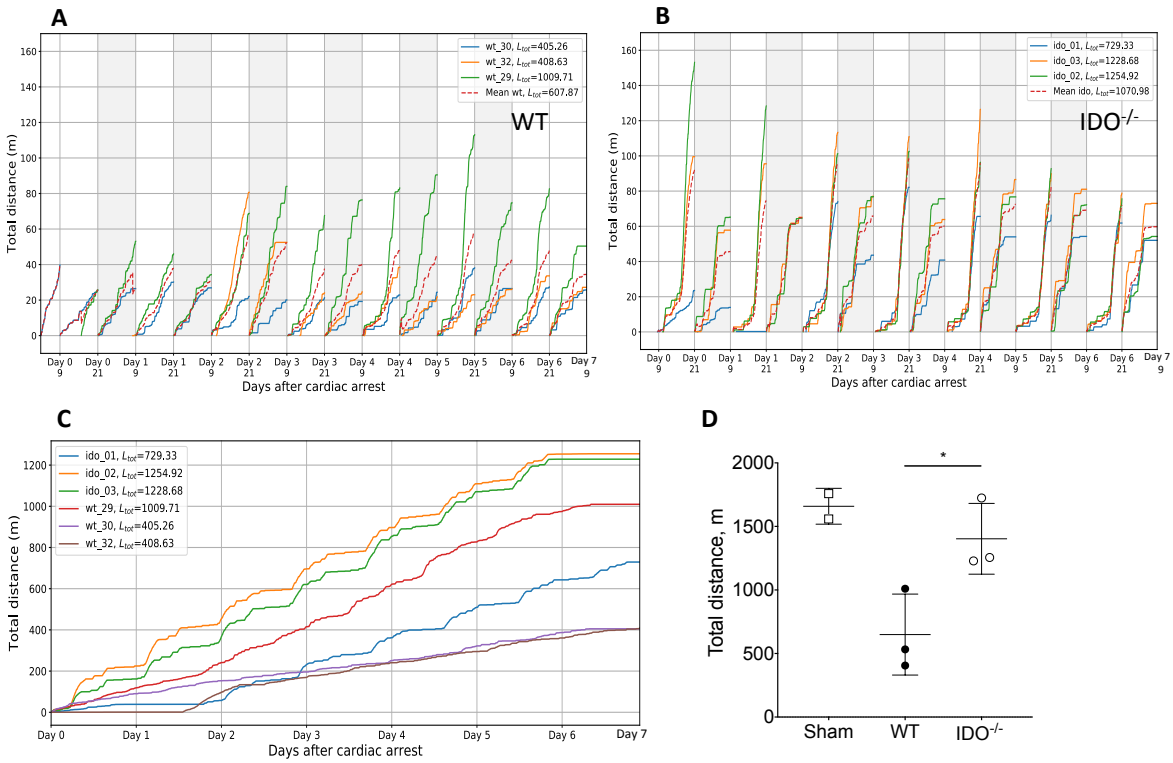

Figure 4. Spontaneous locomotor activity in the 7 days after cardiac arrest/cardiopulmonary resuscitation (CA/CPR). **A.** Cumulative distance covered by WT mice. **B.** Cumulative distance covered by IDO$^{-/-}$ mice during the dark/light periods. **C-D.** Total distance covered by both groups.

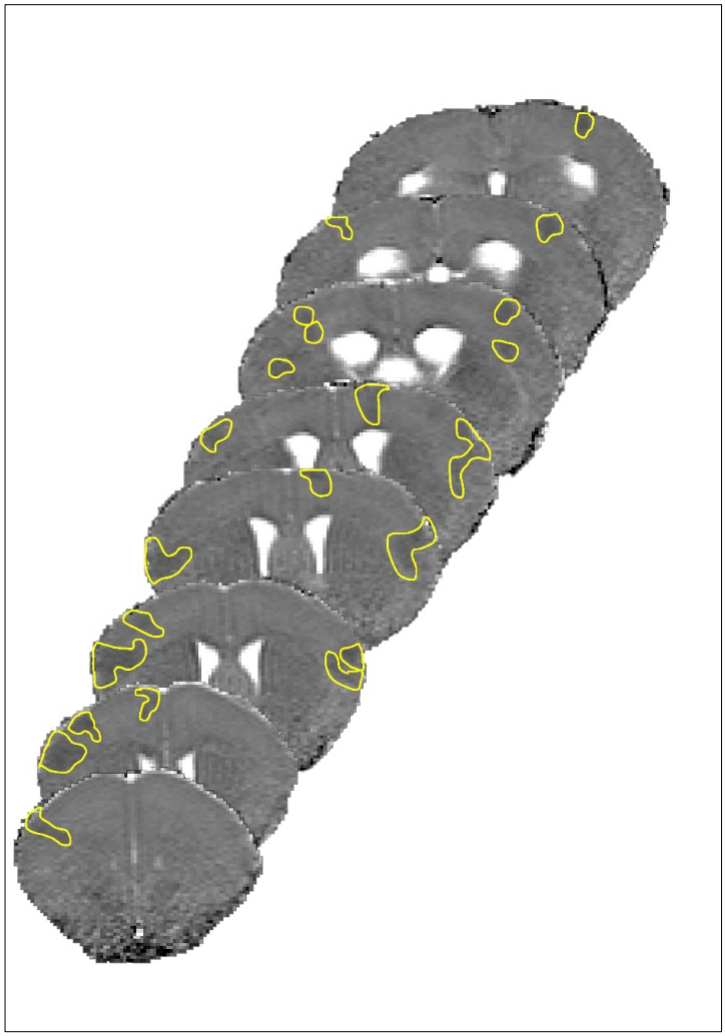

Figure 5. Representative MRI image of the brain of a WT mouse 24 hours after resuscitation. Yellow circles indicate areas of hypointense signal. The ADC map was obtained from DWI sequences. ADC= Apparent Diffusion Coefficient; DWI=diffusion weighted imaging.

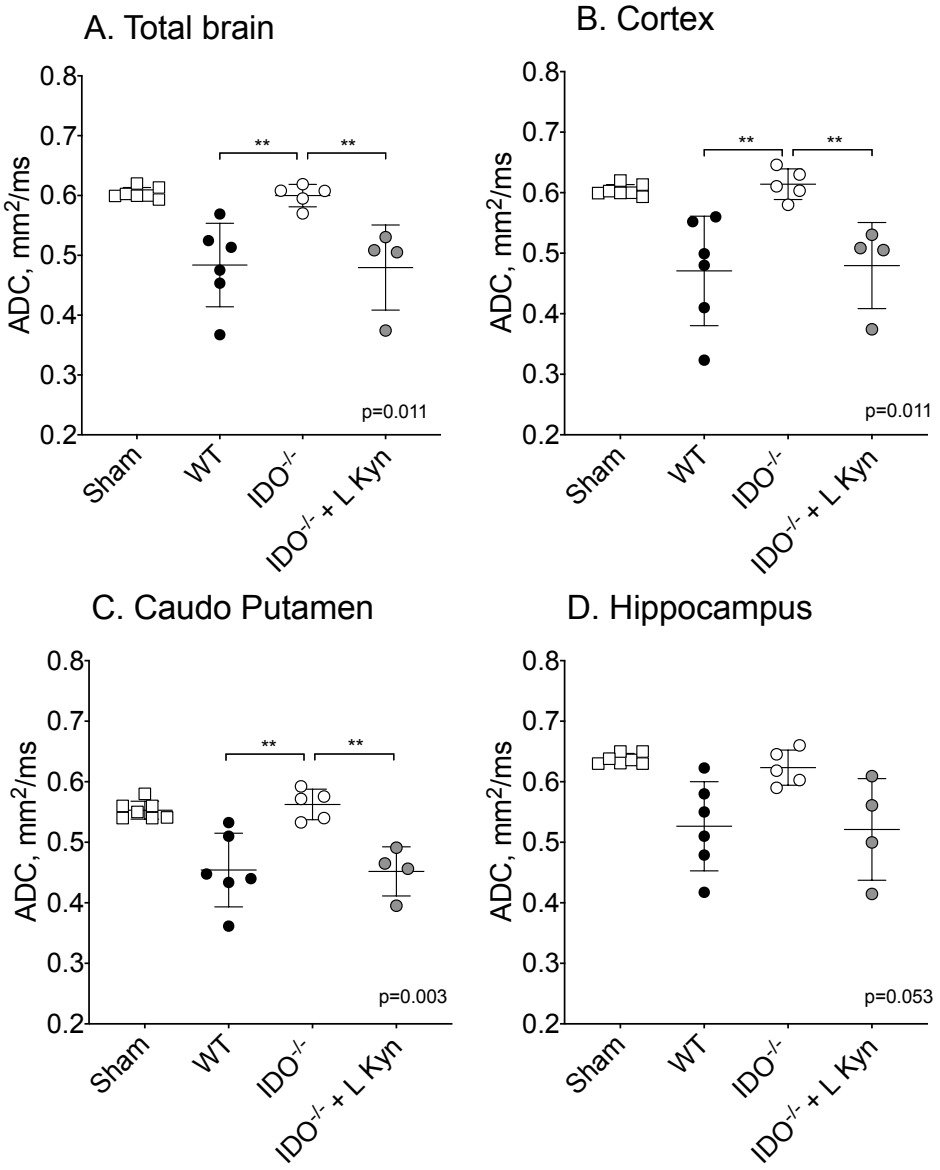

Figure 6. Average ADC values of each region of interest across all planes in Sham-operated animals (n=7), WT mice (n=6), $IDO^{-/-}$ mice (n=5) and $IDO^{-/-}$+L Kyn mice (n=4) are shown at 24 hours after CA/CPR. ADC= Apparent Diffusion Coefficient

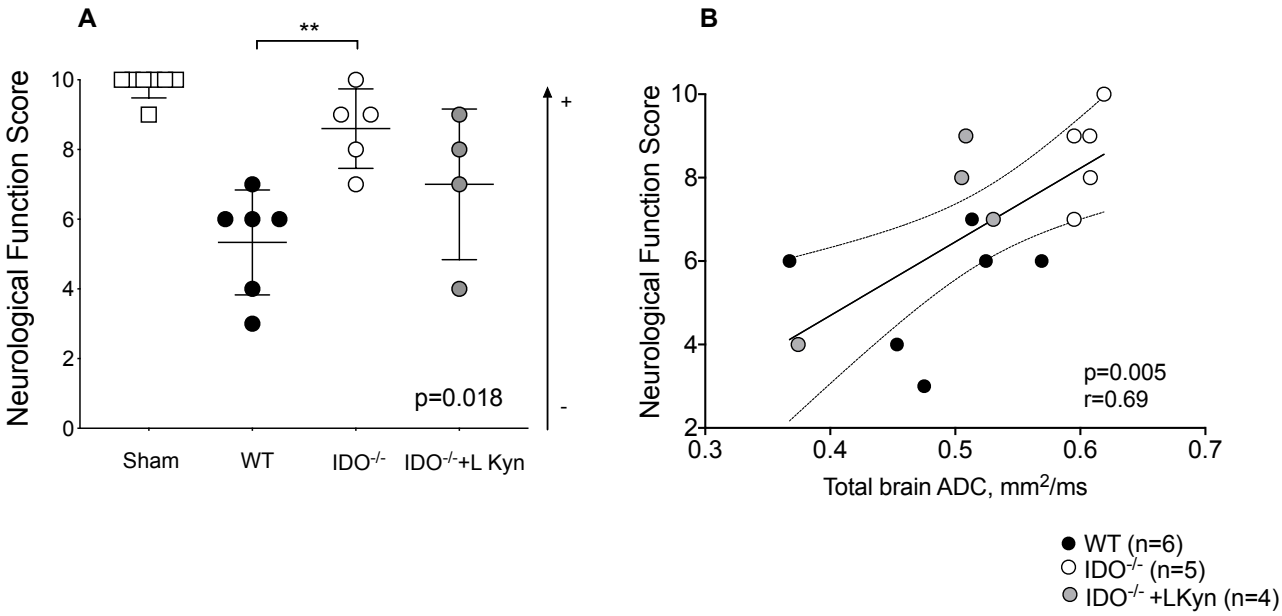

Figure 7. A. Neurological function score in Sham-operated animals (n=7), WT mice (n=6), $IDO^{-/-}$ mice (n=5) and $IDO^{-/-}$+L Kyn mice (n=4) at 24 hours after CA/CPR. **B.** Correlation between total brain ADC and neurological function score at 24 hours after CA/CPR. ADC= Apparent Diffusion Coefficient

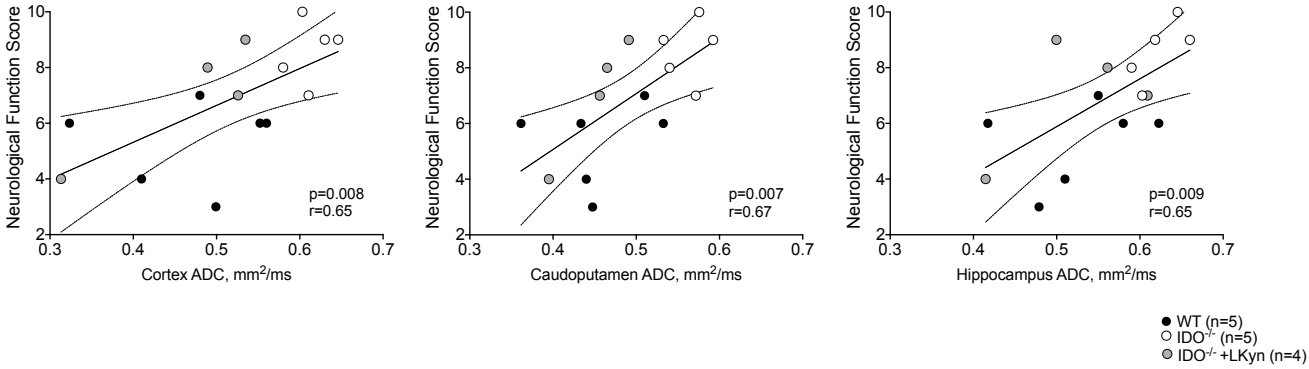

Figure 8. Correlation between ADC in the cortex **A.** caudoputamen **B.** and hippocampus **C.** and neurological function score at 24 hours after CA/CPR. ADC= Apparent Diffusion Coefficient

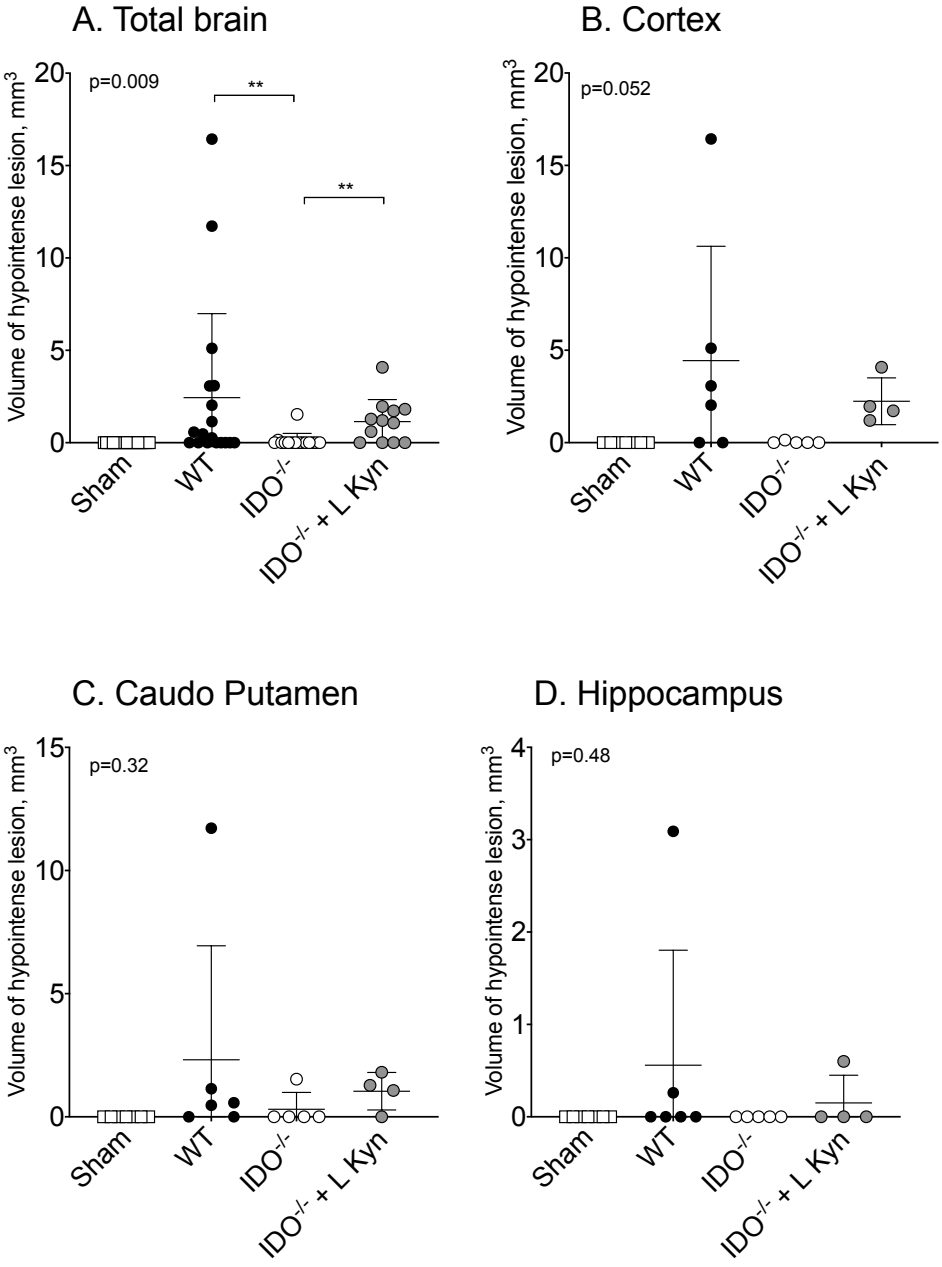

Figure 9. Volumes of the hypointense regions in ADC maps for each region of interest at 24 hours after CA/CPR in Sham-operated animals (n=7), WT mice (n=6), $IDO^{-/-}$ mice (n=5) and $IDO^{-/-}$+L Kyn mice (n=4). ADC= Apparent Diffusion Coefficient

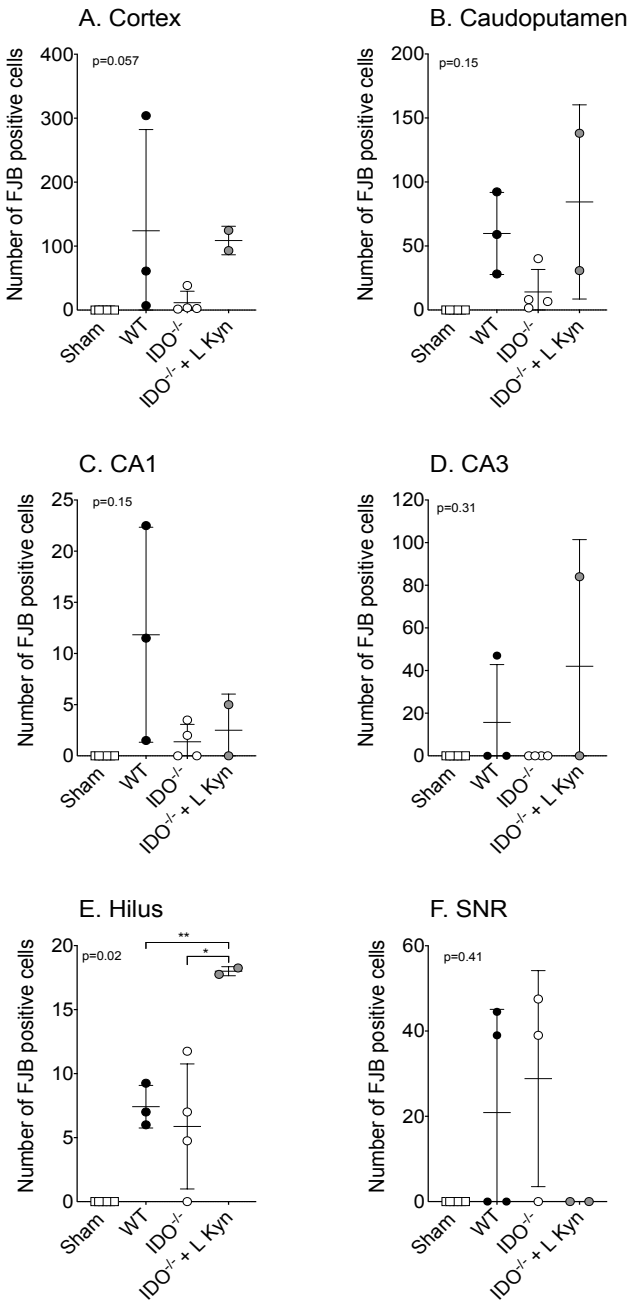

Figure 10. Number of FJB-positive cells in in the cortex, caudoputamen, and hippocampus (CA1, CA3 and hilus) and substantia nigra reticular parts (SNR).

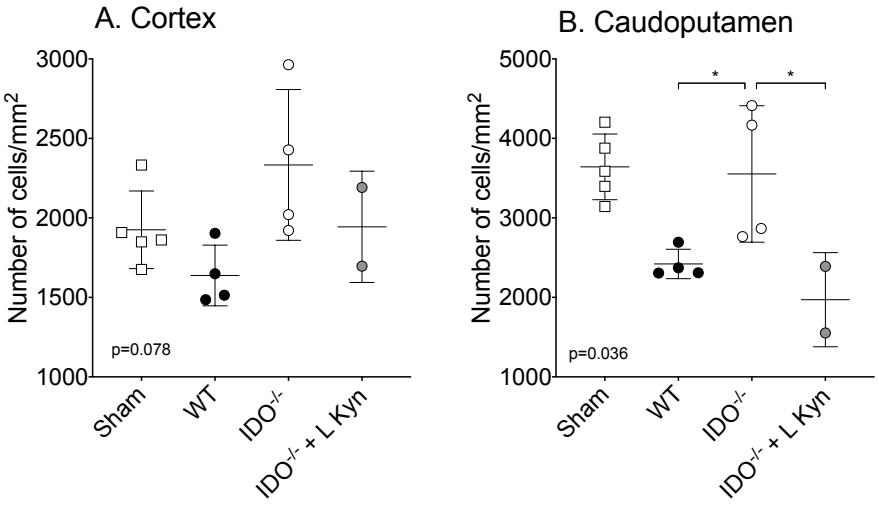

Figure 11. Density of neuronal cells in the cortex **A.** and in the caudoputamen **B.** at 24 hours after CA/CPR in sham-operated mice (n=4), WT mice (n=4), $IDO^{-/-}$ mice (n=4) and $IDO^{-/-}$+L Kyn mice (n=2). Cresyl Violet staining was used to quantify neuronal cell.

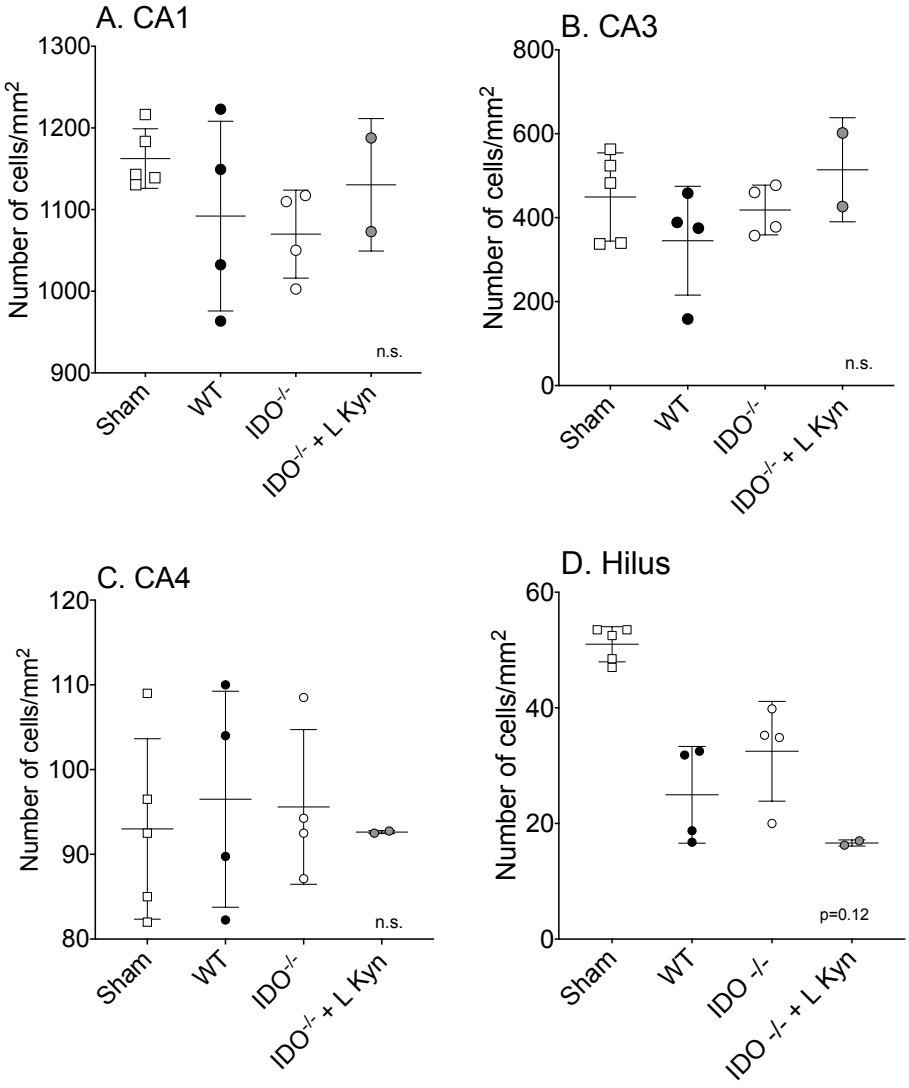

Figure 12. Density of neuronal cells in the regions of hippocampus at 24 hours after CA/CPR in sham-operated mice (n=4), WT mice (n=4), $IDO^{-/-}$ mice (n=4) and $IDO^{-/-}$+L Kyn mice (n=2). Cresyl Violet staining was used to quantify neuronal cell.

References

48. Benjamin EJ, Muntner P, Alonso A, et al. Heart disease and stroke statistics 2019 update: a report from the American Heart Association. Circulation 2019;139:e56e528.

49. Adrie C, Adib-Conquy M, Laurent I. Successful cardiopulmonary resuscitation after cardiac arrest as a "sepsis-like" syndrome. Circulation. 2002;106:562-568

50. Adrie C, Laurent I, Monchi M. Postresuscitation disease after cardiac arrest: A sepsis- like syndrome? Curr Opin Crit Care. 2004;10:208-212

4. Neumar RW, Nolan JP, Adrie C. Post-cardiac arrest syndrome: Epidemiology, pathophysiology, treatment, and prognostication. A consensus statement from the international liaison committee on resuscitation. Circulation. 2008;118:2452-2483

5. Laver S, Farrow C, Turner D, Nolan J. Mode of death after admission to an intensive care unit following cardiac arrest. Intensive Care Med 2004;30:2126—8.
6. Ristagno G, Fries M, Brunelli L. Early kynurenine pathway activation following cardiac arrest in rats, pigs, and humans. Resuscitation. 2013;84:1604–1610

7. Ristagno G, Latini R, Vaahersalo J. FINNRESUSCI Investigators. Early activation of the kynurenine pathway predicts early death and long-term outcome in patients resuscitated from out-of-hospital cardiac arrest. J Am Heart Assoc 2014;4:3

8. Schefold JC, Fritschi N, Fusch G. Influence of core body temperature on Tryptophan metabolism, kynurenines, and estimated IDO activity in critically ill patients receiving target temperature management following cardiac arrest. Resuscitation 2016;107:107– 114

9. Yoshida R, Imanishi J, Oku T. Induction of pulmonary indoleamine 2,3-dioxygenase by interferon. Proc Natl Acad Sci U S A. 1981;78:129-32

10. Werner ER, Hirsch-Kauffmann M, Fuchs D. Interferon-gamma-induced degradation of tryptophan by human cells in vitro. Biol Chem Hoppe Seyler. 1987;368:1407-1412

11. Wang Y, Liu H, McKenzie G. Kynurenine is an endothelium-derived relaxing factor produced during inflammation. Nat Med. 2010;16:279–285
12. Heyes MP , Saito K, Crowley JS. Quinolinic acid and kynurenine pathway metabolism in and non-inflammatory neurological disease. Brain. 1992;115:1249–1273

13. Kita T, Morrison PF, Heyes MP. Effects of systemic and central nervous system localized inflammation on the contributions of metabolic precursors to the L-kynurenine and quinolinic acid pools in brain. J Neurochem. 2002;82:258–268

14. Schwarcz R, Pellicciari R. Manipulation of brain kynurenines: Glial targets, neuronal effects, and clinical opportunities. J Pharmacol Exp Ther. 2002;303:1–10

15. Owe-Young R, Webster NL, Mukhtar M. Kynurenine pathway metabolism in human blood-brain-barrier cells: implications for immune tolerance and neurotoxicity. J Neurochem. 2008;105:1346–1357

16. Tasset I, Pérez-De La Cruz V, Elinos-Calderón D, Carrillo-Mora P, González-Herrera IG, Luna-López A, Konigsberg M, Pedraza- Chaverrí J et al (2010) Protective effect of tert-butylhydroquinone on the quinolinic-acid-induced toxicity in rat striatal slices: role of the Nrf2-antioxidant response element pathway. Neurosignals 18(1):24–31

17. Tavares RG, Tasca CI, Santos CES, Alves ĹB, Porciúncula LO, Emanuelli T, Souza DO (2002) Quinolinic acid stimulates synaptosomal glutamate release and inhibits glutamate uptake into astrocytes. Neurochem Int 40(7):621–627

18. Braidy N, Grant R, Adams S, Brew BJ, Guillemin GJ (2009) Mechanism for quinolinic acid cytotoxicity in human astrocytes and neurons. Neurotox Res 16(1):77–86

19. Mellor AL, Baban B, Chandler P. Cutting edge: induced indoleamine 2,3 dioxygenase expression in dendritic cell subsets suppresses T cell clonal expansion. J Immunol 2003; 171:1652-1655

20. Minamishima S, Kida K, Tokuda K. Inhaled nitric oxide improves outcomes after successful cardiopulmonary resuscitation in mice. Circulation. 2011;124:1645-1653

21. Kida K, Shirozu K, Yu B. Beneficial effects of nitric oxide on outcomes after cardiac arrest and cardiopulmonary resuscitation in hypothermia-treated mice. Anesthesiology. 2014;120:880-889

22. Nishida T, Yu JD, Minamishima S, Sips PY. Protective effects of nitric oxide synthase 3 and soluble guanylate cyclase on the outcome of cardiac arrest and cardiopulmonary resuscitation in mice. Crit Care Med. 2009;37:256-262

23. Minamishima S, Bougaki M, Sips PY . Hydrogen sulfide improves survival after cardiac arrest and cardiopulmonary resuscitation via a nitric oxide synthase 3-dependent mechanism in mice. Circulation. 2009;120:888-896

24. Hayashida K Improvement in outcomes after cardiac arrest and resuscitation by inhibition of S-Nitrosoglutathione reductase

25. Ikeda K, Liu X, Kida K. Thiamine as a neuroprotective agent after cardiac arrest. Resuscitation. 2016;105:138-144

26. Abella BS, Zhao D, Alvarado J. Intra-arrest cooling improves outcomes in a murine cardiac arrest model. Circulation. 2004;109:2786-2791

27. Iannello F. Non-intrusive high throughput automated data collection from the home cage. Helyon Volume 5, Issue 4, April 2019, e01454

28. Moro F, Fossi F, Magliocca A, Pascente R, Sammali E, Baldini F, Tolomeo D, Micotti E, Citerio G, Stocchetti N, Fumagalli F, Magnoni S, Latini R, Ristagno G, Zanier E. Efficacy of acute administration of inhaled argon on traumatic brain injury in mice. Br J Antesh 2020 Sep 22;S0007-0912(20)30686-3.doi: 10.1016/j.bja.2020.08.027.Online ahead of print.

29. Frigerio F, Pasqualini G, Craparotta I, Marchini S, van Vliet EA, Foerch P, Vandenplas C, Leclercq K, Aronica E, Porcu L, Pistorius K, Colas RA, Hansen TV, Perretti M, Kaminski RM, Dalli J, Vezzani A. Brain. 2018 Nov 1;141(11):3130-3143. doi: 10.1093/brain/awy247.

30. Combined Genetic Deletion of IL (Interleukin)-4, IL-5, IL-9, and IL-13 Does Not Affect Ischemic Brain Injury in Mice. Perego C, Fumagalli S, Miteva K, Kallikourdis M, De Simoni MG. Stroke. 2019 Aug;50(8):2207-2215.

31. Macrophages are essential for maintaining a M2 protective response early after ischemic brain injury. Perego **C**, Fumagalli S, Zanier ER, Carlino E, Panini N, Erba E, De Simoni MG. Neurobiol Dis. 2016 Dec;96:284-293. doi: 10.1016/j.nbd.2016.09.017.

32. Perego C, Fumagalli S, De Simoni MG. J Neuroinflammation. 2011 Dec 10;8:174. doi: 10.1186/1742-2094-8-174.

33. Hoshi M, Matsumoto K, Ito H, Ohtaki H, Arioka Y, Osawa Y, Yamamoto Y, Matsunami H, Hara A, Seishima M, Saito K. 2012. L-tryptophan-kynurenine pathway metabolites regulate type I IFNs of acute viral myocarditis in mice. J. Immunol. 188:3980 –3987.

34. Masato Hoshi, Yosuke Osawa, Hiroyasu Ito , Hirofumi Ohtaki Tatsuya Ando, Manabu Takamatsu, Akira Hara, Kuniaki Saito, Mitsuru Seishima Blockade of indoleamine 2,3-dioxygenase reduces mortality from peritonitis and sepsis in mice by

regulating functions of CD11b+ peritoneal cells. Immun 2014 Nov;82(11):4487- 95. doi: 10.1128/IAI.02113-14.

35. Romergryko G Geocadin, Clifton W Callaway, Ericka L Fink, Eyal Golan, David M Greer, Nerissa U Ko, Eddy Lang, Daniel J Licht, Bradley S Marino, Norma D McNair, Mary Ann Peberdy, Sarah M Perman, Daniel B Sims, Jasmeet Soar, Claudio Sandroni, American Heart Association Emergency Cardiovascular Care Committee. Standards for Studies of Neurological Prognostication in Comatose Survivors of Cardiac Arrest: A Scientific Statement From the American Heart Association. Circulation 2019 Aug 27;140(9):e517-e542.doi: 10.1161/CIR.0000000000000702.Epub 2019 Jul 11.

36. Neumar RW. Molecular mechanisms of ischemic neuronal injury. *Ann Emerg Med*. 2000;36:483–506.

37. Darlington LG, Mackay GM, Forrest CM. Altered kynurenine metabolism correlates with infarct volume in stroke. Eur J Neurosci. 2007;26:2211–2221.

38. Adams Wilson JR, Morandi A, Girard TD. The association of the kynurenine pathway of tryptophan metabolism with acute brain dysfunction during critical illness. Crit Care Med. 2012;40:835–841.

39. Affatato R, Lucchetti J, Ceriani S. Inhibition of the Kynurenine Pathway Improves Neurological Recovery in a Rat Model of Cardiac Arrest. Circulation. 2015;132:A15237.

40. http://dx.doi.org/10.14336/AD.2017.0221 (aged mice locomotor acitvity)

41. Nao Hirata, Satoko Hattori**.** Comprehensive behavioral analysis of indoleamine 2,3-dioxygenase knockout mice**.** Neuropsychopharmacology Reports. 2018;38:133–144. DOI: 10.1002/npr2.12019

42. Greer DM, Scripko PD, Wu O, Edlow BL, Bartscher J, Sims JR, Camargo EE, Singhal AB, Furie KL (2013) Hippocampal magnetic resonance imaging abnormalities in cardiac arrest are associated with poor outcome. J Stroke Cerebrovasc Dis 22:899–905.

43. Jang J, Oh SH, Nam Y, Lee K, Choi HS, Jung SL, Ahn KJ, Park KN, Kim BS (2019) Prognostic value of phase information of 2D T2*-weighted gradient echo brain imaging in cardiac arrest survivors: a preliminary study. Resuscitation 140:142–149.

44. Jeon CH, Park JS, Lee JH, Kim H, Kim SC, Park KH, Yi KS, Kim SM, Youn CS, Kim YM, Lee BK (2017) Comparison of brain computed tomography and diffusion-weighted magnetic

resonance imaging to predict early neurologic outcome before target temperature management comatose cardiac arrest survivors. Resuscitation 118:21–26.

45. Kim JH, Kim MJ, You JS, Lee HS, Park YS, Park I, Chung SP (2018) Multimodal approach for neurologic prognostication of out-of-hospital cardiac arrest patients undergoing targeted temperature management. Resuscitation 134:33–40.

46. Ryoo SM, Jeon SB, Sohn CH, Ahn S, Han C, Lee BK, Lee DH, Kim SH, Donnino MW, Kim WY (2015) Predicting outcome with diffusion-weighted imaging in cardiac arrest patients receiving hypothermia therapy: multicenter retrospective cohort study. Crit Care Med 43:2370–2377.

47. Son SH, Lee IH, Park JS, Yoo IS, Kim SW, Lee JW, Ryu S, You Y, Min JH, Cho YC, Jeong WJ, Oh SK, Cho SU, Ahn HJ, Kang C, Lee DH, Lee BK, Youn CS (2020) Does combining biomarkers and brain images provide improved prognostic predictive performance for out-of-hospital cardiac arrest survivors before target temperature management? J Clin Med.
48. Kim J, Kim K, Hong S, Kwon B, Yun ID, Choi BS, Jung C, Lee JH, Jo YH, Kim T, Rhee JE, Lee SH (2013) Low apparent diffusion coefficient cluster-based analysis of diffusion-weighted MRI for prognostication of out-of- hospital cardiac arrest survivors. Resuscitation 84:1393–1399.

49. Moon HK, Jang J, Park KN, Kim SH, Lee BK, Oh SH, Jeung KW, Choi SP, Cho IS, Youn CS (2018) Quantitative analysis of relative volume of low apparent diffusion coefficient value can predict neurologic outcome after cardiac arrest. Resuscitation 126:36–42.

50. Hirsch KG, Fischbein N, Mlynash M, Kemp S, Bammer R, Eyngorn I, Tong J, Moseley M, Venkatasubramanian C, Caulfield AF, Albers G (2020) Prognostic value of diffusion-weighted MRI for post-cardiac arrest coma. Neurology 94:e1684–e1692.

51. María I. Cuartero, Iván Ballesteros, Juan de la Parra, Andrew L. Harkin, Aine Abautret-Daly, Eoin Sherwin, Pedro Fernández-Salguero, Ángel L. Corbí, Ignacio Lizasoain and María A. Moro AN. L-Kynurenine/Aryl Hydrocarbon Receptor Pathway Mediates Brain Damage After Experimental Stroke. *Circulation.* published online October 30, 2014 DOI: 10.1161/CIRCULATIONAHA.114.011394

52. Gellért L, Knapp L, Németh K, Herédi J, Varga D, Oláh G, Kocsis K, Menyhárt A, Kis Z, Farkas T, Vécsei L, Toldi J. Post-ischemic treatment with L-kynurenine sulfate exacerbates neuronal damage after transient middle cerebral artery occlusion. *Neuroscience.* 2013;247C:95- 101.

53. G. Mazarei, D.P. Budac, G. Lu, H. Lee, T. Möller, B.R. Leavitt. The absence of indoleamine 2,3-dioxygenase expression protects against NMDA receptor-mediated excitotoxicity in mouse brain. Experimental Neurology 249 (2013) 144–148

54. Jung ID, Lee MG, Chang JH. Blockade of indoleamine2,3-dioxygenase protects mice against lipopolysaccharide-induced endotoxin shock. J Immunol, 2009, 182:3146–3154

55. Blockade of indoleamine 2,3-dioxygenase reduces mortality from peritonitis and sepsis in mice by regulating functions of CD11b+ peritoneal cells

56. George C Prendergast, William P Malachowski, James B DuHadaway, Alexander J Muller. Discovery of IDO1 Inhibitors: From Bench to Bedside. Cancer res 2017 Dec 15;77(24):6795-6811. doi: 10.1158/0008-5472.CAN-17-2285.

57. Soliman HH, Jackson E, Neuger T, Dees EC, Harvey RD, Han H, et al. A first in man phase I trial of the oral immunomodulator, indoximod, combined with docetaxel in patients with metastatic solid tumors. Oncotarget. 2014; 5:8136–46.

58. https://clinicaltrials.gov/ct2/results?cond=&term=IDO-inhibitors&cntry=&state=&city=&dist=

Chapter 5. Summary, conclusions and future perspectives

Cardiac arrest (CA) is a leading cause of death worldwide (1). Despite early initiation of cardiopulmonary resuscitation (CPR) and prompt defibrillation have increased the rate of return of spontaneous circulation (ROSC), CA outcome remains poor. Only 12% of out-of-hospital CA patients survive to hospital discharge, and barely 8% of these survivors regain good neurological recovery (1).

The present thesis focuses on different strategies targeting the two main aspects of CA treatment, namely: cardiopulmonary resuscitation interventions and post-resuscitation care. It includes both experimental and translational studies directed to improve hemodynamic support during CPR, to define pulmonary dysfunction related to CPR, and to improve post-resuscitation outcomes.

Cardio-Pulmonary Resuscitation Interventions: Hemodynamic Support

In a preclinical model of CPR performed in a moving ambulance, a piston-based mechanical chest compressions (CC) allowed for a significantly greater hemodynamic support and systemic perfusion, as represented by higher coronary perfusion pressure, and arterial pressure, and lower arterial lactate, compared with manual CC. Mechanical CC accounted also for a better CC quality, with a lesser rescuer's physical effort requirements, compared with manual compression. This study provides evidence to suggest and encourage the use of mechanical devices during ambulance transport to assure ongoing high-quality CC, tissue perfusion, and rescuers' safety (2).

These findings have several clinical implications:

- Provides evidence to the current knowledge gap on mechanical CPR during transport as claimed in the 2015 International Consensus on Cardiopulmonary Resuscitation and Emergency Cardiovascular Care Science with Treatment Recommendations.
- The study may have a potential impact on the rescuers' decision on whether stay on the scene or transport the cardiac arrest patient to the hospital with an ongoing mechanical CPR.
- The study results encourage the use of mechanical CPR devices during ambulance transport to assure ongoing high-quality CC, adequate hemodynamic support and tissue perfusion, and rescuers' safety.

Cardio-Pulmonary Resuscitation Interventions: Lung damage

In a translational study we provide a comprehensive description of lung abnormalities following cardiopulmonary resuscitation, with similar techniques, in both pigs and humans. The consistent clinical and experimental findings allow us to introduce the concept of "Cardiopulmonary-Resuscitation Associated Lung Edema" (CRALE). Lung abnormalities were first investigated in a porcine model of CA and prolonged mechanical vs manual CPR and then in a cohort of out-of-hospital CA patients undergoing mechanical or manual CC with a lung CT scan performed after resuscitation.

Our observations highlight the presence of lung abnormalities, likely representing a Cardiopulmonary-Associated Lung Edema which were

more pronounced after mechanical versus manual CC, with a derangement in mechanical properties and gas exchange. These alterations are transient and appear related with the intensity of intratoracic pressure swings during CC (3).

The novelty of this work is that despite a strong rationale supporting the idea that successfully resuscitated cardiac arrest patients may suffer from authentic lung injury, the concept of post-resuscitation disease had been so far essentially considered from a hemodynamic perspective. CRALE will be from now on an additional piece of this complex puzzle that must be taken into account in the management of cardiac arrest patients. These findings are of high clinical value since some studies previously suggested that ARDS following cardiac arrest significantly affect ICU stay and chance of survival (4).

Further reasarch should be focused on the identification of the optimal ventilation strategy in order to prevent or reduce the occurence of CRALE.

Indeed, the pathophysiological mechanisms of lung injury after CPR are not completely understood. Currently, the only treatment recommendation in CA patients with a secure airway receiving continuous CC is to maintain a ventilation rate of 10 bpm. The optimal ventilation strategy during mechanical CC is still elusive: how to provide adequate blood oxygenation and carbon dioxide (CO_2) removal while minimizing lung injury remains uncertain. Future work should be aimed at investigate whether the optimization of ventilation during mechanical CC could prevent lung injury. Specifically, whether a protective ventilation strategy could improve the respiratory system compliance, oxygenation and regional distribution of tidal

ventilation by alveolar recruitment of the lung collapsed during chest compressions should be further evaluated.

Post Resuscitation Care: Modulation of Kynurenine Pathway To Prevent Brain Injury After Cardiac Arrest.

In an experimental model of CA we provide evidence that kynurenine pathway (KP) inhibition through genetic deletion of its rate-limiting enzyme (IDO) markedly improves survival and neurological outcome. The neuroprotective effects of IDO-deletion were associated with attenuation of CA-induced abnormality in water diffusion detected with brain magnetic resonance imaging at 24 hours after resuscitation and with prevention of neuronal degeneration in the hilus and in the frontal cortex. The protective effect of IDO-deletion was also associated with reduced neuronal cell loss in the caudoputamen. Moreover, IDO-deletion accelerated the recovery of spontaneous locomotor function up to 7 days after CA. Finally, administration of L-Kyn in $IDO^{-/-}$ mice abrogated the protective effects of IDO-deletion on neurological function, ischemic brain edema and neuronal degeneration after CA. Future work should be focused on evaluating the effects of pharmacological inhibition of KP after CA. From the viewpoint of translating the present results into clinical benefit, the pharmacological inhibition of KP after resuscitation would add relevance to the present findings.

Different IDO inhibitors have been developed in the last years (5), in preclinical settings the most used IDO inhibitor is represented by 1-methyl-tryptophan (1MT). In clinical settings various compounds have been studied, in the field of oncology they have been used as

immunometabolic adjuvants since 2008 (6); and phase I-II clinical trials are still ongoing (7).

References

1. Benjamin EJ, Muntner P, Alonso A, Bittencourt MS, Callaway CW; on behalf of the American Heart Association Council on Epidemiology and Prevention Statistics Committee and Stroke Statistics Subcommittee. Heart disease and stroke statistics—2019 update: a report from the American Heart Association. *Circulation*. 2019;139:e56–e528. doi: 10.1161/CIR.0000000000000659.

2. Magliocca A, Olivari D, De Giorgio D, Zani D, Manfredi M, Boccardo A, Cucino A, Sala G, Babini G, Ruggeri L, Novelli D, Skrifvars MB, Hardig BM, Pravettoni D, Staszewsky L, Latini R, Belloli A, Ristagno G. LUCAS Versus Manual Chest Compression During Ambulance Transport: A Hemodynamic Study in a Porcine Model of Cardiac Arrest. J Am Heart Assoc. 2019;8(1):e011189.

3. Magliocca A, Rezoagli E, Zani D, Manfredi M, De Giorgio D, Olivari D, Fumagalli F, Langer T, Avalli L, Grasselli G, Latini R, Pesenti A, Bellani G, Ristagno G. Cardiopulmonary Resuscitation-Associated Lung Edema (CRALE) - A

Translational Study.Am J Respir Crit Care Med. 2020 Sep 8. doi: 10.1164/rccm.201912-2454OC. Online ahead of print.

4. Geri G, et al. Cardiopulmonary Resuscitation Associated Lung Edema: The Price to Pay to Get the Heart Beat? Am J Respir Crit Care Med. 2020. PMID: 32966750 No abstract available.

5. George C Prendergast, William P Malachowski, James B DuHadaway, Alexander J Muller. Discovery of IDO1 Inhibitors: From Bench to Bedside. Cancer res 2017 Dec 15;77(24):6795-6811. doi: 10.1158/0008-5472.CAN-17-2285.

6. Soliman HH, Jackson E, Neuger T, Dees EC, Harvey RD, Han H, et al. A first in man phase I trial of the oral immunomodulator, indoximod, combined with docetaxel in patients with metastatic solid tumors. Oncotarget. 2014; 5:8136–46.
7. https://clinicaltrials.gov/ct2/results?cond=&term=IDO-inhibitors&cntry=&state=&city=&dist=

Publications:

- **Magliocca A**, Olivari D, De Giorgio D, Zani D, Manfredi M, Boccardo A, Cucino A, Sala G, Babini G, Ruggeri L, Novelli D, Skrifvars MB, Hardig BM, Pravettoni D, Staszewsky L, Latini R, Belloli A, Ristagno G. LUCAS Versus Manual Chest Compression During Ambulance Transport: A Hemodynamic Study in a Porcine Model of Cardiac Arrest. J Am Heart Assoc. 2019;8(1):e011189

- **Magliocca A**, Rezoagli E, Zani D, Manfredi M, De Giorgio D, Olivari D, Fumagalli F, Langer T, Avalli L, Grasselli G, Latini R, Pesenti A, Bellani G, Ristagno G. Cardiopulmonary Resuscitation-Associated Lung Edema (CRALE) - A Translational Study.Am J Respir Crit Care Med. 2020 Sep 8. doi: 10.1164/rccm.201912-2454OC. Online ahead of print.

- **Magliocca A**, Manfredi M, Olivari D, De Giorgio D, Cucino A, Zani DD, Ristagno G. High quality chest compression: Don't be afraid of breaking ribs to gain a life! Heart Lung. 2019 Mar-Apr;48(2):173-174. doi: 10.1016/j.hrtlng.2018.12.004. Epub 2019 Jan 10

- Rezoagli E, **Magliocca A**, Ristagno G, Bellani G. CO_2 Oscillation during Cardiopulmonary Resuscitation: The Role of Respiratory System Compliance. Am J Respir Crit Care Med. 2019 May 15;199(10):1290-1291. doi: 10.1164/rccm.201812-2331LE.

- **Magliocca A**, Omland T, Latini R Dipeptidyl peptidase 3, a biomarker in cardiogenic shock and hopefully much more.
  .Eur J Heart Fail. 2020 Feb;22(2):300-302. doi: 10.1002/ejhf.1649. Epub 2019 Dec 15.

- Moro F, Fossi F, **Magliocca A**, Pascente R, Sammali E, Baldini F, Tolomeo D, Micotti E, Citerio G, Stocchetti N, Fumagalli F, Magnoni S, Latini R, Ristagno G, Zanier ER Efficacy of acute administration of inhaled argon on traumatic brain injury in mice. Br J Anaesth. 2020 Sep 22:S0007-0912(20)30686-3. doi: 10.1016/j.bja.2020.08.027. Online ahead of print.

- Porceddu E, Rezoagli E, Poli D, **Magliocca A**, Scoditti U, Di Minno MND, De Stefano V, Siragusa S, Ageno W, Dentali F; CEVETIS (CErebral VEin Thrombosis International Study) Investigators Sex-related characteristics of cerebral vein thrombosis: A secondary analysis of a multicenter international cohort study.Thromb Res. 2020 Sep 17;196:371-374. doi: 10.1016/j.thromres.2020.09.023. Online ahead of print

- Olivari D, De Giorgio D, Staszewsky LI, Fumagalli F, Boccardo A, Novelli D, Manfredi M, Babini G, Luciani A, Ruggeri L, **Magliocca A**, Zani DD, Masson S, Belloli A,

Pravettoni D, Maiocchi G, Latini R, Ristagno GSearching for Preclinical Models of Acute Decompensated Heart Failure: a Concise Narrative Overview and a Novel Swine Model.Cardiovasc Drugs Ther. 2020 Oct 24. doi: 10.1007/s10557-020-07096-5. Online ahead of print.